

## For Reference

---

NOT TO BE TAKEN FROM THIS ROOM


## For Reference

---

NOT TO BE TAKEN FROM THIS ROOM

Ex LIBRIS  
UNIVERSITATIS  
ALBERTAENSIS





Digitized by the Internet Archive  
in 2018 with funding from  
University of Alberta Libraries







THE UNIVERSITY OF ALBERTA

Thesis  
1961  
# 36

INFRARED SPECTROSCOPY OF XANTHATE COMPOUNDS  
IN THE SOLID, SOLUTION AND ADSORBED STATES

A Thesis

Submitted to the Faculty of Graduate Studies

In Partial Fulfilment of the Requirements

for the Degree of Master of Science

DEPARTMENT OF MINING AND METALLURGY

by

GEORGE WESLEY POLING

EDMONTON, ALBERTA

APRIL 1961





## ABSTRACT

The infrared spectra of several alkali and heavy metal xanthates and closely related compounds are presented. Assignments are given for the absorption bands associated with stretching vibrations of the C=O, C=S, and C-S groups in xanthate molecules.

An accessory reflectance attachment to the spectrophotometer for monolayer adsorption studies is described. The ability to produce absorption bands of reasonable intensity from a monomolecular layer is illustrated by the recording of spectra of monolayer films deposited by the Langmuir-Blodgett technique onto the sample mirrors used in the reflectance accessory.

Lead sulfide films evaporated onto either aluminum mirrors (for study by reflectance) or infrared transmitting windows (for transmission studies), are shown to contain lead thiosulfate as the predominant oxidation product. The reflection spectrum of polished natural galena resembles lead thiosulfate more closely than it does lead sulfate or lanarkite. The latter have previously been identified as galena oxidation products using an electron diffraction technique. Evidence is presented that the thiosulfate may have been further oxidized to sulfate in the electron diffraction camera.

Preliminary spectroscopic studies of the adsorption of xanthate from an aqueous solution onto galena show that the oxidation product has been completely replaced by lead xanthate multilayers. Most of the multilayers were washed away in hot acetone but the xanthate remaining on the surface constituted more than a single monolayer.



## ACKNOWLEDGMENTS

I wish to express sincere gratitude to Dr. J. Leja for his valuable advice and direction of the work connected with this thesis. The assistance and suggestions of Dr. R.J. Crawford of the Chemistry Department (U. of A.) and Dr. L.H. Little (presently at the University of Western Australia, Perth), who collaborated in some of this work, have also been appreciated. The encouragement and administrative assistance of Professor E.O. Lilge has greatly facilitated this work.

I have also appreciated the assistance of Mrs. S. Brahms, Miss M. Schwerman, Messrs. W. Yakymyshyn and J. Moissl in work connected with this thesis.

The receipt of a Province of Alberta Graduate Scholarship and an equipment grant (Number E-140) from the National Research Council of Canada are gratefully acknowledged.



## TABLE OF CONTENTS

	Page
INTRODUCTION	1
INFRARED SPECTROSCOPY	
I. THEORY OF INFRARED SPECTROSCOPY	5
A. General Remarks	5
B. Classical Infrared Theory	7
C. Quantum Mechanical Infrared Theory	9
D. Vibrations of Complex Molecules	12
E. Spectral Presentation	18
F. Molecular Structure Determinations	22
II. INFRARED INSTRUMENTATION	
A. Instrument Description	24
B. Sensitivity Requirement of Instrument	28
EXPERIMENTAL PROCEDURES	
I. MATERIALS	
A. Preparations of Xanthates and Related Compounds	30
B. Vacuum Evaporation Technique	31
II. INFRARED SPECTROSCOPIC PROCEDURES	35
A. Infrared Spectra of Solids	35
B. Infrared Spectra of Solutions	36
C. Adsorption Spectral Studies	37
III. LANGMUIR-BLODGETT FILM TECHNIQUE	45
RESULTS AND DISCUSSION	
I. INFRARED SPECTRA OF XANTHATES AND RELATED COMPOUNDS IN SOLID AND SOLUTION STATES	48
A. Absorption Band Assignments	50
B. Group Vibrational Interactions	57
II. NATURE OF THE ADSORBENT	76



## TABLE OF CONTENTS

	Page
III. SPECTRA OF LANGMUIR-BLODGETT MONO-LAYER DEPOSITS ON ALUMINUM MIRRORS	87
IV. INFRARED SPECTRA OF XANTHATES ADSORBED ON SULFIDE MINERALS FROM THE SOLUTION PHASE	
A. Preliminary Attempts	91
B. Multiple Reflection Studies	93
V. SUMMARY	99
VI. PROPOSALS FOR FURTHER STUDIES	100
REFERENCES	101





## LIST OF TABLES

Page

Table 1	C=O Stretching Frequencies in Various Compounds	18
Table 2	Assignment of Vibrational Frequencies of Xanthate Compounds	56
Table 3	Electronegativity Values and Partial Ionic Character of the Metal-Sulphur Bonds	73



## LIST OF FIGURES

	Page
Fig. 1     The Infrared Spectral Region	6
Fig. 2     Characteristic Vibrations of a Triatomic Molecule	7a
Fig. 3     Infrared Vibration-Rotation Transitions	11
Fig. 4     Half Width of an Absorption Band	21
Fig. 5     Spectral Energy Distribution Function	21
Fig. 6     Perkin Elmer 221 Spectrophotometer Optical Schematic	25
Fig. 7     Optical Arrangement for Reflection Spectral Studies	42
Fig. 8     Selected Carbonyl and Thiocarbonyl Compounds	52
Fig. 9     Ethyl and Butyl Xanthates of Copper and Dixanthogens	53
Fig. 10    Zinc Alkyl Xanthates	54
Fig. 11    Alkali Metal Xanthates	55
Fig. 12    Potassium Xanthate Homologues Group Frequency Shifts (Solid State Spectra)	59
Fig. 13    Aqueous Solution Spectra of Potassium Xanthate Homologues	60
Fig. 14    Potassium Xanthate Homologues Group Frequency Shifts (Aqueous Solution Spectra)	61
Fig. 15    Normal and Secondary Xanthates: Comparison of C-O Stretching Frequencies (Solid State Spectra)	63
Fig. 16    Zinc Alkyl Xanthates Group Frequency Shifts (Solid State Spectra)	65
Fig. 17    Lead Alkyl Xanthates	66
Fig. 18    Lead Alkyl Xanthates Group Frequency Shifts (Solid State Spectra)	66
Fig. 19    Schematic Molecular Configuration of Zn Alkyl Xanthate	67



# LIST OF FIGURES

		Page
Fig. 19A	Molecular Models of Zinc n-Heptyl Xanthate and n-Heptyl Xanthate Anion	68
Fig. 19B	Molecular Model of Lead n-Heptyl Xanthate Unit Cell (After Hagihara <sup>35</sup> )	68
Fig. 20	Metal Ethyl Xanthates, Solid State Spectra	70
Fig. 21	Metal n-Butyl Xanthates, Solid State Spectra	71
Fig. 22	Metal Ethyl Xanthates, Group Frequency Shifts	72
Fig. 23	Metal n-Butyl Xanthates, Group Frequency Shifts	72
Fig. 24	Lead Sulfide and Oxidation Products	81
Fig. 25	Infrared Spectra of Lead n-Cetyl Xanthate Monolayers	88
Fig. 26	Spectra of Xanthate "Reaction Product" and $K_2S_2O_3$	93
Fig. 27	Adsorption of K n-Nonyl Xanthate onto Evaporated PbS Film	96



## INTRODUCTION

Flotation technology is largely based on the formation of water repellent or hydrophobic films on solid substances by the adsorption of suitable molecules from aqueous solutions. The heteropolar type molecules employed for this purpose in flotation are called "collectors". The most important species of anionic collectors are the "xanthates"

( $\text{R-O-C} \begin{smallmatrix} \nearrow \text{S} \\ \searrow \text{S} \end{smallmatrix} \text{-Me}$ ) since they are effective in rendering the surfaces of many sulfide minerals hydrophobic.

Since C.H. Keller introduced xanthates as collectors for sulfide minerals in 1923, this molecule has been extensively investigated in the hope of gaining some insight into its powerful collecting ability. A knowledge of the nature of the adsorption of xanthate onto a mineral is thus of fundamental significance.

Xanthates, normally employed as collectors (containing 2 to 6  $\text{CH}_2$  groups in the hydrocarbon radical) are considered to be highly ionized in alkaline aqueous solutions. The majority of the suggested mechanisms for the adsorption of these reagents has been the interaction of the xanthate anion with a metal site on the mineral surface to form Metal-Sulfur bonds. In recent years, however, a controversy between neutral molecule (free acid) adsorption and ion exchange adsorption has arisen. Cook and Nixon<sup>1</sup>, Last and Cook<sup>2</sup> have proposed the free acid adsorption theory in which the xanthate is first hydrolyzed to xanthic acid which is then adsorbed on the mineral surface. Sutherland and Wark<sup>4</sup> maintain that xanthate anions compete with hydroxyl ions for adsorption sites on the mineral. Cook and Nixon<sup>1</sup> pointed out that if such an ionic mechanism were to apply, counter-





ions (i. e.  $H^+$ ) must be adsorbed concurrently with the anions in order to account for the charge neutrality of the floated mineral and of the solution left behind. This, in effect, means that the ionic mechanism must involve "ion pair" adsorption. Sutherland<sup>4</sup> claims, however, that since the adsorption of a xanthate anion would be accomplished by an exchange mechanism, probably involving a hydroxyl ion, electroneutrality is insured. In any case, since the end products in the solution are the same for either free acid or ionic adsorption, normal analytical methods cannot distinguish between the two possibilities. Both schools of thought appear to have successfully correlated experimental data with the chemical equilibria equations describing the reaction<sup>2,4</sup>. However, the expressions for the chemical equilibria are basically dependent on the initial assumptions involved and they can therefore be criticized. An independent experimental procedure which would provide direct evidence of the types of bonds formed in xanthate adsorption is therefore very desirable.

Infrared spectroscopy can produce valuable information not only as to the existence or non-existence of a particular bond but also as to the extent to which the bonding is perturbed by its particular environment. In recent years infrared spectroscopy has shown great promise in the study of adsorption phenomena and it was felt that a spectroscopic investigation of xanthate adsorption was warranted. If, for example, a metal sulfur bond is formed in the adsorption process this should be detectable as a characteristic infrared absorption band. A study of changes of the C-O, C=S and C-S groups, when the xanthate molecule is adsorbed, may also provide information concerning their perturbations or contributions to the adsorption process. Eyring and Wadsworth<sup>5</sup>, in studying the adsorption



of n-Hexanethiol on zinc minerals by infrared spectroscopy, found that on ZnO and ZnS the hydroxyl concentration at the surface was decreased and invariably the S-H bond was destroyed. However no distinction could be made between neutral molecule adsorption and ion pair adsorption. The results from the adsorption studies of hexanethiol on willemite ( $\text{Zn}_2\text{SiO}_4$ ) can, however, be explained only by neutral molecule (or ion pair) adsorption and not by hydroxyl ion competition, since the latter was incompatible with their observations. The potential of infrared spectroscopy in adsorption studies on minerals is well illustrated by the above work of Eyring and Wadsworth. Ultimately the combination of spectroscopy, controlled kinetic investigations and other techniques, should provide an answer to the nature of xanthate adsorption by sulfide minerals.

Very few infrared spectroscopic data pertaining to xanthate type compounds are available, therefore the first stage in this investigation consisted of a spectral study of these molecules in the solid and solution states. In this regard a paper is being published by Little, Poling and Leja<sup>6</sup> presenting some absorption band assignments. Since the submission of this paper, additional work on absorption band assignments has been conducted. The purpose of this work was to further confirm the C=S absorption band assignment presented in the paper and also to provide assignments distinguishing between the two C-O stretching modes in xanthates.

Before attempting a spectroscopic study of the adsorption of xanthate onto sulfide minerals it was also necessary to investigate the nature of the mineral surface. Galena was chosen as the substrate for detailed study because of its comparative transparency to infrared radiation. The oxidation state of the surface of galena had been intensively studied



using electron diffraction techniques,<sup>22, 45</sup> but no infrared spectroscopic data were available. Therefore a spectral study of both natural and evaporated galena films has been conducted. Although this investigation is as yet incomplete, tentative conclusions have been reached on the nature of the surface oxidation state of this compound.

A spectroscopic investigation of xanthate adsorption employing an auxiliary reflection attachment with the spectrophotometer has been initiated. Preliminary data for the adsorption of potassium xanthate onto galena, both from acetone and aqueous solutions, are reported. Additional accessories to the reflectance attachment will be constructed in the future to permit preparation, treatment and recording of the spectra to be accomplished under either a vacuum or a controlled atmosphere.





# I N F R A R E D   S P E C T R O S C O P Y

## I. THEORY OF INFRARED SPECTROSCOPY

### A. General Remarks

Spectroscopy deals with interactions between electromagnetic radiation and matter in which energy is either abstracted (absorbed) or added to the radiation field (emission by the matter). The infrared spectral region of the electromagnetic spectrum holds special interest in the study of molecular interactions since this radiation promotes molecular transitions between rotational and vibrational energy levels of the ground energy state. As implied by the name, the infrared spectral region covers the wavelength range above that of red in the visible spectrum, ( $\lambda$ , wavelength =  $1\mu$ ) and merges with the microwave region near 1000 microns wavelength. Since electromagnetic radiation is quantized, the energy of a single quantum (photon) is given by the expression:

$$E = h\nu$$

where:  $h$  = Planck's constant,

$$6.624 \times 10^{-27} \text{ erg. sec.}$$

$\nu$  = the frequency of the radiation,  $\text{sec}^{-1}$ .

A more convenient unit for the infrared spectral region is the "wavenumber" -  $\nu'$  defined as:

$$\frac{\nu}{c} = \text{the number of waves per centimeter}$$

where:  $c$  is the velocity of the radiation,

$$2.99776 \times 10^{10} \text{ cm sec}^{-1}.$$

Also since  $\lambda \cdot \nu = c$

$$\nu' = \frac{10^4}{\lambda}$$





where:  $\lambda$  is the wavelength in microns.

Thus the energies of the infrared quanta are generally given in  $\text{cm}^{-1}$  (wavenumbers). This energy unit is converted into ergs on multiplying by  $hc$ . The following chart (Fig. 1) shows the infrared spectral region with energy equivalents.

$\lambda =$	$1 \mu$	$10 \mu$	$1000 \mu$
$\nu =$	$10,000 \text{ cm}^{-1}$	$1000 \text{ cm}^{-1}$	$10 \text{ cm}^{-1}$
VISIBLE	NEAR I. R.	FAR I. R.	MICRO WAVE
Energy:			
ergs per single quantum =	$1.9856 \times 10^{-12}$	$1.9856 \times 10^{-13}$	$1.9856 \times 10^{-15}$
kcal per N quanta =	$2.858 \times 10$	2.8586	$2.8586 \times 10^{-2}$
(N = Avogadro's number, $6.023 \times 10^{23} \text{ mole}^{-1}$ )			

Fig. 1 The Infrared Spectral Region

Molecular absorption spectroscopy deals with photon energies between 0 and 200 kcal per mole. Since chemical reactions generally involve 10 - 300 kcal/mole, irradiation of matter with photons of energy greater than  $10^5 \text{ cm}^{-1}$  ( $\lambda = 1/10 \mu$ ) leads either to dissociation of the molecule or scattering of the radiation.



## B. Classical Infrared Theory

Even though the very nature of spectroscopy makes us realize that the energies of molecules and atoms can only be changed in definite steps and cannot therefore be governed by Newtonian, "mechanical", laws, the classical approach is very useful in that it is more easily visualized. For example, we can construct a molecular model from balls proportional in weight to the respective atomic weights involved and make the spring strengths proportional to the bond strengths. If we suspend the model and strike it a blow -- the balls will be seen to vibrate with definite frequencies when viewed with a stroboscopic light. If the molecule contains  $N$  atoms, it possesses  $3N$  degrees of freedom. Any free non-linear molecule possesses 3 degrees of translational freedom, 3 of rotational freedom and  $3N-6$  degrees of vibrational freedom (linear molecule =  $3N-5$ ). Normally, molecules in the solid and liquid phases possess no rotational motion.

In classical electromagnetic theory emission and absorption of radiation are associated with periodic changes of space position and/or magnitude of an electric dipole. If the frequency of the periodic motion is  $\nu_m$ , the frequency of the radiation is also  $\nu_m$ . It is, therefore, natural to suppose that only those vibrations that cause a change of the dipole moment of the molecule will be infrared active, i.e. show absorption in the infrared region. (This is the classical equivalent of the quantum mechanical selection rules governing transition probabilities - see p. 12). Dipole moment changes can be illustrated by considering a 3-atom molecule such as  $\text{CO}_2$  (neglecting for the moment the fact that it is degenerate).

Since  $N = 3$ , the molecule should have  $3N-6=3$  normal vibrations, as shown in Figure 2.



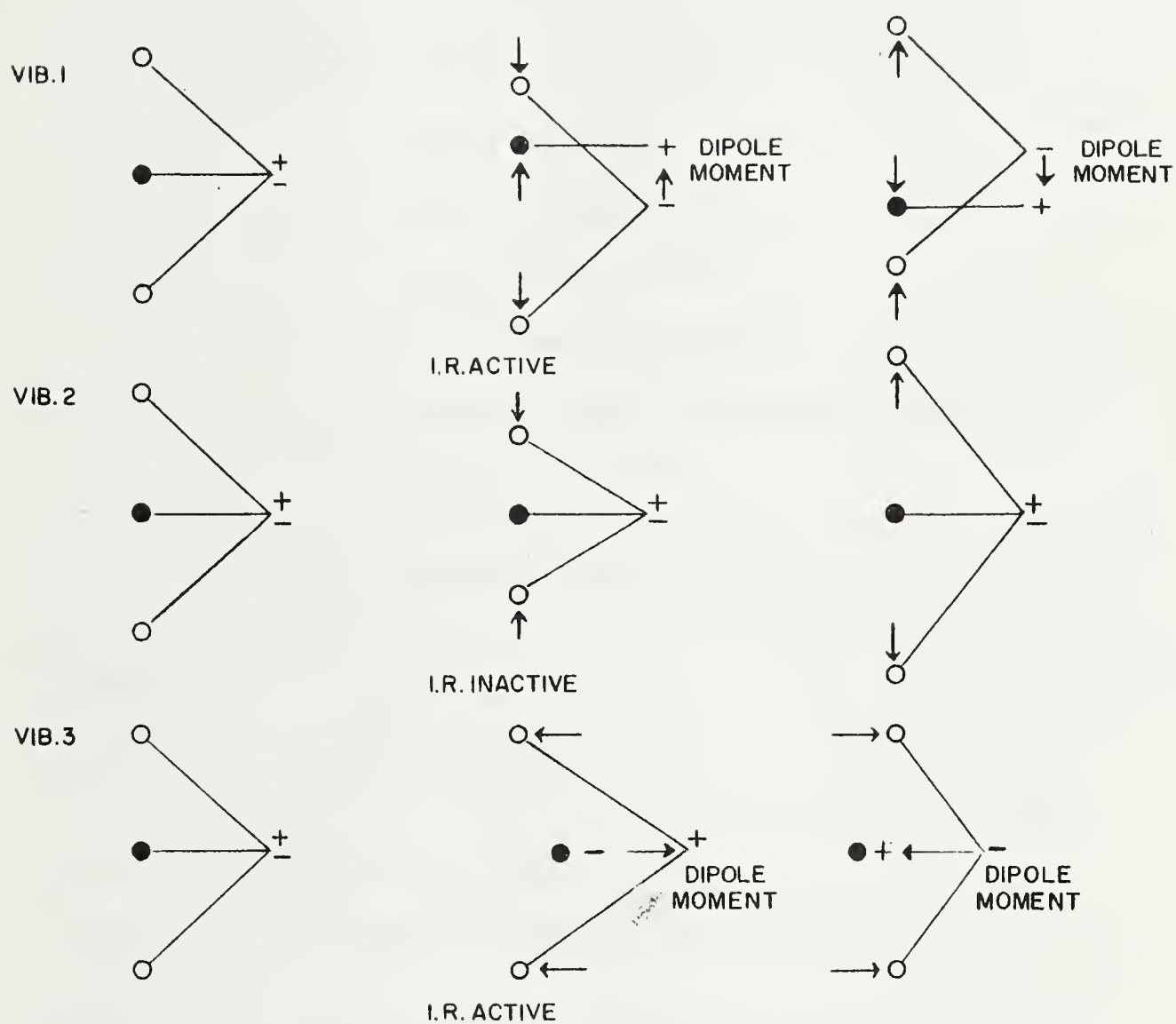


Fig. 2 Characteristic Vibrations of a Triatomic Molecule



If we consider these vibrations to be simple harmonic (which is, in fact, a good approximation) then their vibrational frequencies can be derived as follows:

For a diatomic molecule: (masses  $m_1$  and  $m_2$ )

$$-\frac{\partial V}{\partial r} = -k(r-r_e) = \frac{\mu_m \partial^2 r}{\partial t^2} = \frac{\mu_m \partial^2 (r-r_e)}{\partial t^2}$$

= valence restoring force

= mass x acceleration

where:  $V$  = the potential energy  
 $r$  = the interatomic distance  
 $r_e$  = the equilibrium interatomic distance  
 $k$  = the force constant

$$\mu_m = \text{reduced mass} = \frac{m_1 m_2}{m_1 + m_2}$$

Setting:  $(r-r_e) = x$

$$kx = -\frac{\mu_m \partial^2 x}{\partial t^2}$$

Since  $x = A \sin 2\pi \nu_m t$

where:  $\nu_m$  is the frequency of the vibration,

then  $-\frac{kx}{\mu_m} = \frac{\partial^2 x}{\partial t^2} = -4\pi^2 \nu_m^2 \cdot A \sin 2\pi \nu_m t$

$$\therefore \nu_m = \frac{1}{2\pi} \sqrt{\frac{k}{\mu_m}} \quad \therefore \nu' = \frac{1}{2\pi c} \sqrt{\frac{k}{\mu_m}}$$

If a molecule contains more than 2 atoms, there arise interactions between all the atoms comprising the molecule; the mathematical derivation of their normal vibration frequencies becomes then very com-





plicated. The complicated motion of the system can, however, always be described by a superposition of the  $3N-6$  normal vibrations.

### C. Quantum Mechanical Infrared Theory

If radiation is either emitted or absorbed by a molecule, that molecule is capable of existence in two stationary states  $E_1$  and  $E_2$ , separated by an energy difference  $\Delta E = E_2 - E_1$  such that, according to the Bohr frequency relation:

$$\Delta E = h\nu$$

Molecules in the gas phase possess translational, rotational and vibrational energies, which are quantized, i.e. can assume only discrete energy values. Radiation is absorbed if a molecule moves from a lower to a higher energy level. The spacing of the translational energy levels is sufficiently small that continuous spectral activity results. The Heisenberg uncertainty principle shows that the indeterminacy involved is more than sufficient to "blur" the system of discrete energy levels. This indeterminacy is vanishingly small however when considering the rotational and vibrational energy levels of gases.

A solution of the Schrödinger wave equation for a diatomic molecule<sup>7</sup> gives values of the rotational and vibrational energy levels of the molecule, viz.,

#### (1) Rotational

$$E_{\text{rot}} = \frac{h^2}{8\pi^2 I} J(J+1)$$

where  $I$  = the moment of inertia of the molecule

$$I = \left( \sum m_i r_i^2 \right); m = \text{mass of atom } i$$



$r$  = distance from molecular center of mass to atom  $i$

$J$  = the rotational quantum number = 0, 1, 2, 3, ...

A rotational transition from  $J = 1$  to  $J = 2$  yields therefore:

$$E_{\text{rot}} = \frac{h^2}{8\pi^2 I} (6-2) = \frac{h^2}{2\pi^2 I} = h\nu$$

$$\therefore \nu' = \frac{\nu}{c} = \frac{h}{2\pi^2 c I} \text{ cm}^{-1}$$

Changes in molecular rotational energies generally occur in the far infrared and in the microwave spectral regions.

## (2) Vibrational

$$E_{\text{vib}} = \frac{h}{2\pi} \sqrt{\frac{k}{\mu_m}} \left(n + \frac{1}{2}\right)$$

where  $\mu_m$  = reduced mass

$k$  = force constant

$n$  = vibrational quantum number = 0, 1, 2, 3, ...

Note that even for  $n = 0$  there remains a finite vibrational energy in the molecule; the so-called "zero point energy".

A vibrational transition from  $n = 0 \rightarrow 1$  yields

$$\Delta E_{\text{vib}} = \frac{h}{2\pi} \sqrt{\frac{k}{\mu_m}} = h \nu_{\text{abs.}}$$

Hence

$$\nu' = \frac{1}{2\pi c} \sqrt{\frac{k}{\mu_m}} \text{ cm}^{-1}$$

For example:

$$\text{HCl: } \mu_m \stackrel{a}{=} 1.6 \times 10^{-24} \text{ gms.}$$

$$\text{HCl: } k \stackrel{a}{=} 5 \times 10^5 \text{ dynes/cm.}$$

$$\therefore \nu' = 3000 \text{ cm}^{-1} \text{ (calculated)}$$

$$\nu' = 2885 \text{ cm}^{-1} \text{ (observed in gas phase).}$$



Note that a vibrational transition from  $n=0$  to  $n=1$  yields the same formula for the vibrational frequency as that derived previously using classical theory.

In the gas phase, vibrational transitions are normally accompanied by the exchange of smaller rotational energy quanta during an absorption process. This is illustrated below:

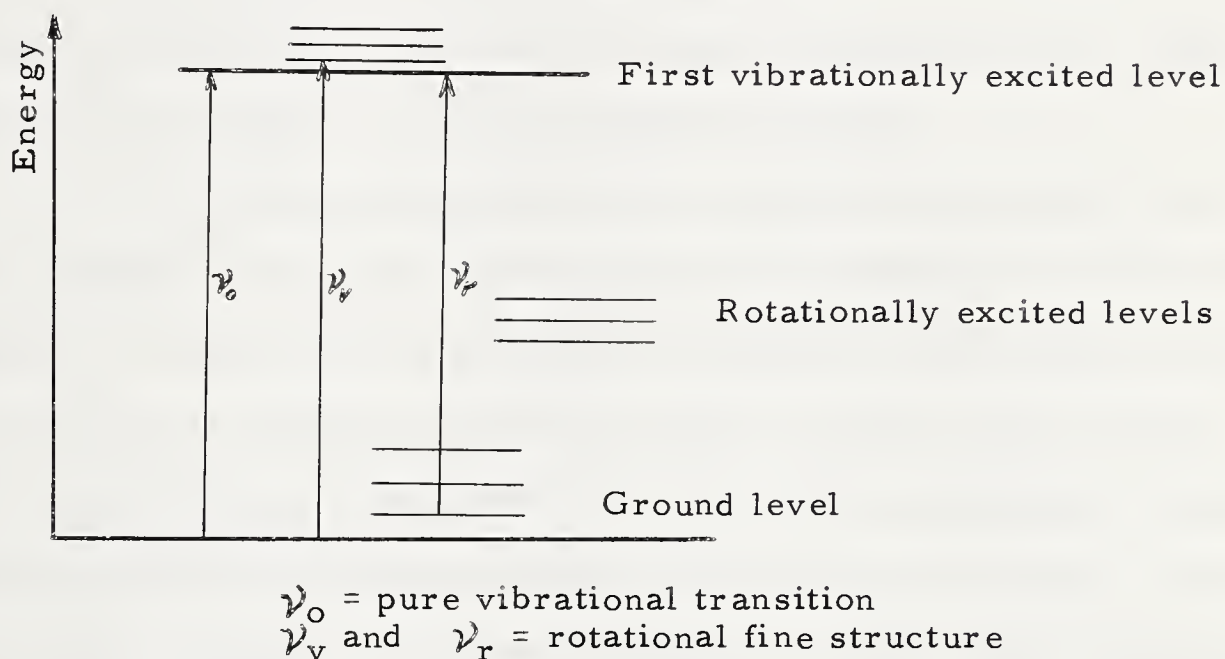


Fig. 3 Infrared Vibration - Rotation Transitions

Selection Rules: The classical concept of the change in dipole moment required for radiation to be absorbed or emitted is analogous to quantum mechanical selection rules governing transition probabilities. The intensity of a spectral absorption line or band is determined by the probability of the transition which gives rise to the line.

If we consider a spontaneous transition from state  $n_1$  to  $n_2$  with the absorption of light of frequency  $\nu_{n_1, n_2} = \frac{E_2 - E_1}{h}$ , the probability ( $A_{n_1 n_2}$ ) of such a transition is expressed by <sup>7</sup>:





$$A_{n_1 n_2} = \frac{64 \pi^2 \nu^3}{3 h c^3} \left[ \mu_x^2_{n_1 n_2} + \mu_y^2_{n_1 n_2} + \mu_z^2_{n_1 n_2} \right]$$

where:  $\mu_{x n_1 n_2} = \int \psi_{n_1}^* \mu_x \psi_{n_2} d\tau$  is a quantum mechanical exchange integral or an expression of the component of the electric moment of the system.

If  $\mu_x$ ,  $\mu_y$  and  $\mu_z$  are all zero for a given transition  $n_1$  to  $n_2$ , that transition will not give rise to absorption of radiation.

The observed absorption band intensities are usually lower than those predicted by the above formula due to the phenomenon of "induced emission". When matter is subjected to radiation, and absorbs some of this radiation, transitions occur from lower to higher energy states. These higher energy states are not the most stable configurations and the state may revert to the ground level by the emission of radiation. Since this emitted radiation is of the same frequency as the incident radiation, it is said to be coherent with it and thus reduces the absorption of radiation by the sample. For this reason visible and ultraviolet spectroscopes are nearly 100 times as efficient as microwave instruments where the induced emission reduces the net absorption to about 1%.

#### D. Vibrations of Complex Molecules

An infrared spectrum of a molecule consists not only of the strongly absorbing fundamental transitions but "overtone" and combination vibrations also occur. For example, if the fundamental vibrations of a molecule produce absorption bands at  $\nu_1$  and  $\nu_2$ , subject to selection rules, weaker "overtone" bands may also occur at  $2 \nu_1$ ,  $3 \nu_1$ ,  $4 \nu_1$ ;





2  $\nu_2$ , 3  $\nu_2$ , 4  $\nu_2$ , etc. The "combination" bands  $\nu_1 + \nu_2$  and  $\nu_1 - \nu_2$  may also occur. If the oscillations are considered to be perfectly harmonic then only fundamental vibrations will occur; however if, as is always the case, the oscillations are slightly anharmonic, overtone and combination bands will occur. Further complications arise when two vibrational levels (bands) in a polyatomic molecule "happen" to have nearly the same energy level, i.e. they are said to be "accidentally degenerate". Such a resonance (Fermi resonance) leads to a perturbation of these energy levels and they repel each other resulting in a shift of one band to higher, and the other band to lower, frequencies. Any alteration of the molecular structure disturbs the fundamental vibrational modes and the entire spectrum may change. Because of this fact, the vibrational spectrum of an organic compound has been singled out as the most characteristic of all the physical properties of that compound.

Specific Group Frequencies: Certain atomic groups give rise to vibration bands at nearly the same frequencies regardless of their environments. Such bands can be used to characterize an absorbing group. N.B. Colthup<sup>8</sup> has published a fairly complete set of Spectra-Structure correlation charts in which he gives the general positional range of various absorbing groups. For example the C-H stretching band is found from 3300 - 2700  $\text{cm}^{-1}$ , and the C=O stretching band is found from 1800 - 1600  $\text{cm}^{-1}$ .

Bond vibrational modes are divided into two distinct types, i.e. stretching or bending (sometimes called deformation) vibrations. The stretching force constant of an A-B vibration is about ten times as large as the deformation constant. Thus, for example, the O-H stretching frequency in  $\text{H}_2\text{O}$  is at 3650  $\text{cm}^{-1}$  while the O-H deformation frequency is



around  $1600\text{ cm}^{-1}$ . In general, multiple bonds (i.e. C=S, C=C, etc.) and R-H (stretching) bonds (where R is any atom) are least affected by internal structural changes, but they are more susceptible to external environmental changes. The exception to this is the case of intramolecular hydrogen bonding. Single bond stretching vibrations between atoms of the same or similar mass are markedly influenced by internal structural changes (i.e. C-O).

Effects of Changes in State: Vibrational spectra can be studied in gaseous, liquid and solid states, and pronounced changes may occur in the spectrum of a compound in each state. Molecules studied in the gaseous phase can be regarded as being free from the influence of other molecules. Gas molecules can undergo translational, rotational and vibrational transitions. Many molecules, however, cannot be studied in the vapor state, because they either readily decompose on heating or they do not have sufficient vapor pressure.

Liquids: The infrared spectra of liquids are very different from gaseous spectra in that the vibrating molecules are surrounded by other molecules which may alter their frequency and/or intensity by either changing the dielectric constant of the medium or by molecular association. Molecular association may take the form of hydrogen bonding which results in the weakening of the intramolecular bonds involved with consequent frequency shifts and band intensity changes. Hydrogen bonding involving O-H groups causes the largest frequency shifts (up to  $500\text{ cm}^{-1}$ ) with lesser ones involving N-H, S-H and P-H groups. Intramolecular hydrogen bonding, intermolecular hydrogen bonding and chelation (very strong intramolecular hydrogen bonding), can be distinguished by infrared spectroscopy. The O-H





stretching frequencies of intramolecular hydrogen bonded substances are independent of dilution, whereas dilution in a non-polar solvent affects the frequencies of an intermolecular hydrogen bonded O-H compound due to a sharp reduction in the extent of this bonding. Intramolecular hydrogen bonds produce sharp absorption bands since they are confined to single molecules. Intermolecular hydrogen bonding between two molecules (dimeric) also yields sharp absorption bands, whereas that between several molecules (polymeric) results in broad absorption bands.

Another form of molecular association is dipole-dipole interaction which may cause the formation of loose chain linkages due to the electrostatic forces which in turn induce additional charge effects and can thus increase the overall polarity of a specific group.

As a general rule, molecular associations lead to lower stretching frequencies and higher deformation frequencies. In pure liquids or solutions, rotational isomerism (total or partial rotation about single bonds) may cause broadening of a vibrational absorption band since each configuration of the molecule will be associated with a slightly different vibrational frequency.

Solids: Frequency shifts due to a change from the liquid to the solid state are generally small and are caused by a further increase in the intermolecular forces. The relationship between the structure and the vibrational spectrum of a solid must be based on the unit cell of the material and not on a single molecule. This relationship becomes more pronounced, the more polar is the compound. Due to the increased order in the crystalline state (orientation) certain bands may disappear from the spectrum, particularly those associated with rotational isomerism. New bands may





also appear due either to lattice absorptions or "in phase -- out of phase" vibrations of the same group in two different molecules which causes splitting of a single band into two.

The orientation of molecules in studying a single crystal or an oriented film can exert a pronounced effect on the infrared spectrum. If the direction of the electric vector associated with a localized group is approximately parallel to the radiation beam, the absorption band associated with this group will be weak if not entirely absent. Thus the use of polarized radiation can aid in the elucidation of oriented molecular structures. When solids are examined in the form of alkali halide pressed discs (to reduce loss of radiation by scattering) spectral changes may occur due to interactions between vibrations of the sample and the alkali halide lattice.

Anomalous dispersion may occur in the spectra of crystalline solids when either the refractive index of the solid substance becomes 1.0 or it becomes equal to the refractive index of the dispersive medium. This phenomenon is called the "Christiansen Effect".<sup>9</sup>

Solvent Effects: Solvent association may occur as a general orientation of its molecules around the whole solute molecule or it may be limited to one particular group. Non-polar solvents such as  $\text{CS}_2$  and  $\text{CCl}_4$  (which have high molecular transparency due to their molecular symmetry) have a minimum influence on the vibrations of solute molecules. Polar solvents may exercise a selective effect on certain absorption bands, particularly the  $\text{C}=\text{O}$ ,  $\text{N}-\text{H}$  and  $\text{O}-\text{H}$  stretching vibrations. Attempts have been made to correlate solvent shifts with dielectric constants or refractive indices and while most non-polar solvents obey this relationship, many



polar solvents do not. As yet no entirely satisfactory theoretical solution to the problem of solute-solvent interactions is available. However, an empirical treatment of the effects of various solvents on observed frequency shifts can yield valuable information, with selected vibrational groups, as to the physical properties of individual groups comprising the molecule under study. For example, the linear shift of the C=O band to lower frequencies, established on examination of the material in a sequence of solvents (generally ranging from non-polar to strongly polar solvents) can be used in identification of this vibrational mode.<sup>10</sup>

Mass and Coupling Effects: The probable effects of mass changes in a molecule, either by substitution or simply by additions which do not involve coupled vibrations, can be predicted from basic theory (i. e.  $\nu'_m \propto \sqrt{\frac{1}{\mu_m}}$ ). The vibrations which are least sensitive to mass changes are thus R-H stretching and deformation modes since here the hydrogen atom undergoes most of the vibrational motion. One approach which is often useful in R-H substitutional work is to deuterate the compound giving an R-D frequency  $\sim \frac{1}{\sqrt{2}} \nu'_{(R-H)}$ . Single bond vibrations which do not involve hydrogen are very sensitive to mass and coupling effects. For example, the C-O stretching vibration occurs over a very wide frequency region (1350 to 890  $\text{cm}^{-1}$ ) but can be recognized within limited environments. Table 1 shows the general assignment of the most intense band attributed to the C-O stretching modes in various compounds.



Table 1.C-O Stretching Frequencies in Various Compounds<sup>11</sup>

Type of Compound	C-O Band cm <sup>-1</sup>
Alkyl ethers . . . . .	1150 - 1060
Alcohols . . . . .	1140 - 1010
Hemi-acetals . . . . .	1150 - 1020
Carboxylic acids . . . . .	1320 - 1210
Aryl ethers . . . . .	1270 - 1230
Esters . . . . .	1245 - 1185
Carbonates . . . . .	1280 - 1250

Vibrational coupling occurs when two groups having the same symmetry and vibrating with nearly the same frequencies are in close proximity. When this occurs, an extremely strong interaction results which causes wide separation of the symmetrical and asymmetrical frequencies. For example, in sulphones, sulphates, etc. the symmetrical and asymmetrical frequencies of the  $\text{-SO}_2$  - group are generally about 150 to 200 cm<sup>-1</sup> apart.

E. Spectral Presentation

There are many variations as to the units employed in graphical representations of infrared spectra. In recording band positions both wavelength ( $\lambda$  in microns) and wavenumbers ( $\nu$  in cm<sup>-1</sup>) are in common use. In the study of molecular structures the use of frequency





units offers decided advantages over the wavelength units in that the former presents a linear energy scale, permits a direct comparison of Raman and infrared data (since Raman data have always been presented in  $\text{cm}^{-1}$  units) and, most important, the integrated absorption intensities (areas under the curves) can be directly related to dipole moment changes that occur during the vibration. The recognition of overtone and combination bands also becomes much easier when dealing with wavenumber units.

Absorption and Transmission Units: If a beam of monochromatic radiation is passed through a sample, and some absorption by the sample occurs, then the percentage transmittance can be expressed as  $100 \times \frac{I}{I_0}$ , where  $I$  is the intensity of the transmitted radiation and  $I_0$  that of the incident radiation. Most spectrophotometers have the pen movement calibrated in percentage transmittance units. When spectra are plotted on a percentage transmittance scale the regions of high absorption appear as minima.

Other units in common use are: percentage absorption =  $\frac{100 (I_0 - I)}{I_0}$  and optical density or absorbance =  $\log_{10} \left( \frac{I_0}{I} \right)$ . The quantity  $\log_e \left( \frac{I_0}{I} \right)$  may also be encountered, particularly in computations of integrated absorption intensities. Optical density units are preferred since absorption plotted on this scale is directly proportional to the amount of absorbing material in the beam. Spectral chart paper is available with a logarithmic ordinate scale which permits direct readings of absorbance.





Absorption Band Intensities: A fundamental law governing the absorption of monochromatic radiation by a solution is:

$$I = I_0 10^{-kcl} \quad \text{or} \quad kcl = \log_{10} \left( \frac{I_0}{I} \right)$$

= Optical density

where  $k$  = extinction coefficient (absorptivity)

$c$  = concentration of substance in g/l

$l$  = sample thickness in cm.

If the concentration  $c$  is given in g moles/liter the symbol  $k$  is replaced by  $\epsilon$  and is called the "molar extinction coefficient".

$$\text{i.e.} \quad \epsilon = \frac{I}{cI} \log_{10} \left( \frac{I_0}{I} \right)$$

$\epsilon$  generally 1 - 1500

The above relationships are generally referred to as "Beer's Law", however, they are actually a combination of Beer's and Lambert's Laws. Strong<sup>12</sup> has discussed the theories behind these relationships.

The values  $\epsilon_{\max}$  or  $k_{\max}$  may be used to characterize the order of magnitude of a band intensity. The determination of the integrated absorption intensity ( $A$ ) is, however, of greater theoretical significance and is nearly independent of the instrument's "slit width".

$$A = 2.303 \int \epsilon d\nu \quad \text{or} \quad A = 2.303 \int k d\nu$$

depending on the concentration units used.

In addition, it is also convenient to have a recognized measure of the breadth of an absorption band. The half band width ( $\frac{\Delta\nu_1}{2}$ ) serves such a purpose and is measured where the band intensity is equal to 0.5

$\epsilon_{\max}$  or  $0.5 k_{\max}$  (see Fig. 4).



The above relationships apply to strictly monochromatic radiation, however, in a spectrometer this is never achieved since, due to the finite slit width, there is a distribution of spectral energy which is "seen" by the instrument's detector. The energy distribution can be represented by a triangular function such as that shown in Fig. 5.

The "spectral slit width"  $S$  represents the separation of two monochromatic lines such that they just fail to be resolved; it can be calculated upon knowing the instrument data.<sup>13</sup>

Due to a finite slit width, the extinction coefficients and absorption intensities are generally termed "apparent", to emphasize the deviation from ideality.

Several attempts have been made to derive empirical equations to fit the envelopes of infra red absorption bands. Most are slight modifications of the Lorentz function<sup>14</sup>, given by Ramsay<sup>15</sup> as:

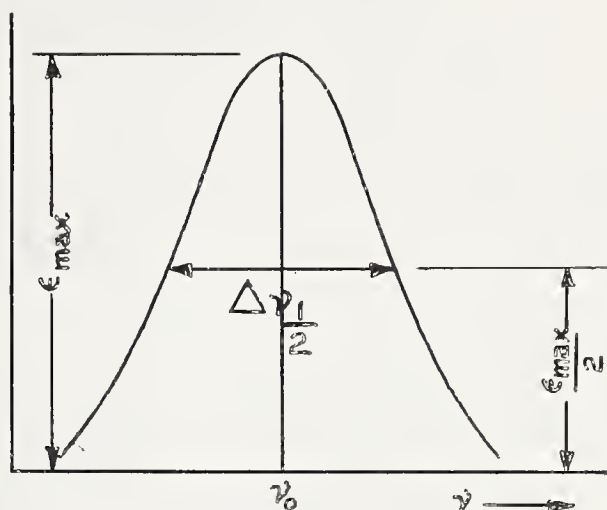


Fig. 4 Half Width of an Absorption Band

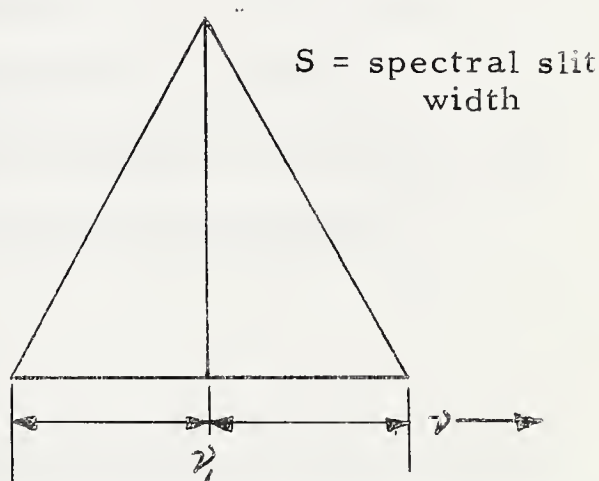


Fig. 5 Spectral Energy Distribution Function



$$\log_e \left( \frac{I_0}{I} \right) = \frac{a}{\left( (\nu - \nu_0)^2 + b^2 \right)}$$

where:  $a$  and  $b$  are constants.

$$\frac{a}{b^2} = \log_e \left( \frac{I_0}{I} \right)_{\max}$$

$$2b = \Delta \nu_{\frac{1}{2}}$$

whence the integrated area (A) becomes

$$A = \frac{\pi}{2} \Delta \nu_{\frac{1}{2}} \log_e \left( \frac{I_0}{I} \right)_{\max}$$

For single, isolated absorption bands this provides the simplest method of computing true integrated absorption intensities from absorption curves.

Integrated intensity measurements are coming into increased use in studies of molecular structure since intensity comparisons with other infrared bands in the same spectrum can be misleading.

#### F. Molecular Structure Determinations

Most vibrational group frequencies occur within a limited range and spectra-structure correlation charts are available to aid in the assignments of particular frequencies<sup>8</sup>. However, a vibrational group containing similar atoms (i.e. C-O stretching, C=S stretching etc.) may give rise to bands spread over a wide frequency range in various compounds, thereby necessitating specific assignments to these modes within each of the specified structural groups. The assignments are generally carried out by the method of substitution of an atom or group which may be similar in behaviour but has a different mass. Care must be taken that the compound being studied is as pure as possible, so that accurate chemical





analysis must accompany any infrared frequency assignment data.

The use of polarized radiation can also aid in structural determinations of crystals or oriented films. Unintentional partial polarization occurs as a result of reflections of the radiation from the many mirrors in all spectrometers and, in the absence of intentional polarization, this may cause confusion.

The measurements of integrated absorption band intensities (described under "Spectral Presentation") can be very significant in studying the changes occurring in a molecular structure in the transfer from a solvated state to an adsorbed state where, for example, frequency shifts may or may not be significant.





## II. INFRARED INSTRUMENTATION

### A. Description of Instrument

Infrared spectrophotometers contain three components basic in the construction of all spectrographs. These are: a source of radiation yielding a continuous spectrum, a dispersive element to enable selection of a narrow frequency range, and a detector which measures the energy in this band of radiation. There are many varieties of spectrographs embodying these basic features. The double beam type described below is the most common:

A Perkin-Elmer 221-G Spectrophotometer was employed in the spectral measurements to be described later. This instrument is a double beam automatic recording spectrophotometer which utilizes a servo-driven attenuator to produce a true radiation null at the detector. The optical schematic of the instrument is shown in Figure 6.

The source of radiation consists of a Nernst filament (a mixture of sintered cesium and thorium oxides) which is electrically heated to  $\pm 1500^{\circ}\text{C}$  and produces a continuous spectrum of infrared radiation. The maximum energy from the Nernst glower occurs at about  $7000\text{ cm}^{-1}$  and falls to nearly  $\frac{1}{1000}$  of this value at  $600\text{ cm}^{-1}$ . This is particularly significant in the low frequency region ( $1000 - 300\text{ cm}^{-1}$ ) since here the source energy is extremely low.

Radiation from the source is split into two beams of equal intensity (i. e. reference beam and sample beam). After passing through the sampling area the radiation beams are chopped by a 13 cps hemispherical chopper mirror  $M_7$  which lets the detector alternately "see" the reference beam energy and the sample beam energy.







The chopped beam then enters the monochrometer section through the entrance slits  $S_1$  and is collimated by a paraboloid mirror  $M_{11}$  before reaching the dispersive element, the prism.

The prism is cut from a single crystal of sodium chloride which possesses good transmission and dispersive qualities in the "normal" infrared spectral region of  $5000 - 650 \text{ cm}^{-1}$ . For lower frequencies cesium bromide prisms are available which enable the region from  $700 - 250 \text{ cm}^{-1}$  to be studied.

The radiation is refracted through the prism onto a Littrow mirror,  $M_{12}$ , (or grating - for added dispersion, as is the case of the PE-221-G) and back through the prism again before entering the detector section through the exit slits,  $S_2$ , and being focused on a high sensitivity thermocouple detector. The scanning of the spectrum is accomplished by the movement of the Littrow mirror which is hinged at one end.

The instrument operates on a "null" principle. If, for example, the sample is placed in the sample beam of the instrument and at a certain frequency it absorbs energy, then the detector produces a 13 cps voltage. This voltage is fed to an amplification circuit which in turn supplies energy to a motor that moves the optical attenuator wedge into the reference beam until no ac signal is produced at the detector. The attenuator is made in such a way that its linear movement in the reference beam is linear with respect to the percentage transmittance. The movement of the attenuator wedge thus records the percent transmittance of energy through the sample.

The double beam principle of the spectrophotometer has many advantages over a single beam instrument in that:





1. atmospheric absorption bands are cancelled out;
2. variations in source radiation are automatically compensated;
3. undesirable solvent absorption bands can be compensated in differential spectra.

Some of the special features of the instrument which made it suitable for molecular structural studies are:

1. The instrument employs a prism-grating combination as a dispersive element from 4000 - 1430  $\text{cm}^{-1}$ . This feature allows an optimum resolution of  $\sim 1.5 \text{ cm}^{-1}$  over this region. The grating serves as a Littrow mirror from 1430 - 650  $\text{cm}^{-1}$ , in the region where the NaCl prism alone has adequate dispersion.

2. The instrument is equipped with a readily interchangeable CsBr prism interchange which enables spectral surveys to be conducted to 250  $\text{cm}^{-1}$ .

3. A feature particularly suited for solvent-solute differential spectra is the automatic gain control. Over regions of high solvent absorption the pen amplifier gain is normally too low. With the use of the automatic gain control the pen servo-amplifier gain is automatically regulated according to solvent absorption in the reference beam.

4. Ordinate Scale Expansion is a particularly useful feature which increases the effective sensitivity of the instrument by 5, 10 or 20 times. This is important in solution spectra where the solute is only very slightly soluble or in cases where the concentration of absorbing groups in the beam is very small.



### B. Sensitivity Requirement of Instrument

In monomolecular adsorption studies, one difficult obstacle is to achieve the combination of high instrument sensitivity together with a large number of molecules in the beam. This is illustrated by the following simple calculation:

Under normal operating conditions an absorption band with an  $I/I_0$  value of 0.99 is detectable (1X Ordinate expansion). If we now employ the Beer-Lambert Law we can calculate the necessary number of absorbing groups in the beam to produce such a band:

$$\text{i. e.} \quad I = I_0 e^{-kc}$$

where  $c$  = the number of absorbing groups per  $\text{cm}^2$  of the beam's cross section

$k$  = the extinction coefficient expressed in  $\text{cm}^2$  per group.

If we consider the xanthate molecules adsorbing on a suitable solid adsorbent using an area, per xanthate molecule, of  $27\text{\AA}^2$  and assuming that there is one monolayer of xanthate groups on the adsorbent, then the number of groups per  $\text{cm}^2$  is:

$$\frac{1 \text{ cm}^2}{27\text{\AA}^2} = \frac{10^{16}}{27} = 3.7 \times 10^{14} \text{ group/cm}^2$$

Using an approximate figure of  $400 \frac{\text{cm}^2}{\text{mole}}$  for the molecular extinction coefficient for the C=S group (slightly less than for the normal C=O group) we find that the extinction coefficient expressed in  $\text{cm}^2/\text{group}$

$$k = \frac{400 \times 1000}{6.02 \times 10^{23}} = 0.7 \times 10^{-17} \text{ cm}^2/\text{group}.$$

Hence

$$\frac{I}{I_0} = e^{-0.7 \times 3.7 \times 10^{-3}}$$

$$\frac{I}{I_0} = .997 \text{ (Detectability limit} = 0.99)$$



This value of  $I/I_0$  is beyond the limit of detectability under normal instrument sensitivity conditions. However, if one can increase the surface area of the absorbent considerably beyond its geometrical surface area and in addition employ 10x or 20x ordinate scale expansion, it can readily be seen that a reasonable absorption band can be attained with a single monolayer of adsorbate. R.P. Eischens<sup>16</sup> and others have used high area oxide materials with a thickness of  $\approx 12$  mg/cm<sup>2</sup> and a specific area of approximately 200 m<sup>2</sup>/gm. In this way Eischens attains a very high surface area of adsorbent per cross sectional area of the beam of light traversing it, viz.,

$$\frac{200 \times 10^4 \times 12}{1000} = 2.4 \times 10^4 \frac{\text{cm}^2 \text{ surface area}}{\text{cm}^2 \text{ beam cross section}}$$

If reasonable transmission can be maintained, using such a high specific surface area material, the normal instrument sensitivity (i. e. 1X Ordinate scale) is sufficient to detect monolayer coverages.

Eischens<sup>17</sup> has also described infrared studies of adsorption on evaporated platinum films. He claims the film was quite porous in that its actual surface area was estimated to be ten times its geometrical area. By stacking several such films in the beam path, studies of gaseous carbon monoxide adsorption onto the platinum film revealed that bands of sufficient intensity were produced.



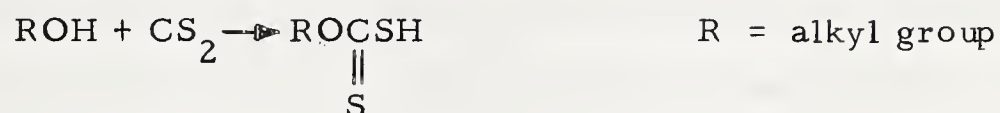


## EXPERIMENTAL PROCEDURES

## 1. MATERIALS

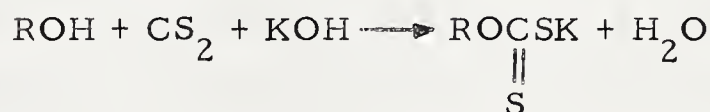
A. Preparation of Xanthates and Related Compounds

(a) Xanthates are salts of xanthic acids which themselves are products of reactions between carbon disulphide and alcohols, viz.;



Xanthic acids are very unstable and revert to the alcohol plus  $\text{CS}_2$ .

Metal Xanthates are normally made from saturated monohydric alcohols (i.e. ethyl, butyl, amyl, etc.) but they can also be produced from more complicated alcohols. Alkali salts of metal xanthates are made from an alkali alcoholate and carbon disulphide or an alkali hydroxide, an alcohol and carbon disulphide, viz.;



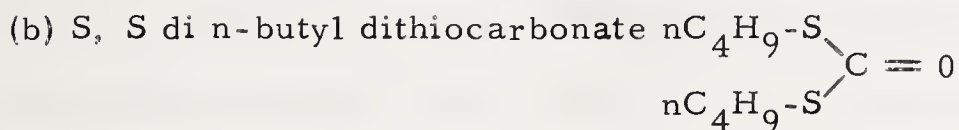
R here represents the hydrocarbon radical - either alkyl or aryl, etc. The alkali metal xanthates studied in this work were all prepared as described in the papers of Little and Leja<sup>18</sup> and Bulmer and Mann<sup>19</sup>. These xanthates after being thoroughly washed with diethyl ether to remove any of the xanthate oxidation product, dixanthogen, analyzed 99% + in purity. (See reprint of paper by Little, Poling and Leja<sup>6</sup> at back of thesis for complete analytical results.)

Heavy metal xanthates were precipitated by mixing solutions of AnalaR grade metal sulfates or chlorides with aqueous solutions of the alkali metal xanthates. Coprecipitation of dixanthogen occurs when preparing xanthates of metals with more than one valency (i.e.  $\text{Cu}^{++}$ ,  $\text{Cu}^+$ ,  $\text{Fe}^{+++}$





and  $\text{Fe}^{+++}$ ) which was then removed by ether washings. Spectroscopic and analytical data cited in the above-mentioned paper by Little, Poling and Leja confirm this.



a substitutional compound employed in the assignment of absorption bands was prepared by the method described by Bulmer and Mann<sup>19</sup>. The other two compounds used in the assignment of xanthate absorption band frequencies (S, S, didodecyl trithiocarbonate and O, S, di-octadecyl dithiocarbonate) were provided by B.D.H. - Poole Eng., and D.S.I.R., Warren Spring Lab., Stevenage, Herts., Eng.

The chloroformates and carbonates were commercial high purity reagents.

(c) Other Reagents. In the solution work most of the organic solvents were Eastman Kodak Spectral Grade but, where this grade was unavailable, reagent grade solvents were used.

All water used was fresh doubly distilled, with the second distillation from an all pyrex still. (No attempt was made to remove the dissolved oxygen from the water).

Other reagents used were of commercial high purity grade.

### B. Vacuum Evaporation Technique

An Edwards Model 6E vacuum coating unit was used both for the preparation of front-surface aluminum mirrors for accessory attachments to the spectrophotometer (see reflectance I.R. work) and also for the preparation of high area mineral samples for study in the infrared by transmission and reflection techniques.



The vacuum coating unit consists of a rotary pump - two stage oil diffusion pump combination providing a pumping speed of 8 litres/sec. and an ultimate vacuum of  $10^{-5}$  -  $10^{-6}$  mm Hg. The working chamber is a 6 inch diameter x 8 1/2 inch high bell jar which is sealed to the base plate with a rubber L ring. The unit is equipped with two voltage sources: one low tension filament source rated at 7.5 volts at 20 amperes continuous service or 30 amperes for durations of 1 minute, and a 1000 volt ac high tension source for ionic bombardment.

Evaporation of Aluminum: A tungsten wire filament bent in a zig-zag pattern was normally used for evaporating aluminum. Small aluminum strips were hung onto the filament after it had previously been cleaned by flashing under high vacuum. Since the molten aluminum wets the tungsten, drops of aluminum were formed at the lower apexes of the filament during evaporation.

The glass to be aluminized was first cleaned in a  $K_2CrO_4$  -  $H_2SO_4$  degreasing mixture, then dried and placed above the filament at a distance of approximately 6 cm. The glass substrate was then further cleaned by ionic bombardment (at 1000 v ac and 10 ma) for approximately 10 minutes prior to evaporation of the aluminum. A vacuum of approximately  $5 \times 10^{-5}$  to  $10^{-6}$  mm Hg was attained before the evaporation of the aluminum was begun. The aluminum was then evaporated very rapidly to produce an opaque, shiny mirror surface.

Evaporation of Minerals: One method employed in attempting to study the infrared spectra of xanthate monolayer adsorption onto sulfide minerals was the preparation of thin transparent films of the minerals by the evaporation technique. In addition to the transparency requirement



(which limits the film thickness) the films also had to have a high specific area. For transmission studies the sulfides were evaporated onto infrared transmitting windows (i. e. NaCl, AgCl,  $\text{CaF}_2$ , etc.)

In an attempt to meet the two requirements stated above, the evaporation onto the window was conducted at a very high incidence angle ( $\approx 80^\circ$ ) to promote "whisker" growth.<sup>20</sup> The window substrate was also cooled to dry ice temperature in an attempt to aid whisker growth by reducing the mobilities of the depositing molecules. Whiskers grown in such a manner were generally 200 - 1000 Å in diameter and oriented toward the evaporant source.

This preferred orientation of the whiskers was evident to the eye since, on viewing the sample from the side of the evaporation source, the deposit appeared sooty while from the opposite side it appeared somewhat shiny.

The minerals PbS, CuS and ZnS were prepared as precipitates by bubbling  $\text{H}_2\text{S}$  gas from a Kipp type generator through solutions of the soluble Pb, Cu and Zn salts respectively. The precipitates were carefully washed and dried before use.

Since these minerals do not wet filaments of tungsten, molybdenum or tantalum, they had to be evaporated from "boat" filaments (generally made from Mo or Ta foil). These minerals are difficult to evaporate since they tend to decrepitate on heating and much of the charge was spattered out of the filament.

The same general procedure was used to evaporate these minerals as was described for the evaporation of aluminum. The exception was that, when whisker growth was desired for transmission work, the







substrate was clamped to a hollow copper backing block which was filled with solid  $\text{CO}_2$  (with an escape vent to the outside of the working chamber). The backing block was tilted in the chamber so that the angle of incidence to the source was from 70-80 degrees.

Most of the studies were conducted on galena ( $\text{PbS}$ ), both with transmission and reflection samples, since it proved to be the most transparent of the three above sulfides in the spectral region of interest. Reflection studies of galena were made by evaporating  $\text{PbS}$  perpendicularly onto a front surface aluminum mirror (prepared as previously described). The  $\text{PbS}$  films deposited in such a manner formed a very thin (approximately  $0.1 \mu$  thick) mirror-like film adjacent to the aluminum substrate with a sooty appearing deposit (whiskers) on top of this. The thickness of the sooty deposit was of the order of 1 micron<sup>21</sup>. H. Wilman<sup>22</sup> has shown by electron microscopy that galena films evaporated in such a way have an average crystallite size (diameter) of from 150 to 500  $\text{\AA}$  and possess a marked degree of crystal orientation with the 001 face parallel to the substrate.

When considering the properties of evaporated films one must always be aware of the influence of residual gases in the evaporation chamber. For example, if the residual oxygen pressure remained at about  $10^{-5}$  mm Hg, it can be shown by a calculation based on kinetic theory that there is sufficient oxygen to form a monomolecular coverage in about one second if every atom striking the sample adsorbs.<sup>23</sup> The significance of this aspect is further exemplified by the fact that coherent aluminum films cannot be evaporated using a mercury diffusion pump, with a solid carbon dioxide and acetone trap, due to the attack of aluminum by mercury. At



the trapping temperature ( $-78^{\circ}\text{C}$ ) the vapor pressure of mercury is only  $3 \times 10^{-9}$  mm Hg. Since the exclusion of residual gases below a certain limit (that has no effect on the film) is impossible, one must be very cautious when citing "purity" in evaporated films. The nature of the substrate will be considered further in the discussion.

## II. INFRA RED SPECTROSCOPIC PROCEDURES

All spectra discussed in this thesis were recorded on a Perkin Elmer 221-G Spectrophotometer using a NaCl prism - grating interchange. Some of the work described in the publication by Little, Poling & Leja (Can. J. Chem., April 1961) was performed with a Beckman IR-4 infrared spectrophotometer using a CsBr prism; and also with a Cary Raman Spectrophotometer.

### A. Infrared Spectra of Solids

Most of the spectra of solid compounds were recorded as mulls in nujol or in hexachlorobutadiene. Mulls of the solids were prepared by grinding a small solid sample with the oil in a mortar and then squeezing this paste sample between two polished NaCl windows. The oil substantially reduced the scattering loss since its refractive index approached that of the solid itself. Hexachlorobutadiene was employed as a mulling agent when the C-H stretching region was of interest. Evaporated films of some solids were also studied both by transmission and reflection infrared techniques. Evaporated films could not, however, be produced with xanthates and their related compounds since these decompose on heating.



## B. Infrared Spectra of Solutions

Xanthates were also studied as solutions in organic solvents and water. For the organic solvent work, normal NaCl sealed cells of 0.05 and 0.10 mm thicknesses were used. These cells were, however, rather unsuitable for use with alkali xanthate solutions in that the spacer material, a Pb-Hg amalgam, was liable to react with the xanthates forming metal xanthates of Pb and Hg. Most of the organic solvent work was, however, conducted with heavy metal xanthates and dioxanthogen (which is the normal oxidation product of the xanthates) in the NaCl sealed cells without any visible exchange reactions. Some difficulty was experienced with alkali metal xanthates in organic solvents in that the presence of a salt window appeared to catalyze a reaction, leaving an insoluble product on the window face. This will be discussed in Part IV of the "Results and Discussion".

The aqueous solution work presented many problems due mainly to an initial lack of proper sample cells. With only NaCl window material available various attempts, such as evaporation of a  $\text{CaF}_2$  film, gold film, germanium film<sup>24</sup> and application of a thin film of paraffin wax onto the salt, were made to protect the salt window from water. Some aqueous solution spectra were also recorded with NaCl cells using saturated salt solutions for solvent. Of these attempts, the wax film and saturated NaCl solution procedures met with some success. They were, however, eliminated with the purchase of water insoluble KRS-5 (Tl-Br-I),  $\text{CaF}_2$  and  $\text{BaF}_2$  window materials. AgCl windows were also tried but copious precipitation of silver xanthate made this material unsuitable. The spectra of the aqueous xanthate solutions, presented in this theses, were made using a demountable type cell with barium fluoride windows.





This window material has low water solubility (0.17 gms/100 cc H<sub>2</sub>O at 10°C) and is transparent to 800 cm<sup>-1</sup>. A mylar (polyester resin) spacer, 25 micron thick, was used in the cell assembly. Such a cell filled with water gave a background spectrum in the region 1400-900 cm<sup>-1</sup> (which covers the C-O and C=S stretching regions in xanthates) of approximately 40% transmittance. Loss of water from the cell by evaporation was negligible if the cell was carefully assembled.

### C. Adsorption Spectral Studies

Copper Foil Cell: Initial attempts to study adsorbed layers of xanthate were made with a cell constructed of copper foil. Approximately 2 feet of copper foil (2 inches wide by 5 thousandths of an inch thick) were folded so that the foil, stretched over a suitably designed rigid frame, maintained the same convergence as the beam. It was hoped that with such a cell the grazing light would traverse a sufficient number of adsorbed molecules to give reasonable absorption bands. The cell failed, however, because on cleaning the stretched foil in an acid it warped, thus effectively blocking the beam path.

Adsorption on Mineral Sols: A second technique tested was that of preparing aqueous sols of the minerals PbS, ZnS and CuS, separating out the extremely fine sol particles (less than 1  $\mu$ ), adsorbing xanthate onto the particles and recording their infrared spectrum by transmission.

Many difficulties were encountered in this technique: to produce stable sols either excess metal ions or S<sup>2-</sup> ions were required to give the particles an electrical charge. The excess of such ions could not be tolerated, however, since their presence affects the adsorption of xanthate either by precipitating metal xanthates in the bulk solution or by depres-





sing the adsorption due to excess  $S^{--}$  ions. On the other hand, a neutralized sol rapidly coagulates and settles out as a coarse precipitate of low intrinsic surface area. To overcome this difficulty the xanthate solution was added to the sol immediately after its neutralization. It was hoped that, with such a procedure, the rapid adsorption of xanthate might prevent the formation of coarse solid particles thus producing a high specific surface area substrate with adsorbed xanthate. These sol particles were then extracted from the solution either by evaporation of the water to dryness or by filtering. The filter employed for this purpose was a "millipore" V.F. (100  $\text{\AA}$  pore size) cellulose filter in an all glass filter apparatus.

The sol particles with the adsorbed xanthates were then either spread dry between two NaCl windows or dispersed in a drop of nujol and spread between two sodium chloride windows for the recording of the spectrum. With the instrument at maximum sensitivity (i.e. 20X expansion) the nujol film itself showed relatively strong bands in the  $1400\text{--}700\text{ cm}^{-1}$  region which were not apparent at 1X expansion, and these made the detection of weak xanthate bands very difficult. Due to high scattering the dry samples were nearly opaque even with very thin layers of the sol.

Only in a few cases were some new bands (due to adsorbed species) detected and as these bands could not be regularly reproduced the method was also temporarily abandoned. F. Kicinski<sup>25</sup> has successfully prepared PbS photoconductive cells by chemical deposition from a lead acetate, thiourea, sodium hydroxide solution. H. Wilman<sup>22</sup> conducted an electron microscopic investigation of deposits of this type and found them to consist of crystallites with a mean crystal size of  $150\text{ \AA}$ . He also found



that these deposits contained less oxidation product than vacuum evaporated films. Films of this type will be studied in future in addition to evaporated films.

Fine precipitates of some sulfides were pressed, at approximately 30,000 psi, into very thin disks (about 0.1 mm) and their spectral characteristics were studied. None of the sulphide disks showed any reasonable transparency in the infrared. They were also very fragile and difficult to handle and so were abandoned in favor of vacuum evaporated deposits.

#### Adsorption Studies by Transmission Through Evaporated

Mineral Films: The vacuum evaporation technique of preparing mineral films of high transparency has been previously described in this thesis. Films, thus prepared, were scanned in the spectrometer, both before and after treatment with an adsorbate, at identical operating conditions.

Since vacuum deposited PbS films showed greater promise than CuS or ZnS films due to higher transparency and relatively high specific surface area, this mineral was chosen to be the substrate for adsorption study. Another point in favor of PbS was that it has been extensively studied by previous investigators. The PbS films deposited onto NaCl windows were taken from the vacuum evaporator and their spectra were recorded as quickly as possible to minimize oxidation and contamination by the atmosphere. The spectra were generally recorded at 1X and 20X scale expansion. The PbS coated window was then immersed in a xanthate solution (using as solvent, benzene, acetone or  $H_2O$ ) and left for periods varying from 15 minutes to 2 days. The sample was then removed, washed carefully with the pure solvent (usually warmed) and air dried. The



spectrum was again recorded using the identical instrument settings as before. If any adsorbed xanthate was detected the sample was then subjected to a sequence of washings in organic solvents other than that used in the adsorption. The purpose of the subsequent washings was to attempt to dissolve any multilayers adsorbed on top of the initial monolayer and thus to obtain the adsorption bands due to the first monolayer. A final washing in pyridine was found to remove all of the adsorbed xanthate and thus the cycle was completed.

Attempts were made to cancel any absorption due to the substrate material (i. e. PbS + oxidation product) by evaporating PbS simultaneously onto 2 windows adjacent to each other and scanning them in the infrared spectrophotometer differentially. At 10X and 20X scale expansion, however, compensation could not be achieved. It did, however, result in a substantial reduction in the intensity of the substrate absorption bands.

One major drawback to the study of xanthate adsorption on PbS films deposited on infrared transmitting windows was the puzzling appearance of a "reaction product" on the window during the treatment of the PbS (plus window) in a xanthate solution (either benzene, alcohol or acetone). This product was also formed with the salt window alone in xanthate solutions and could not be eliminated by organic solvent dissolution. The absorption bands from this "reaction product" were at  $1125\text{ cm}^{-1}$  and  $1000\text{ cm}^{-1}$  which unfortunately are in the same range as xanthate bands themselves. These same bands appeared with NaCl,  $\text{CaF}_2$  and  $\text{BaF}_2$  and so an attempt was made to eliminate the window support. This was achieved by depositing PbS onto NaCl and then floating off the PbS film onto water and subsequently removing it on a fine screen. However, on drying, the film fell apart, probably as a result of the stresses incurred.







This technique was not pursued because a reflection technique appeared more promising at this stage. It is hoped that the purchase of a new infrared transmitting glass called "Irtran 2" will eliminate the substrate problem and future work can be conducted by transmission studies.

Infrared Reflectance Studies: Because of the difficulties described in studying PbS films with transmitted light, a reflection attachment somewhat similar to that described by Francis and Ellison<sup>26</sup>, and reviewed by R.P. Eischens<sup>17</sup>, was constructed. The optical arrangement used is shown in Figure 7.

The arrangement of Francis and Ellison had the sample mirrors directly adjacent to the source housing in the normal optical path from the source to the monochromator housing. Since their sample mirrors were separated 1/8 inch and the convergent beams are normally approximately 3 cm wide by 5 cm high at this point, they had to re-position the source and adjust the mirrors in the source housing so that the beams focused between the sample mirrors. In this way their sample mirrors collected most of the beams' energy. The necessity of this readjustment has been eliminated in our optical arrangement, since by bringing the beams out from the spectrophotometer the normal instrument focus could be positioned between the mirrors which were separated 3/8 inch. Future plans entail enclosing the sample mirrors in a vacuum container (which would have been impossible with Francis and Ellison's arrangement because of insufficient space). A second alteration is that our optical arrangement can readily achieve up to 8 reflections from the two sample mirrors. In this case, however, the angle of incidence of the beam is approximately 35 degrees. (A higher angle of incidence is desirable - see discussion.)







With 6 reflections the angle of incidence is nearly 45 degrees and the area of the beam striking the two sample mirrors is reduced from  $\approx 20 \text{ cm}^2$  with 8 reflections, to  $\approx 15 \text{ cm}^2$  with 6 reflections. When using front surface aluminum mirrors as sample mirrors, 65% of the beam energy is transmitted by the optical arrangement with 6 reflections.

The general procedure in the reflectance spectral study of xanthate adsorption onto evaporated PbS films consisted of the following:

1. The PbS (obtained as a chemical precipitate) was evaporated onto two 2" x 3" clean front-surface aluminum mirrors in, generally, 2 or 3 evaporation cycles (until the coating appeared of uniform density and had a fairly sooty appearance, as previously described). It was experimentally determined that such films evaporated onto clean glass showed negligible if any reflectance nor did glass itself show appreciable reflectance. The PbS film evaporated onto an aluminum mirror, however, gave a reflectance value approximately 1/3 to 1/2 that of the aluminum alone. This clearly showed that the bulk of the reflection occurred at the aluminum-galena interface. Another observation of interest was the fact that the PbS evaporated films served as very efficient filters for the visible light with no appreciable scattering in the infrared. This again indicated that the crystallites or crystallite aggregates were of the order of less than  $1000 \text{ \AA}$ .
2. Background spectra of the fresh PbS films were then recorded both at 1X and 10X (or sometimes 20X) ordinate scale expansions.
3. The PbS sample mirrors were then washed in acetone, air dried, and their spectra again recorded, taking care to duplicate instrument conditions.





4. The PbS samples were then soaked for from 2 hours to 2 days in an organic solution of the xanthate (K n-nonyl xanthate and K n-butyl xanthate were used). They were then thoroughly washed in the pure solvent and their spectra again recorded.
  5. If no appreciable changes in the spectra were noted, the sample was then treated in an aqueous solution of the same xanthate as used in Step 4. This treatment lasted generally for a period of 1 hour. The samples were removed, washed in doubly distilled water, dried, and their spectra recorded.
  6. Since the treatment in (5) invariably produced the spectrum identical to that of bulk metal xanthate with high absorption band intensities, it was assumed that multilayers had formed. An attempt was therefore made to wash off the multilayers with hot acetone. After each acetone treatment the sample was dried and any spectral changes were noted. The solvation treatment was continued until no further change occurred.
  7. At this stage the sample was either set aside in the atmosphere before further treatment in pyridine or soaked and washed immediately in pyridine which completed the sequence.
- (For the spectra obtained in Steps 1 - 7 see Figure 27).

Some of the PbS films were subjected to varying periods of ionic bombardment to study the effect of this vacuum evaporation cleaning procedure on the nature of the film. This aspect is considered in more detail in Part II of the "Discussion".

To study the surface and adsorption of xanthate on natural galena, a polished slab of galena was substituted for one of the aluminum mirrors in the sample beam of the reflectance attachment. A large piece





of natural polycrystalline galena of unknown origin was cut to size (2 x 3 x 1/2 inches) and one side was ground and polished under water to a mirror-like finish. The grain size of this galena averaged about 1 - 2 cm. in diameter which would indicate high purity but a microscopic examination revealed that a significant amount of impurity was present (mainly quartz) at the grain boundaries. The spectrum was recorded immediately upon drying the galena in a hot air blast. Owing to the relatively low reflectance from the galena itself, the three reflections from this surface left very little energy in the sample beam. In order to record its spectrum the slits were opened to "1000" slit schedule and reference beam attenuation was employed to produce reasonable instrument response (the spectrum is shown in Figure 24f).

### III. LANGMUIR BLODGETT FILM TECHNIQUE

Surface active agents which have a low water solubility can be spread as monolayers at an air-water interface. The molecules in these films become oriented when they are compressed into a closely packed structure by a moveable boom. It has been shown<sup>27, 28</sup> that the orientation of these monolayers is such that the hydrocarbon chains are nearly normal to the surface while the planes of the methylene groups are nearly parallel to the surface (in a normal alkyl type hydrocarbon chain). Such oriented monolayer films can then be deposited on a solid surface by the Langmuir-Blodgett technique<sup>29</sup> and the films retain their coherency and orientation.

A Langmuir-Adam trough was employed in the deposition of lead cetyl xanthate monolayers onto aluminum mirrors. The initial purpose of this was to provide an experimental check for the calculations



which indicated that the spectrophotometer and reflectance attachment should be capable of producing reasonable absorption bands from a single monolayer. This would then insure that reasonable intensity absorption bands would be detected on adsorption of xanthate from solution onto a PbS film (evaporated on the aluminum mirror) with markedly higher specific surface area. A study of the orientation effect of the Pb cetyl xanthate film on the vibrational spectrum was also of interest.

The procedure employed in film deposition with the Langmuir-Adam trough was as follows:

The instrument was calibrated by spreading films of n-Hexadecanol ( $C_{15}H_{31}CH_2OH$ ) on the surface of doubly distilled water and the calculated area per molecule of the condensed film was compared with the well established value<sup>30</sup> of  $21.2 \text{ \AA}^2$ . The cetyl alcohol used in this determination was supplied by Dr. J. Leja from the same source as that used by Dr. Bowcott<sup>30</sup>.

Lead cetyl xanthate was then spread from a warm benzene solution on the surface of doubly distilled water in the Langmuir-Adam trough, into which two cleaned aluminum mirrors had previously been placed on a wire holder. The lead cetyl xanthate film was compressed to 12 dynes/cm and the two mirrors were gently lifted out of the trough, thus depositing the monolayer. The mirrors were lifted through the film at about a  $20^\circ$  angle to the horizontal, in order to facilitate the "squeezing" of water from the "wedge" between the substrate and the monolayer. The film remaining on the trough was then recompressed to the original film pressure (12 dynes/cm) and the area of the compact monolayer removed by the mirrors was determined. This was then compared to the geometrical area of the mirrors and in all cases the agreement was within 10 percent



and generally it was within 5%. The sample mirrors were then dried overnight in a dessicator and their spectrum recorded by using them as sample mirrors in the reflectance attachment (See Fig. 7). The spectrum was generally recorded at both 1X and 10X (or 20X) ordinate scale expansion.

To study the effect of ionic bombardment, the mirrors with the Pb cetyl xanthate monolayers were then placed in the vacuum evaporator between two aluminum high tension electrodes and subjected to bombardment. After one-half hour of bombardment their spectrum was again recorded and compared to the previous one (see Fig. 25).





## RESULTS AND DISCUSSION

### I. INFRARED SPECTRA OF XANTHATES AND RELATED COMPOUNDS IN THE SOLID AND SOLUTION STATES

In the preceding section on infrared theory the general origins of group frequency shifts have been considered. We now wish to employ frequency shifts and intensity changes of absorption bands, associated with xanthate molecules, for absorption band assignments and possibly for the elucidation of their molecular structures. A brief description of the xanthate molecule will aid in the subsequent interpretation of spectroscopic data.

The non-polar end of most xanthate collectors consists of an aliphatic hydrocarbon chain containing from one to six  $\text{CH}_2$  groups. The hydrocarbon chain has a width of approximately  $4\text{\AA}$  and each  $\text{CH}_2$  group adds about  $1.3\text{\AA}$  to the length of the molecule. The length of the hydrocarbon chain, together with the degree of hydration of the polar group, determines the water solubility of the molecule<sup>32</sup>.

The water solubility is decreased 4.34 times with the addition of each  $\text{CH}_2$  group<sup>33</sup> and since the process of adsorption from an aqueous solution can be considered as the "reverse" process to solvation, the surface activity increases with a lengthening of the hydrocarbon chain.

The polar group of a xanthate molecule consists of a carbon atom surrounded by two sulfur atoms and one oxygen atom, i. e.

$-\text{O}-\text{C}\begin{smallmatrix} \nearrow \text{S} \\ \searrow \text{S} \end{smallmatrix}-$ . The width of this polar end of the molecule is about  $7\text{\AA}$  and its breadth is  $3.8\text{\AA}$ <sup>32</sup>. The nature of the polar group is largely dependent on the properties of the divalent sulphur ion. Since this atom has a very large size it is readily polarized and can form electrovalent and



homopolar bonds. Klassen and Mokrousov<sup>32</sup> claim that, if the sulphur ion interacts with cations which are also capable of polarization, the mutual polarizations lead to an impoverishment of electrons and a metallic bond can result.

Bellamy<sup>34</sup> claims that the C=S linkage has little or no initial polarity and it therefore closely resembles the C=C linkage whose frequency falls under the influence of either induction or mesomerism. One therefore expects that the frequency of the C=S absorption band in various xanthates will vary within fairly narrow limits. Since it may appear that the C=S linkage directly affects the collecting ability of a sulphydric collector in the flotation of sulfide minerals<sup>35</sup>, an investigation of the behavior of this group in different environments is of fundamental interest.

The C-O-C stretching vibrational modes in esters, ketones, etc. have been shown to be very sensitive to differences in structural environments<sup>10, 36</sup>. Two strong bands are attributed to the stretching vibrations in these two C-O groups and the most intense and invariable one is generally associated with the stretching of the C-O group adjacent to the C=S linkage, which may stabilize it. No systematic assignment work has been conducted, however, to make a sure distinction between the two C-O group absorption bands.

The C-S band in thiols has been shown, by Trotter and Thompson<sup>37</sup>, to vary appreciably in different molecules and they assigned to it a general range of  $600-700\text{ cm}^{-1}$ . The absorption band associated with this group may indeed provide valuable information in the interpretation of infrared spectroscopic data of xanthate adsorption, since undoubtedly this bond would be perturbed by the sulfur-mineral bond.



Although some infrared spectroscopic data on xanthate compounds were previously published<sup>18, 31</sup>, these were qualitative in nature and specific absorption band assignments were not presented for the  $R-O-C \begin{smallmatrix} \nearrow S \\ \searrow S \end{smallmatrix}$  structure. The first task was, therefore, the reliable assignment of the vibrational absorption bands associated with the C-O-C, C=S, C-S (and possibly S-S in dioxanthogen) stretching modes of the xanthate molecule.

### A. Absorption Band Assignments

A paper (in the Canadian Journal of Chemistry) by Little, Poling and Leja<sup>6</sup> entitled:

#### Infrared Spectra of Xanthate Compounds

#### II Assignment of Vibrational Frequencies

is included at the back of this thesis. This paper contains a general review of previous absorption band assignments together with the results of our investigations on alkali metal xanthates, heavy metal xanthates and dioxanthogens. The reader is referred to this paper for details since only a brief summary of the data contained therein is presented here. Since the spectra presented in this paper will be further discussed here, they are incorporated in this thesis for the sake of completeness (Figures 8-11).

Figure 8. presents the spectra of selected pure compounds on which the assignments of the C-O-C and C=S stretching modes were largely based. Figure 9. gives spectral evidence of the co-precipitation of dioxanthogen with heavy metal xanthates whose metals have variable valency. The absorption band at about  $1260\text{ cm}^{-1}$  is very characteristic of dioxanthogen. The spectra of four zinc alkyl xanthates are presented in Figure 10. Note the shift to lower frequencies and the decrease in the intensity of the  $1130\text{-}1100\text{ cm}^{-1}$  band as the hydrocarbon chain length is increased. Spectra





of alkali metal xanthates are shown in Figure 11. Although the spectra are complex, one can readily see that the high frequency band (at  $1185\text{ cm}^{-1}$  in K-methyl xanthate) is shifted to lower frequencies as the hydrocarbon chain length is increased. The implications of the group frequency shifts (cited above) in the light of additional experimental data (obtained since the submission of the paper<sup>6</sup>) are considered in detail in the following section.

The group frequency assignments presented in the published paper are summarized in Table 2.

Evidence has also been presented in the above paper that the resonance hybrid type xanthate structure  $(\text{R}-\text{O}-\text{C} \begin{smallmatrix} \curvearrowright \text{S} \\ \curvearrowleft \text{S} \end{smallmatrix})^-$  suggested by Pearson and Stasiak<sup>31</sup> does not represent the true structure of metal xanthates. Since the xanthate esters (See Figure 8) which do not exist as resonance hybrids, have the same C=S band near  $1060\text{ cm}^{-1}$  as do the heavy metal xanthates, it is concluded that one carbon sulfur link in the xanthate structure retains a true double bond character.





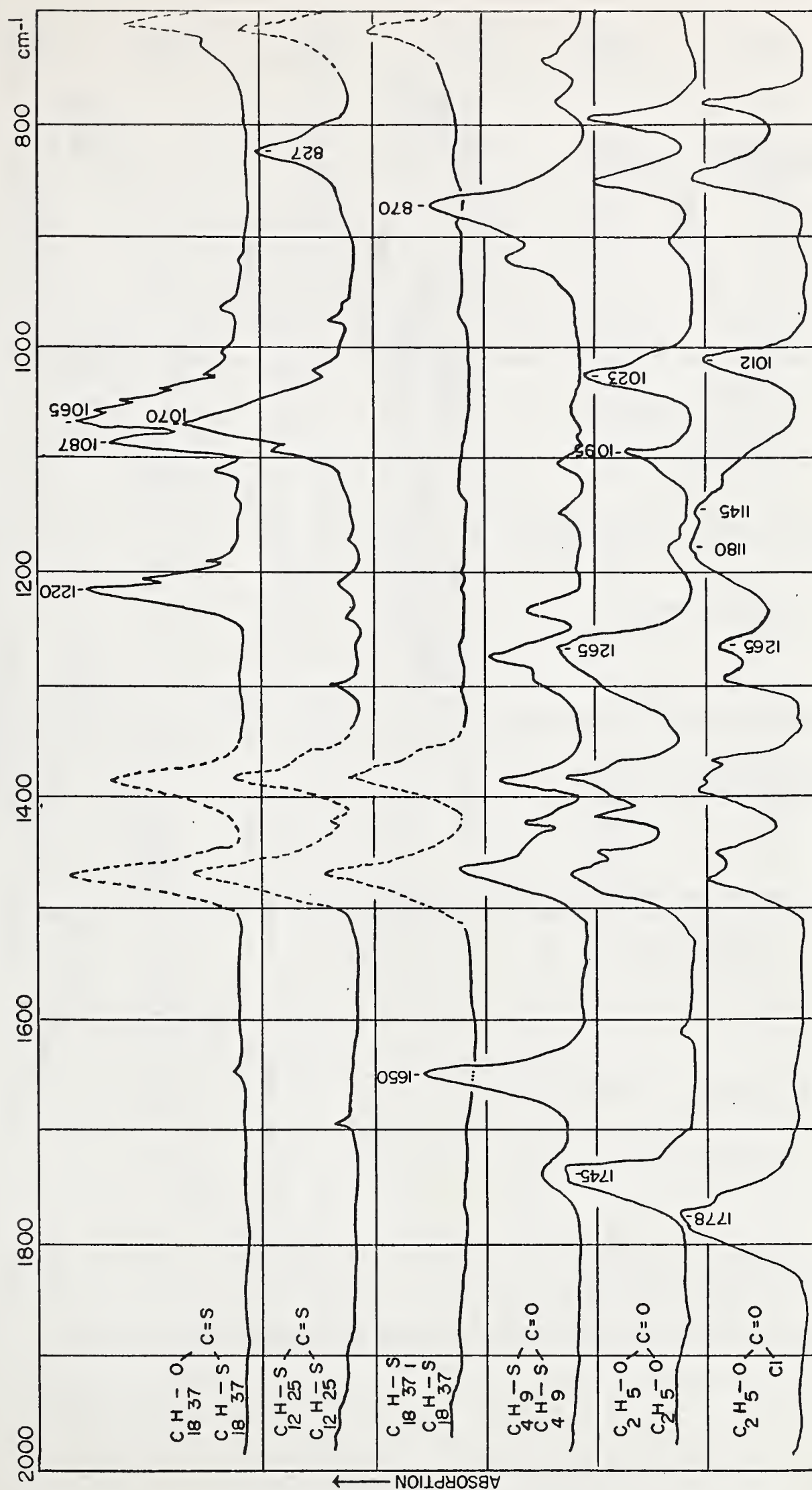


Fig. 8 Selected Carbonyl and Thiocarbonyl Compounds



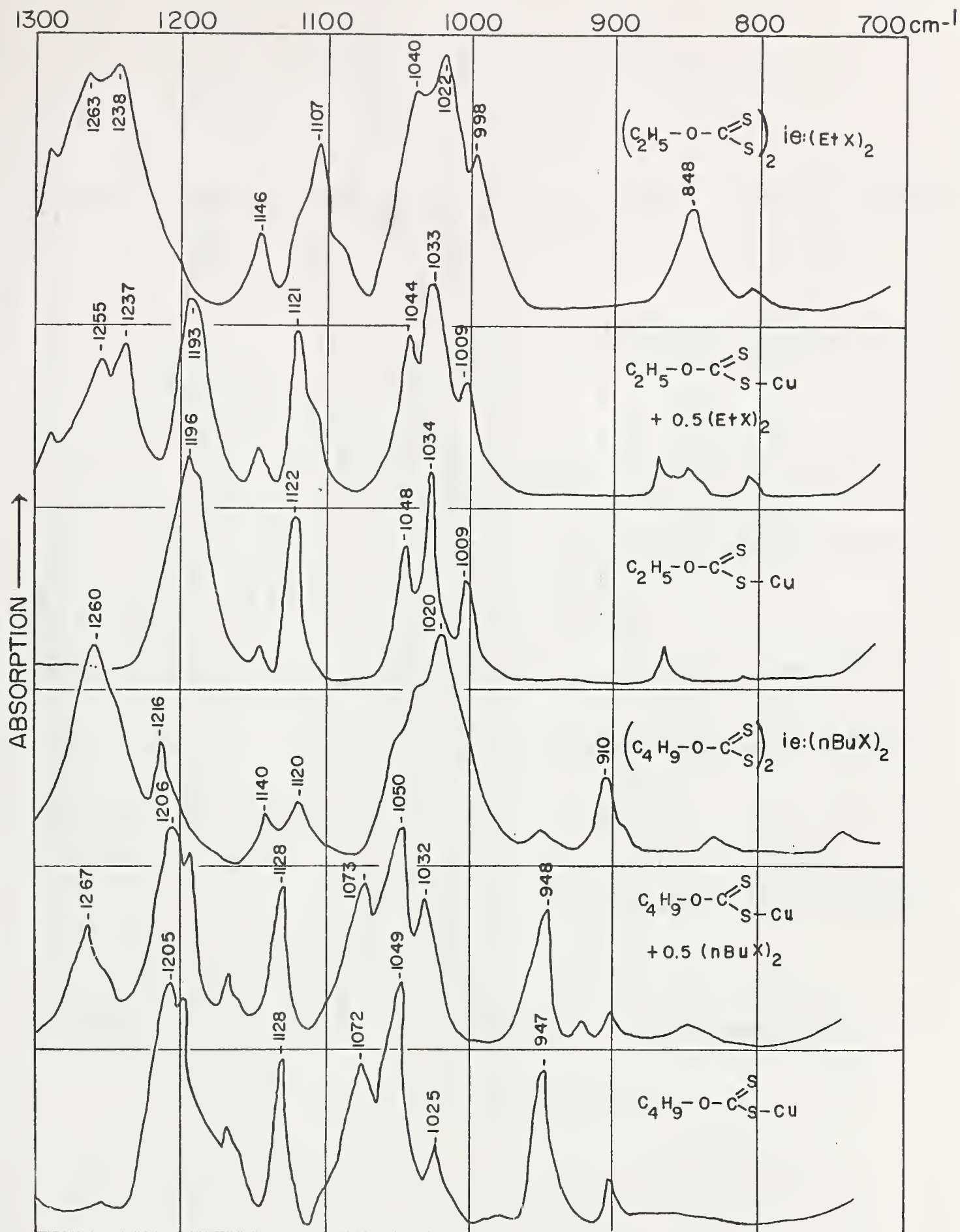


Fig. 9 Ethyl and Butyl Xanthates of Copper and Dixanthogens



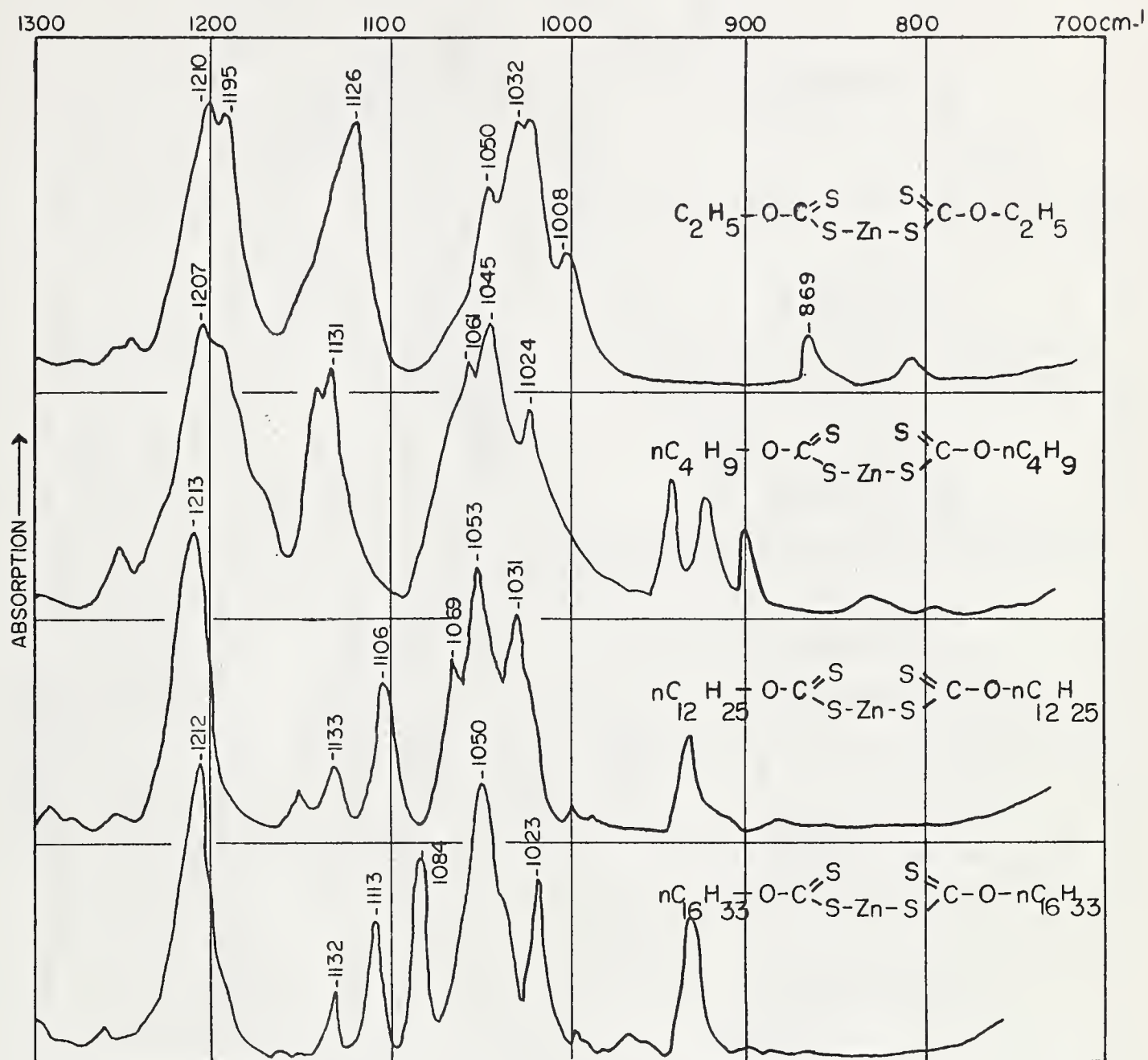


Fig. 10 Zinc Alkyl Xanthates





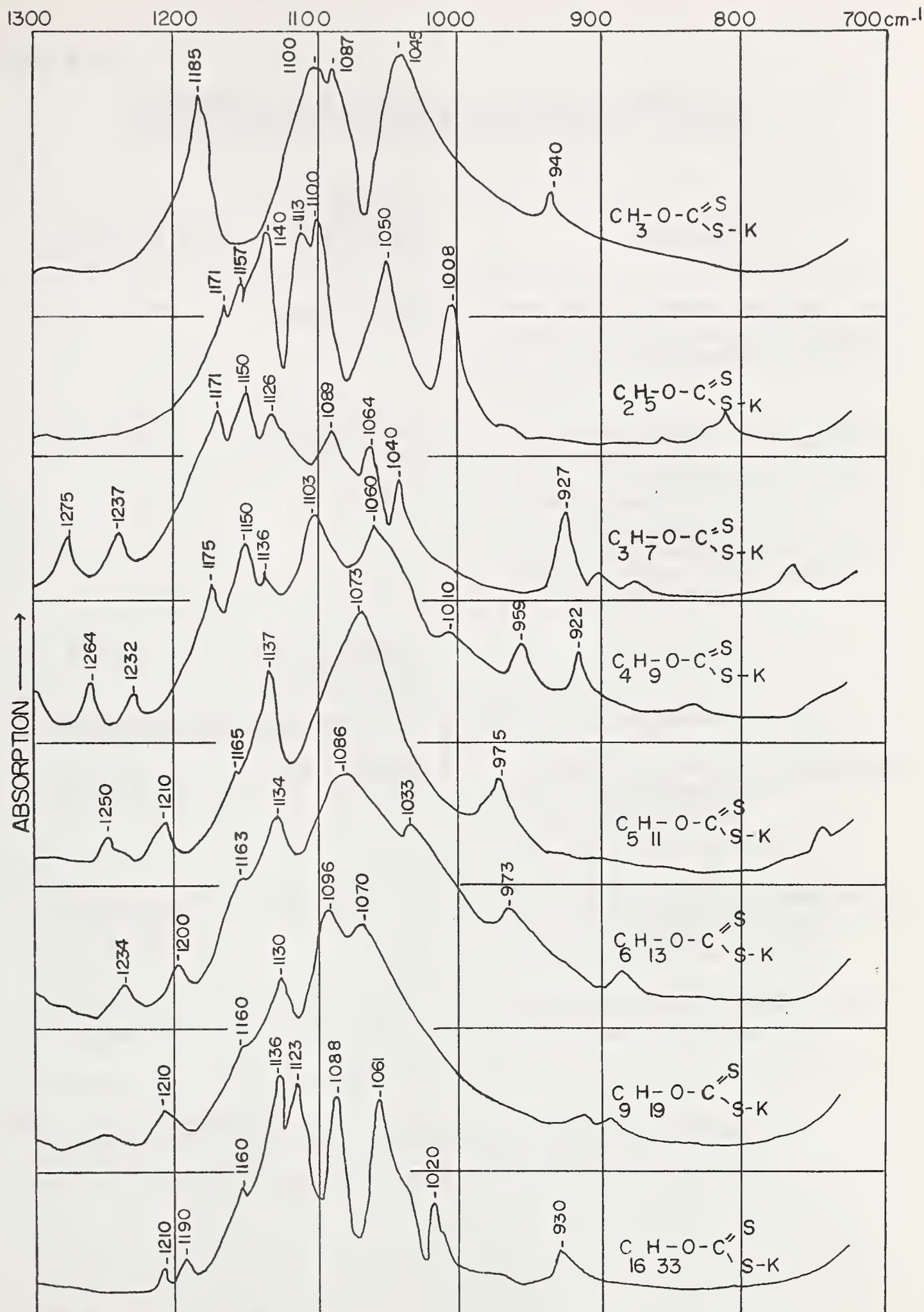


Fig. 11 Alkali Metal Xanthates



TABLE 2

 ASSIGNMENT OF VIBRATIONAL FREQUENCIES OF  
 XANTHATE COMPOUNDS<sup>6</sup> (IN THE SOLID STATE)

Vibrational Mode	Frequency Assignment	Remarks
1. C = S str.*	1020-1070 cm <sup>-1</sup>	Very strong band. Intensity comparable to C=O stretch. Appears as multi peaked band in solid state spectra.
2. C-O-C str.	a) 1200 cm <sup>-1</sup> b) 1100-1140 cm <sup>-1</sup>	Two strong bands - one of which is sensitive to changes in the length of the hydrocarbon chain, as reflected by variations in both its intensity and frequency. In the Zn alkyl xanthates the lower frequency band is the sensitive one. (See Fig. 10)
3. C-S str.	No definite assignments	
Tentative (C-S) assignments for specific compounds are:		
a) C-S-C-S-C asym. str.	830 - 870 cm <sup>-1</sup>	A medium intensity, single peak band in the compounds (nC <sub>12</sub> H <sub>25</sub> S) C=S and (nC <sub>4</sub> H <sub>9</sub> S) <sub>2</sub> C=O (See Fig. 8)
b) C-S-C-S-C sym. str.	600 cm <sup>-1</sup>	An intense Raman absorption band in the compound (nC <sub>4</sub> H <sub>9</sub> S) <sub>2</sub> C=O (See Table III reference 6)
c) C-S-S-C asym. str.	840 cm <sup>-1</sup>	Strong single peak band in ethyl dixanthogen (See Fig. 9)

\* str - stretching mode.

asym and sym = asymmetrical and symmetrical respectively.



### B. Group Vibrational Interactions:

Spectroscopic investigations of many different xanthate molecules, with particular reference to the two C-O-C and the C=S stretching modes in these molecules, have been conducted since the submission of the paper<sup>6</sup> on band assignments. The purpose of this study was to obtain additional confirmation of the C=S band assignment by a procedure employing "solvent effects"<sup>34</sup>, and also the establishment of band assignments distinguishing between the two C-O stretching modes of the C-O-C group. To achieve this last objective many variations were introduced into the hydrocarbon radical of xanthate molecules to note their perturbing effect on the C-O group absorption bands.

Crystalline Spectra: Since xanthates are heteropolar compounds, it is expected that the intermolecular forces present in its crystalline lattice are sufficiently strong to produce marked modifications of its spectrum compared to that obtained from the solution state. Thus, rather than base the vibrational spectrum on an individual xanthate molecule, it should be based on the unit cell of the crystal. A literature survey has, however, revealed that very few structural determinations have been undertaken for xanthate compounds. Wyckoff's Tables of Crystal Structures<sup>38</sup> gave the structures of Arsenic, cobaltic, ferric, and antimony ethyl xanthates as hexagonal while nickel ethyl xanthate was given as orthorhombic. Hagihara<sup>39</sup> has given the crystal structures of K n-butyl xanthate, Pb ethyl xanthate, and Pb n-butyl xanthate as monoclinic and for lead ethyl xanthate he has presented<sup>35</sup> a detailed unit cell configuration. This shows that the lead ethyl xanthate molecule is not symmetrical in itself but a symmetrical unit is developed by the pairing of two such molecules as a result of inter-





action between the doubly bonded sulphur atoms (see Fig. 19B). Until similar information is available for other types of xanthate molecules little can be said in explanation of the complexities of their solid state spectra, particularly in the case of the alkali metal xanthates (See Fig. 11).

**Solution Spectra:** Alkali metal xanthates are quite soluble in water but extremely insoluble in many organic solvents with the exception of acetone and benzene while heavy metal xanthates are extremely insoluble in water and only slightly soluble in a few organic solvents. Because of this, no single solvent can be used for all xanthates and therefore a common environment for spectral comparison of various types of metal xanthates in solution is often impossible.

The study of alkali metal xanthate in aqueous solutions is of particular interest since this is the normal environment for mineral flotation.

Alkali-Metal Xanthates: The solid state spectra of purified straight chain potassium xanthate homologues are shown in Fig. 11. Three absorption bands from each spectrum have been tentatively chosen as belonging to the  $\text{-C-O}$ ,  $\text{O-C}\begin{array}{c} \text{=O} \\ \text{---} \end{array}$   $\text{-C}\begin{array}{c} \text{=S} \\ \text{---} \end{array}$  groups. The positions of these 3 absorption bands are graphed versus the number of  $\text{CH}_2$  groups per molecule in Figure 12. Note that the high frequency C-O stretching band ( $1185\text{-}1135\text{ cm}^{-1}$ ) is the most sensitive to variations in the length (mass effect) of the hydrocarbon chain. This indicates that it is probably the C-O group adjacent to the alcohol residue.





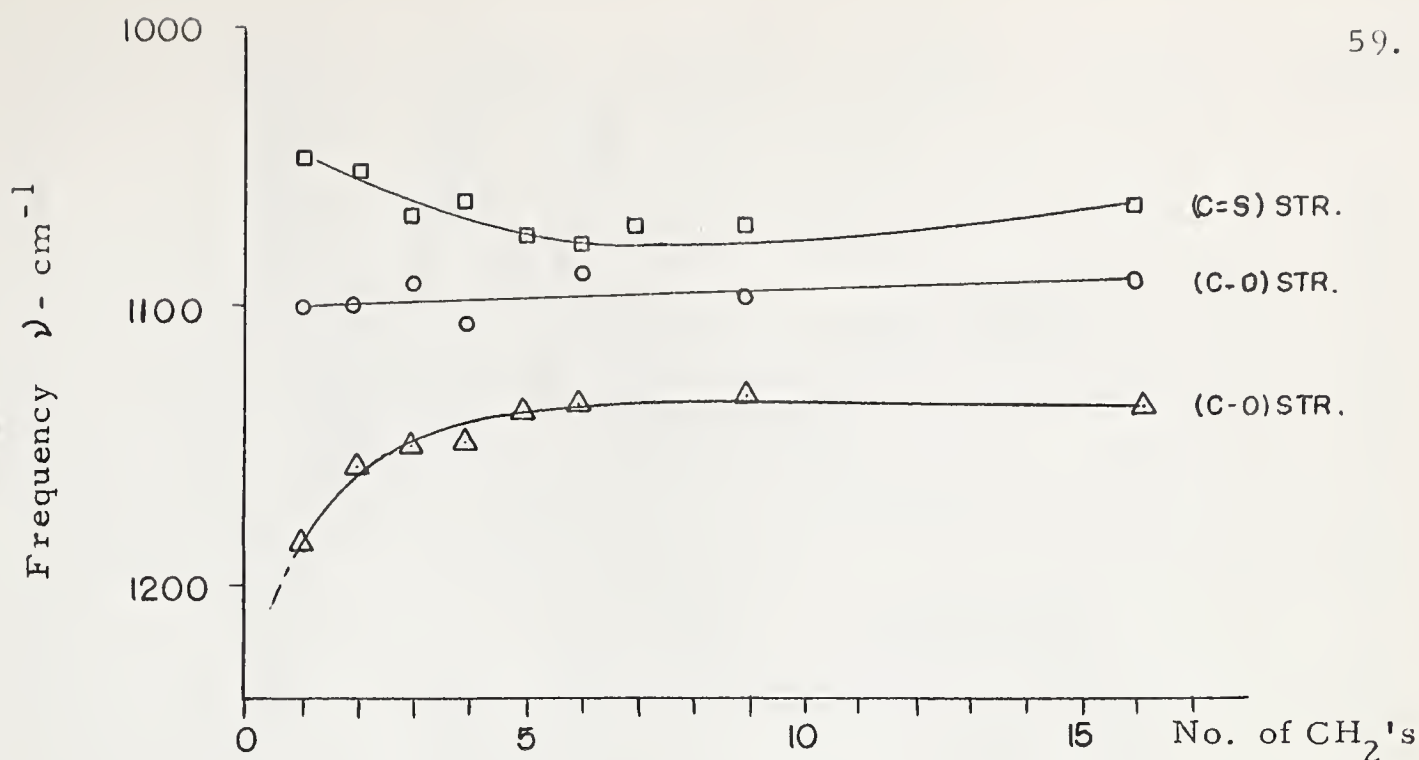


Fig. 12 Potassium Xanthate Homologues  
Group Frequency Shifts  
(Solid State Spectra)

Spectra of the same homologous series of potassium xanthates in aqueous solutions are shown in Figure 13 with the corresponding graph of frequencies versus number of CH<sub>2</sub> groups in Figure 14. The spectra of aqueous solutions of xanthates are much simpler than the solid state spectra since the molecules in solution have more freedom and intermolecular interactions are reduced in magnitudes. Since the polar groups of xanthate anions are all identical, it is expected that any hydration or association of the polar group with water molecules will be practically independent of changes in the hydrocarbon radical. Thus the C=S and adjacent C-O group stretching frequencies should remain fairly constant throughout the series - such is the case if the 1050 and 1110 cm<sup>-1</sup> bands belong to these groups respectively. Again the (1190-1140 cm<sup>-1</sup>) C-O band is most sensitive to changes in the length of the hydrocarbon chain indicating that it is probably due to the C-O group adjacent to the hydrocarbon radical.



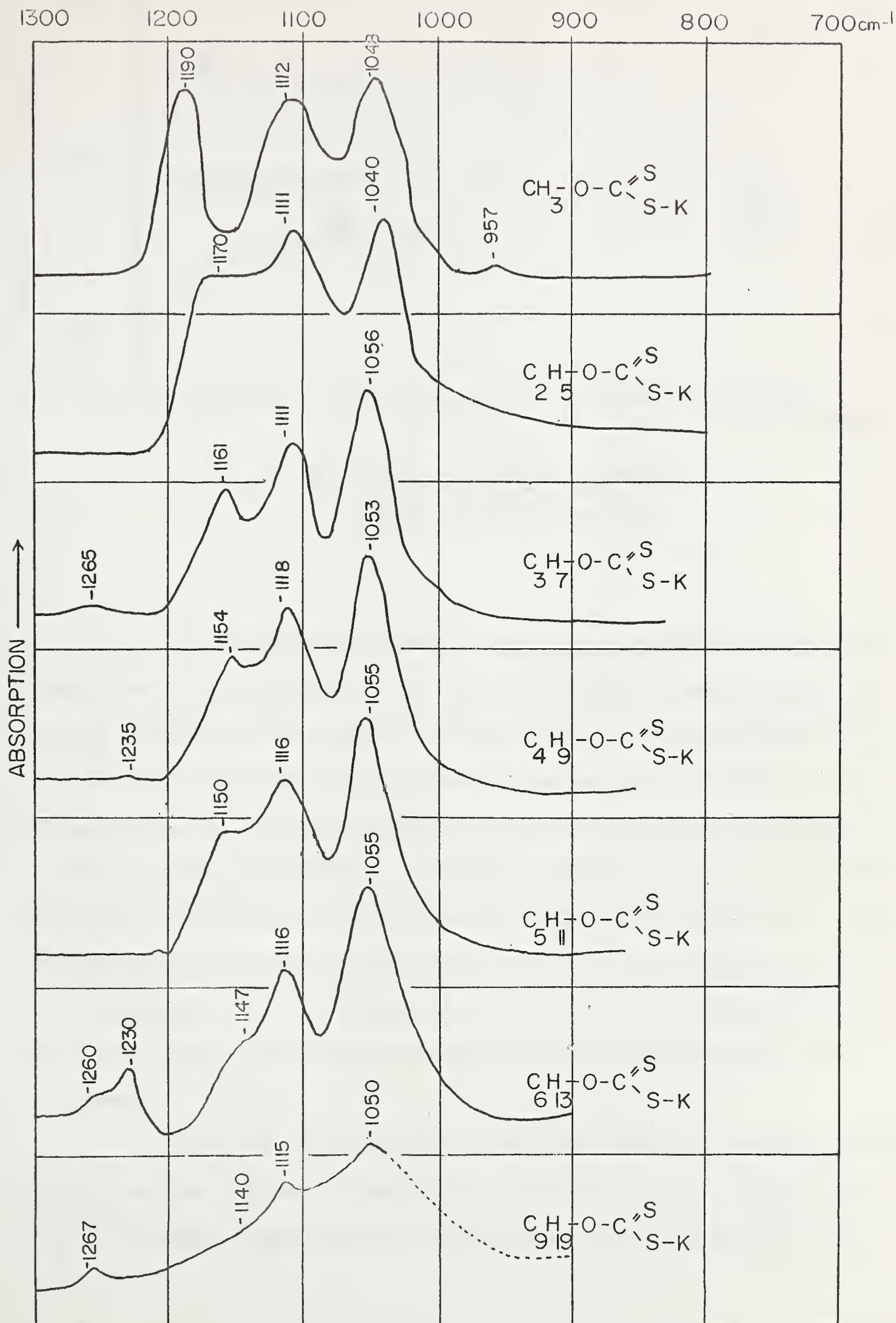


Fig. 13 Aqueous Solution Spectra of Potassium Xanthate Homologues



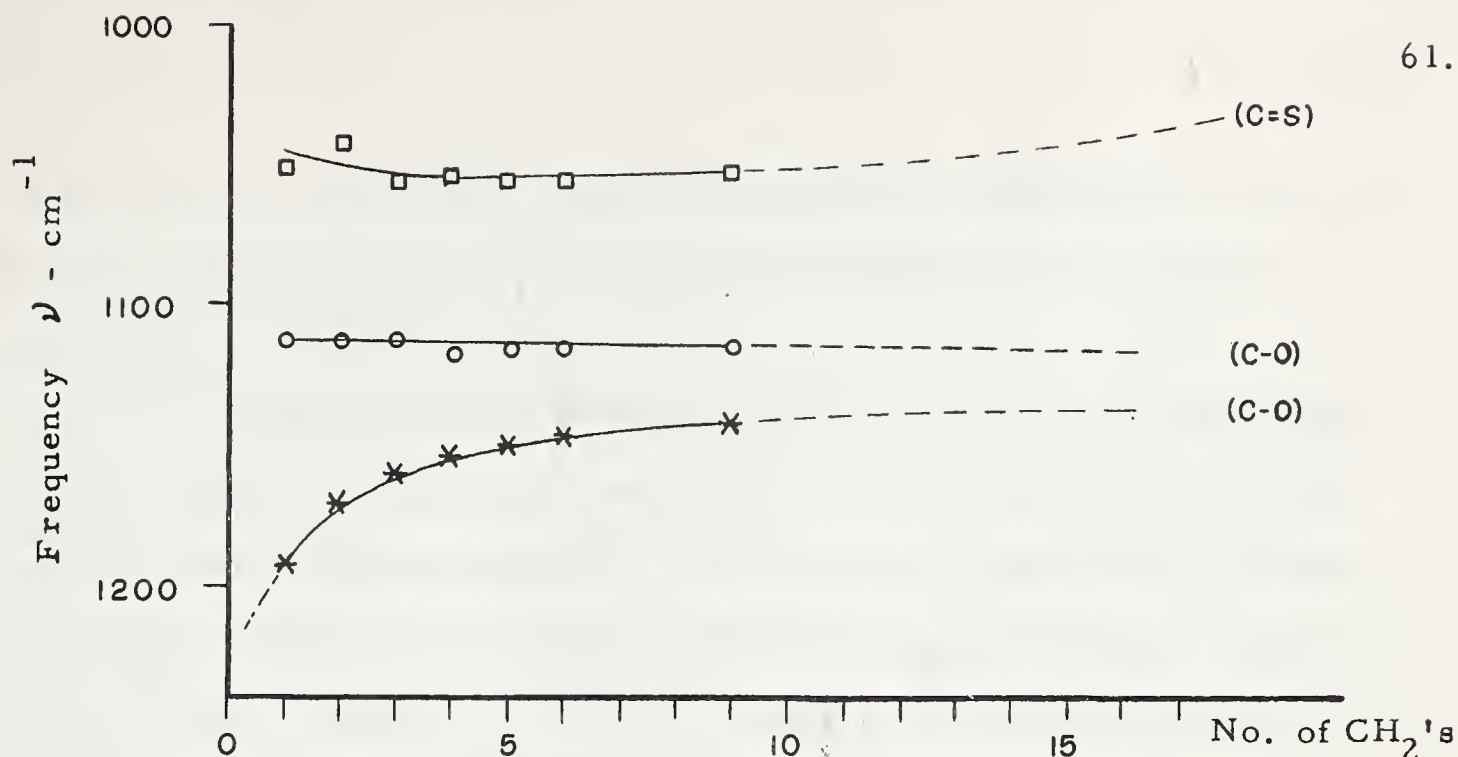


Fig. 14 Potassium Xanthate Homologues  
Group Frequency Shifts  
(Aqueous Solution Spectra)

The spectra of aqueous potassium butyl xanthate solutions were studied over the pH range of 4.5 to 10.0 in an attempt to detect hydrolysis and decomposition of the xanthate. The spectra were recorded within 3 to 10 minutes of regulating the pH of the solution with HCl or NaOH. Over this pH range the spectra of aqueous potassium butyl xanthate remained identical to that given in Figure 13 (for the  $1300\text{-}700\text{ cm}^{-1}$  region). No S-H stretching band, which would indicate hydrolysis to free xanthic acid, could be detected (even at 10X ordinate scale expansion). This does not mean that no xanthic acid exists in aqueous solutions of alkali metal xanthates but rather that its concentration is below the limit of detectability of the instrument.

When concentrated acid was added directly to an aqueous xanthate solution and the spectrum recorded immediately (in 1 min.) a broad weak ( $\sim 2500\text{ cm}^{-1}$ ) band, attributed to hydrogen bonded S-H groups, was detected. This band





disappeared in the period of a few minutes with the simultaneous appearance of bands characteristic of  $\text{CS}_2$  indicating that the xanthic acid rapidly decomposed to  $\text{CS}_2$  and alcohol.

The assignments presented for the two C-O stretching modes in alkali metal xanthates have been further confirmed by the preparation and study of secondary xanthates. Any structural factor which increases the rigidity of the carbon skeleton to motion along the C-O axis raises the C-O stretching frequency. Thus, for example, the C-OH stretching frequencies in straight chain primary, secondary and tertiary alcohols are approximately 1070, 1105 and 1160  $\text{cm}^{-1}$ , respectively, and in phenol it is at 1230  $\text{cm}^{-1}$ . The substitution of a secondary hydrocarbon chain for a primary non-polar xanthate radical should markedly increase the frequency of the C-O group adjacent to the chain while the other O-C band should remain unaffected. (Hereafter these two bands will be differentiated by calling "C-O" the bond adjacent to the hydrocarbon chain, and "O-C" that adjacent to C=S).

For comparison, the solid state spectra of normal and secondary xanthates are shown in Figure 15. The absorption bands marked by dots and circles designate the bands associated with the stretching vibrations of the two C-O groups. It is evident that in the secondary xanthates the high frequency C-O band (●) is shifted to higher frequencies while the low frequency O-C band (○) remains practically unchanged in relation to their positions in the normal xanthate.

The conclusions reached, therefore, are that: in alkali metal xanthates the high frequency C-O band (1190-1140  $\text{cm}^{-1}$ ) is attributed mainly to the stretching of the C-O bond adjacent to the hydrocarbon chain



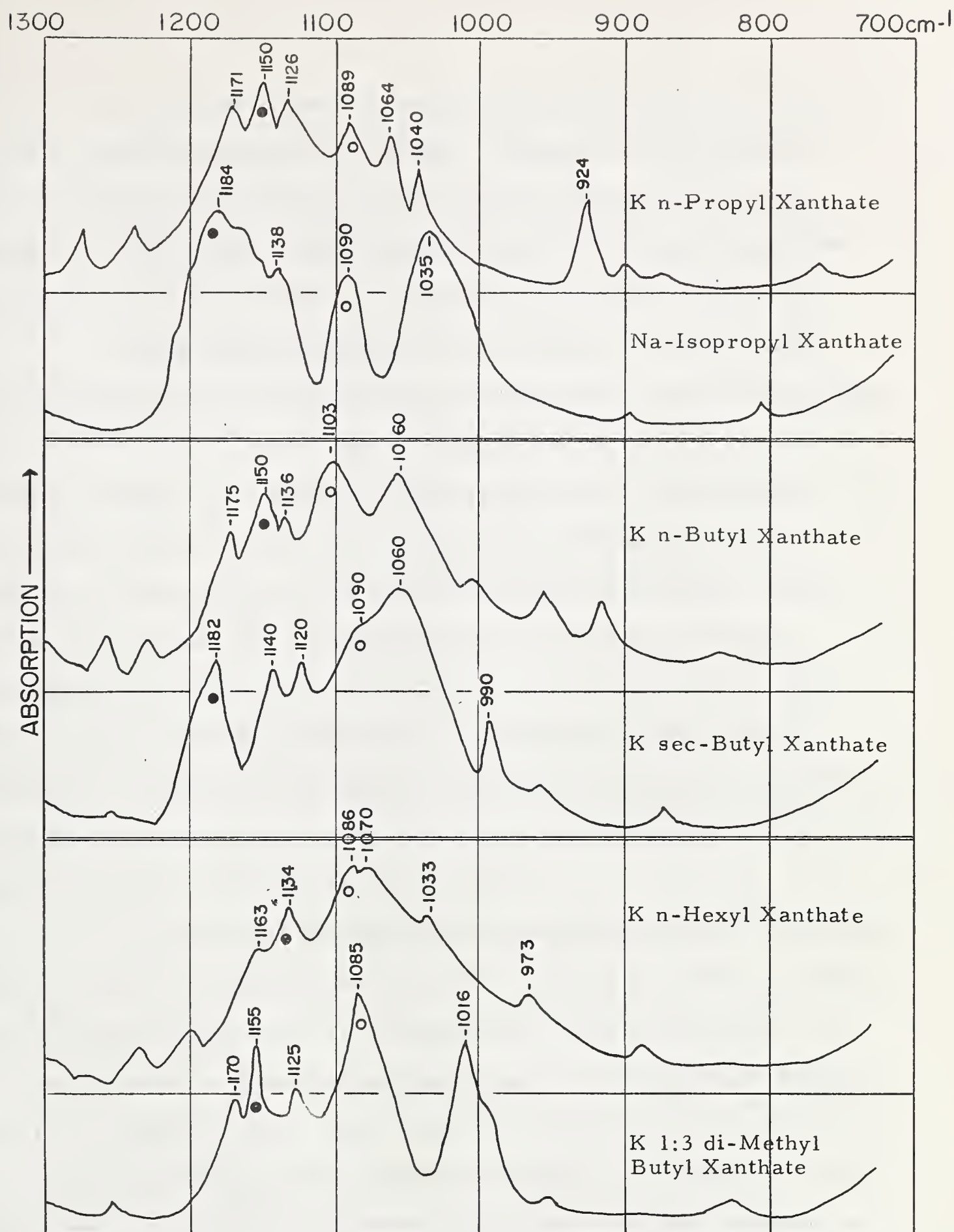


Fig. 15 Normal and Secondary Xanthates:  
Comparison of C-O Stretching Frequencies  
(Solid State Spectra)



while the lower frequency band is associated principally with stretching of the O-C bond adjacent to the C=S group. Although the C-O vibrational modes should probably be described in terms of the vibrations of the entire  $\text{C-O-C}\begin{smallmatrix} \nearrow \text{S} \\ \searrow \text{S} \end{smallmatrix}$  group, since these primarily involve stretching of one or the other of the C-O bonds, the simplified description is justified.

Heavy Metal Xanthates: These compounds are the highly insoluble products of reactions between xanthate anions and any heavy metal ions (i. e.  $\text{Pb}^{++}$ ,  $\text{Zn}^{++}$ ,  $\text{Cu}^+$ , etc.) in aqueous solutions of xanthates. In flotation practice, the presence of heavy metal ions in the medium is detrimental to the process since heavy metal xanthates are precipitated from the solution thus increasing the consumption of collector. Heavy metal xanthates also play an important role in the study of xanthate adsorption onto minerals, since xanthate ions react with mineral oxidation products to form co-adsorbed or co-precipitated heavy metal xanthates. In addition, most theories of xanthate adsorption predict that some type of metal-sulphur bond is formed in the adsorption process, thus producing a metal xanthate surface compound.

On comparing the spectra of cuprous ethyl and butyl xanthates (Fig. 9) and zinc alkyl xanthates (Fig. 10) to the spectra of the potassium xanthate homologues (Fig. 11), the absorption bands of the former are seen to be better resolved and well separated into three distinct groups of bands. The spectra of zinc alkyl xanthates show that the  $1200\text{ cm}^{-1}$  band is unaffected by changes in the length of the hydrocarbon radical while the lower frequency band ( $1130\text{-}1100\text{ cm}^{-1}$ ) is sensitive to such changes, particularly with respect to its intensity.





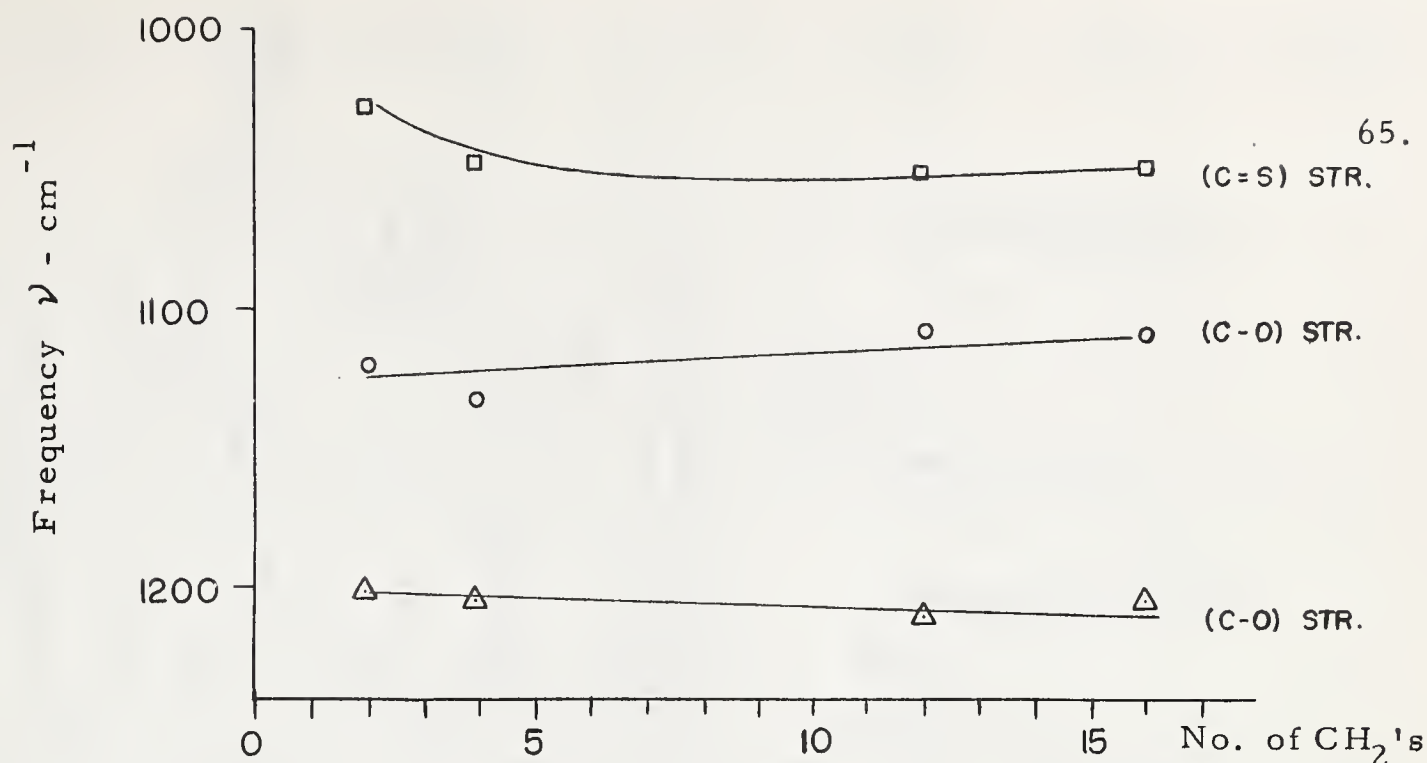


Fig. 16 Zinc Alkyl Xanthates  
Group Frequency Shifts  
(Solid State Spectra)

A graph of the group frequency shifts for the zinc alkyl xanthates is given in Figure 16 which shows that the absorption band positions are relatively unaffected by changes in the hydrocarbon chain length.

The behavior of zinc alkyl xanthates was duplicated in lead alkyl xanthates as shown by the spectra in Figure 17 and the corresponding graph, of group frequency shifts, shown in Figure 18. Such behavior differs markedly from that exhibited by the alkali metal xanthates (see Figures 11, 12, 13 and 14). This indicates that the molecular configuration of the divalent metal xanthates must locate the metal atom in close proximity to the oxygen atoms, where it can have a pronounced influence on the dipole moments of the C-O bonds. Also, since the heavy metal atoms are more electronegative than the alkali metals (i. e.  $X_{Zn} = 1.2$ ,  $X_{Pb} = 1.5$ ,  $X_{Cu} = 2.2$ ,  $X_K = 0.8$  and  $X_{Na} = 0.9$ )<sup>40</sup> they will interact more strongly with the oxygen.





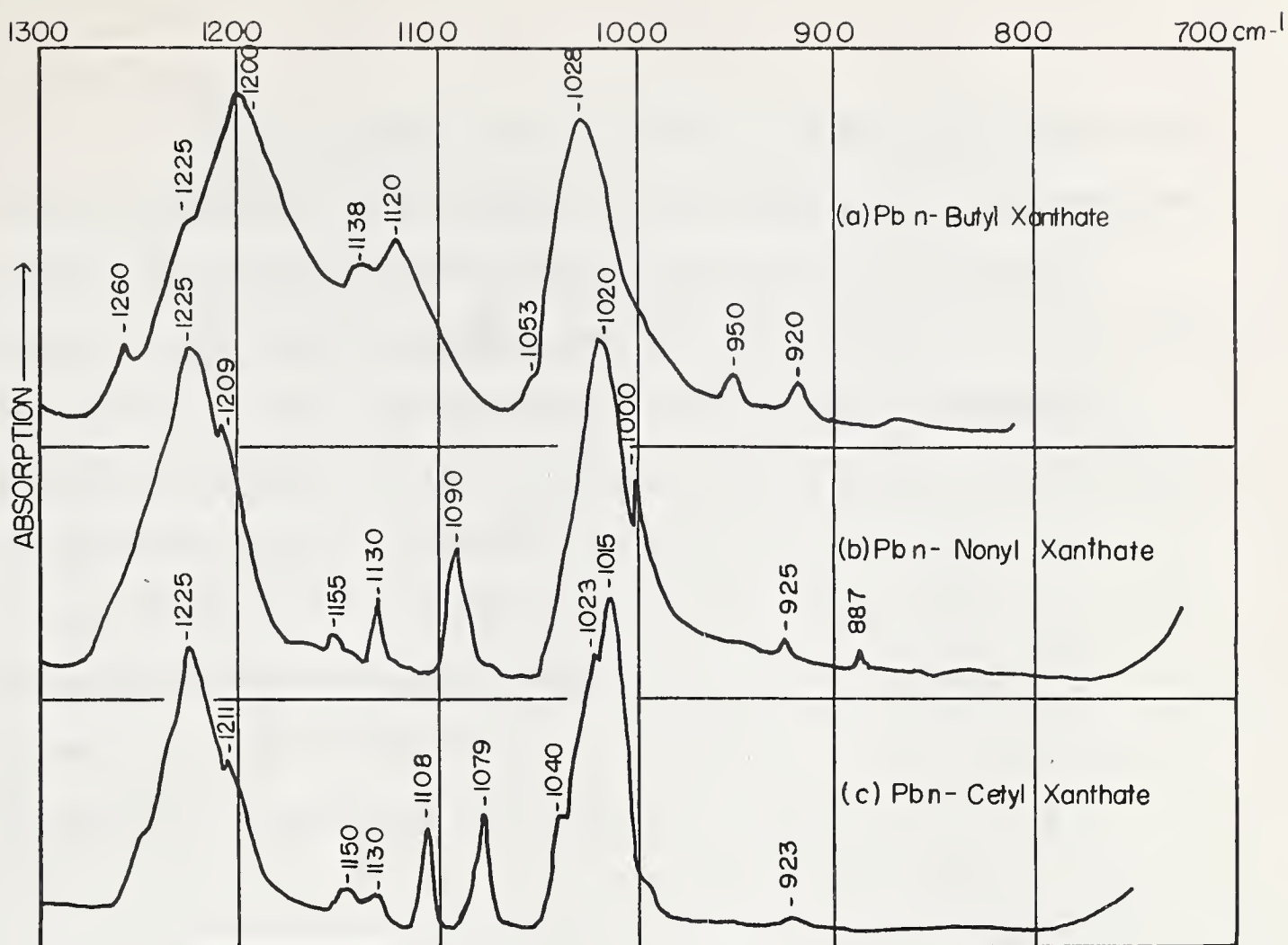
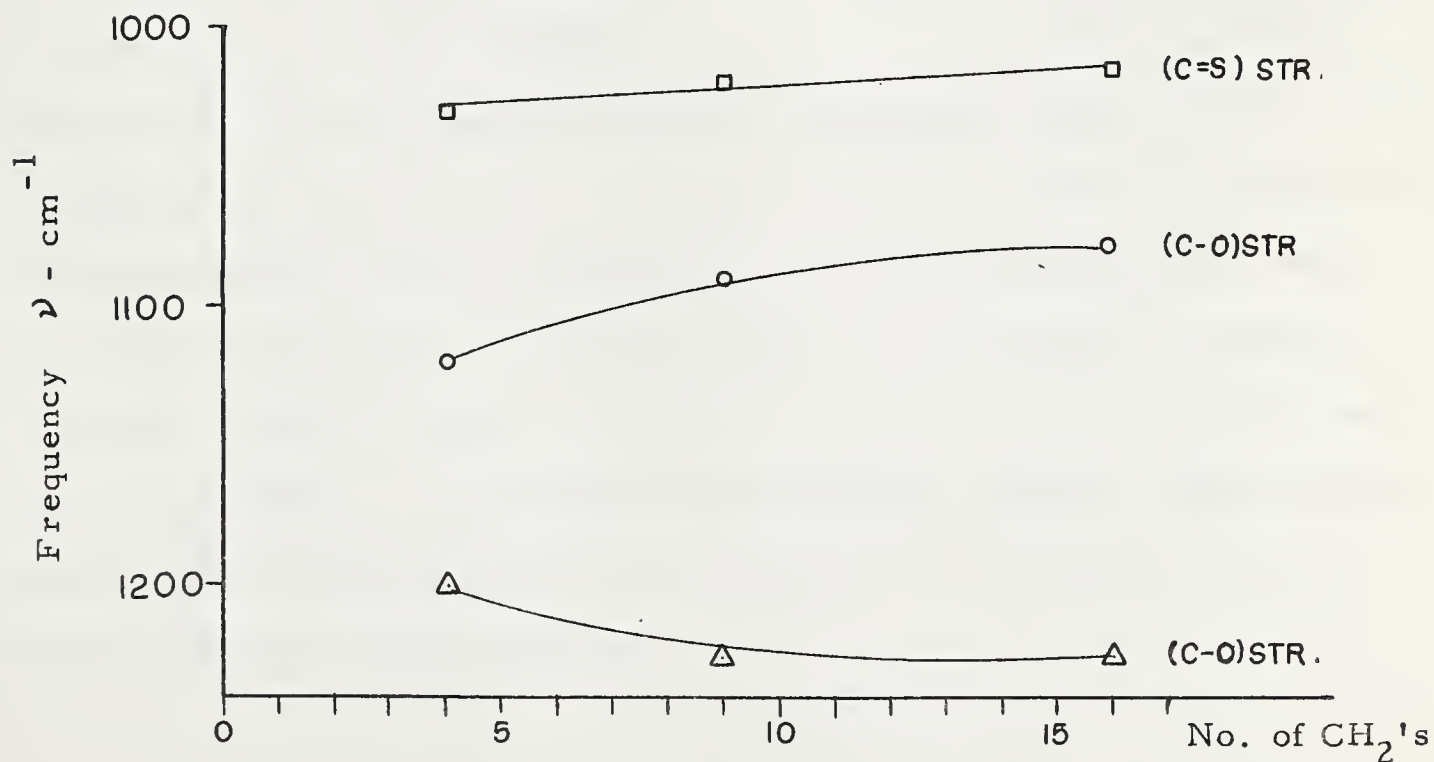


Fig. 17 Lead Alkyl Xanthates

Fig. 18 Lead Alkyl Xanthates:  
Group Frequency Shifts  
(Solid State Spectra)



A configuration, which satisfies both the mutual attractions of the hydrocarbon radicals and the requirement of a close association between the oxygen atoms and divalent metal atoms, is shown in Figure 19 and in the molecular model photograph of Figure 19A. In contrast to this, Figure 19B shows the type of unit cell configuration proposed by Hagiwara<sup>35</sup> on the basis of an X-ray study. This linear type configuration would not allow the metal atom to interact strongly with the oxygen atoms nor would it satisfy the mutual attractions of the hydrocarbon chains within each unit cell.

Additional evidence for the configuration given in Figures 19 and 19A is indicated by the ability of long-chain lead n-cetyl xanthates to spread at the air water interface

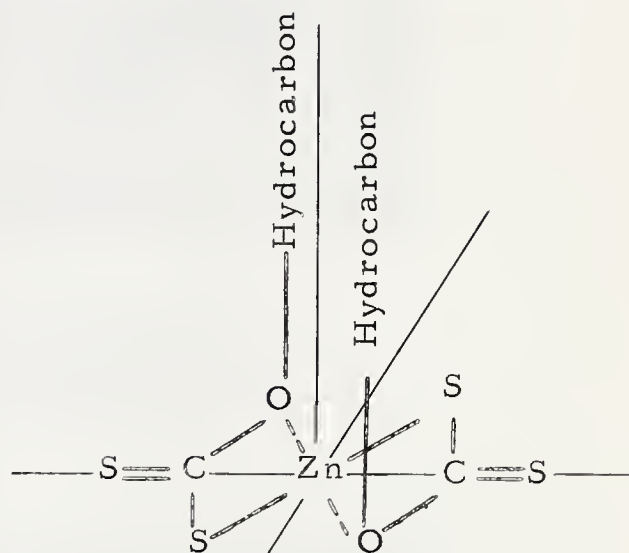


Fig. 19. Schematic Molecular Configuration of Zn Alkyl Xanthate

(described in the succeeding section on "Langmuir Blodgett Films"). This configuration allows the major portion of the polar group to reside in the water while both non-polar chains can protrude from the water. If the molecular configuration of divalent metal xanthates is that as shown in Figures 19 and 19A, the metal atom is confined between two sulphur and two oxygen atoms. A monovalent metal xanthate need not confine the metal atom to such a degree and thus the behaviors of the C-O bonds may be quite different in these two cases.





Fig. 19A      Molecular Models of  
Zinc n-Heptyl Xanthate and  
n-Heptyl Xanthate Anion

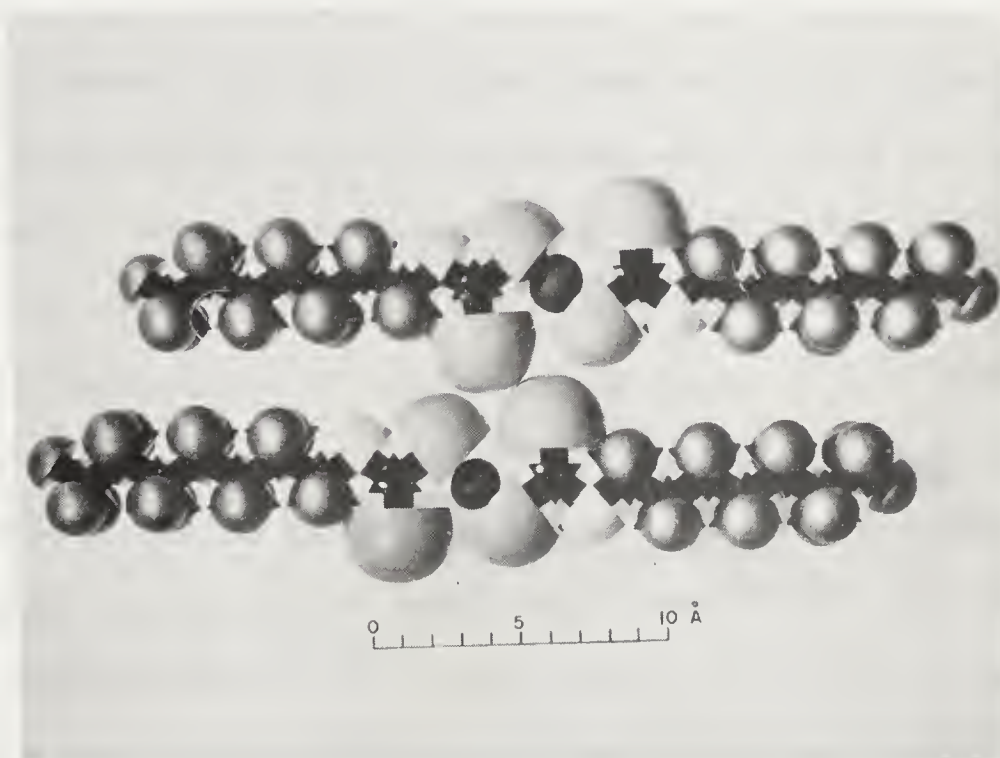


Fig. 19B      Molecular Model of  
Lead n-Heptyl Xanthate Unit  
Cell (After Hagihara<sup>35</sup>)





To investigate the influences of various metal atoms on the C-O bands, the spectra of several mono and divalent metal ethyl and n-butyl xanthates were recorded. Some of these are shown in Figures 20 and 21. Similarly to the spectra of zinc and lead xanthates, all other metal xanthates studied, except potassium and sodium xanthates, showed the high frequency C-O band to be the more intense and least affected by changes in the hydrocarbon radical. In esters the intense high frequency C-O band has previously been assigned to the "O-C" bond<sup>36</sup> (contiguous to the carbonyl group). Such an assignment for the heavy metal xanthates would necessitate a "crossing over" of the C-O and O-C band frequency positions with respect to their positions in the alkali metal xanthates. Graphs of group frequency shifts of metal ethyl and n-butyl xanthates, illustrating the proposed cross over of the C-O and O-C bands, are given in Figures 22 and 23. In these graphs the metal atoms have been characterized by the differences between their electronegativities and that of sulphur. In addition, a distinction has been made between monovalent and divalent metal xanthates. Electronegativity differences ( $X_S - X_{Me}$ ) were chosen for the abscissa scales since they are roughly proportional to the values of the dipole moments for the sulphur-metal bonds. These differences indicate also the partial ionic character of the sulphur-metal bond<sup>41</sup> as given in Table 3. As the covalent character of the metal sulphur bond is increased ( $K-S \rightleftharpoons 50\%$ ,  $S-S \rightleftharpoons 100\%$ ) the xanthate water solubility is progressively decreased<sup>42, 43, 44</sup>. Mercury xanthate is the one exception to this rule since it is even less soluble than copper xanthate. The explanation of this discrepancy may arise from the fact that mercurous compounds always contain pairs of mercury atoms and thus mercurous xanthate probably exists as  $Hg_2X_2$  (where X represents the xanthate anion).



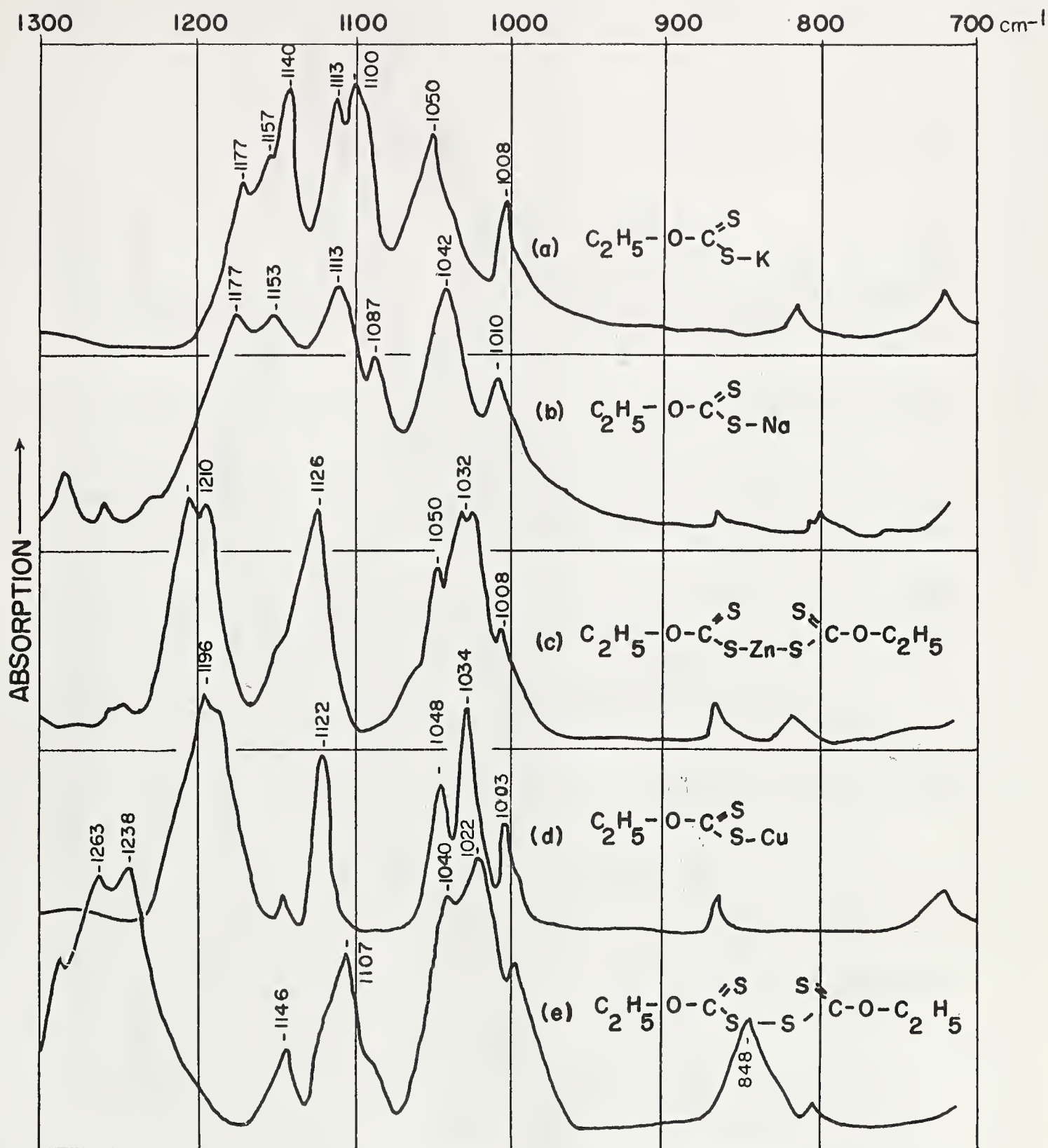


Fig. 20 Metal Ethyl Xanthates (Solid State Spectra)



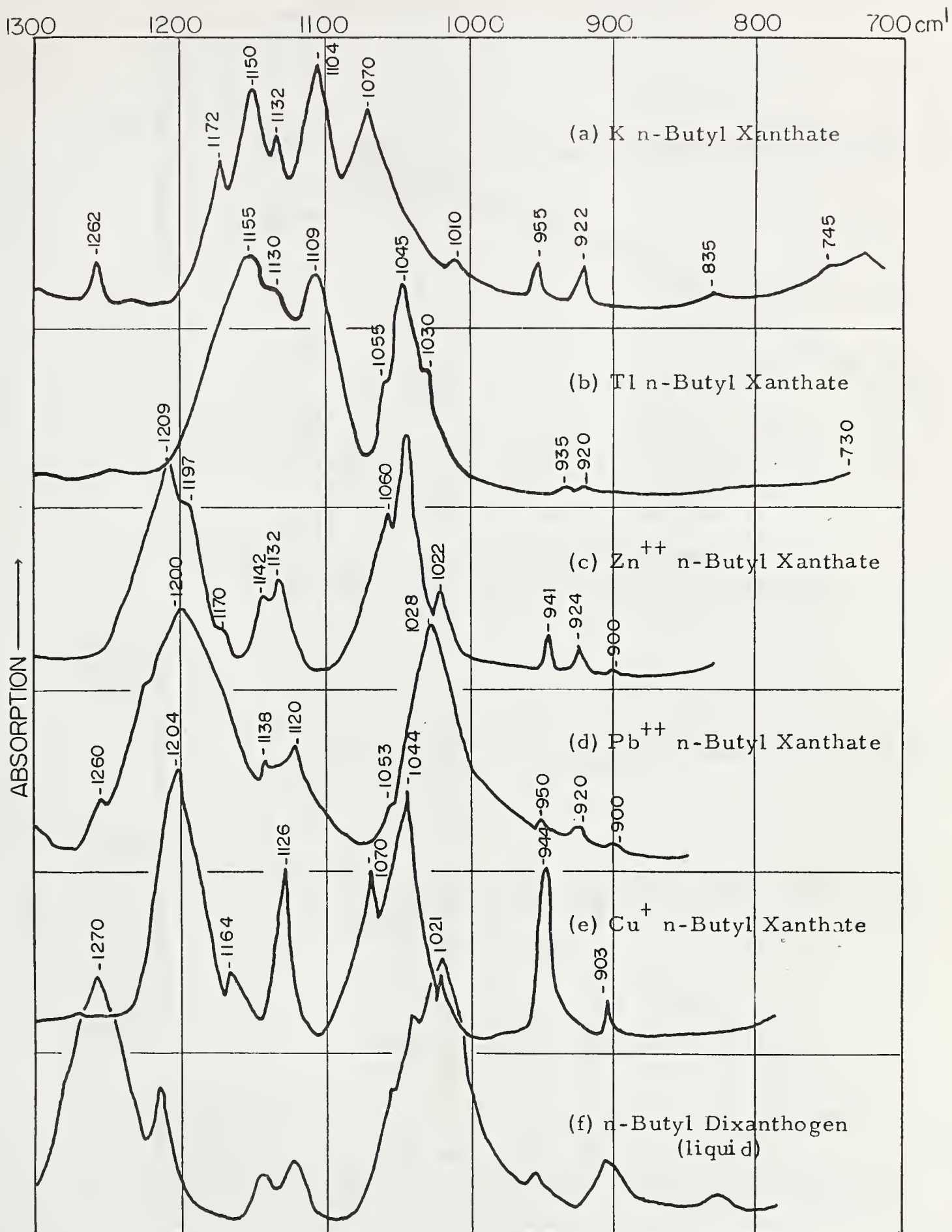


Fig. 21 Metal n-Butyl Xanthates





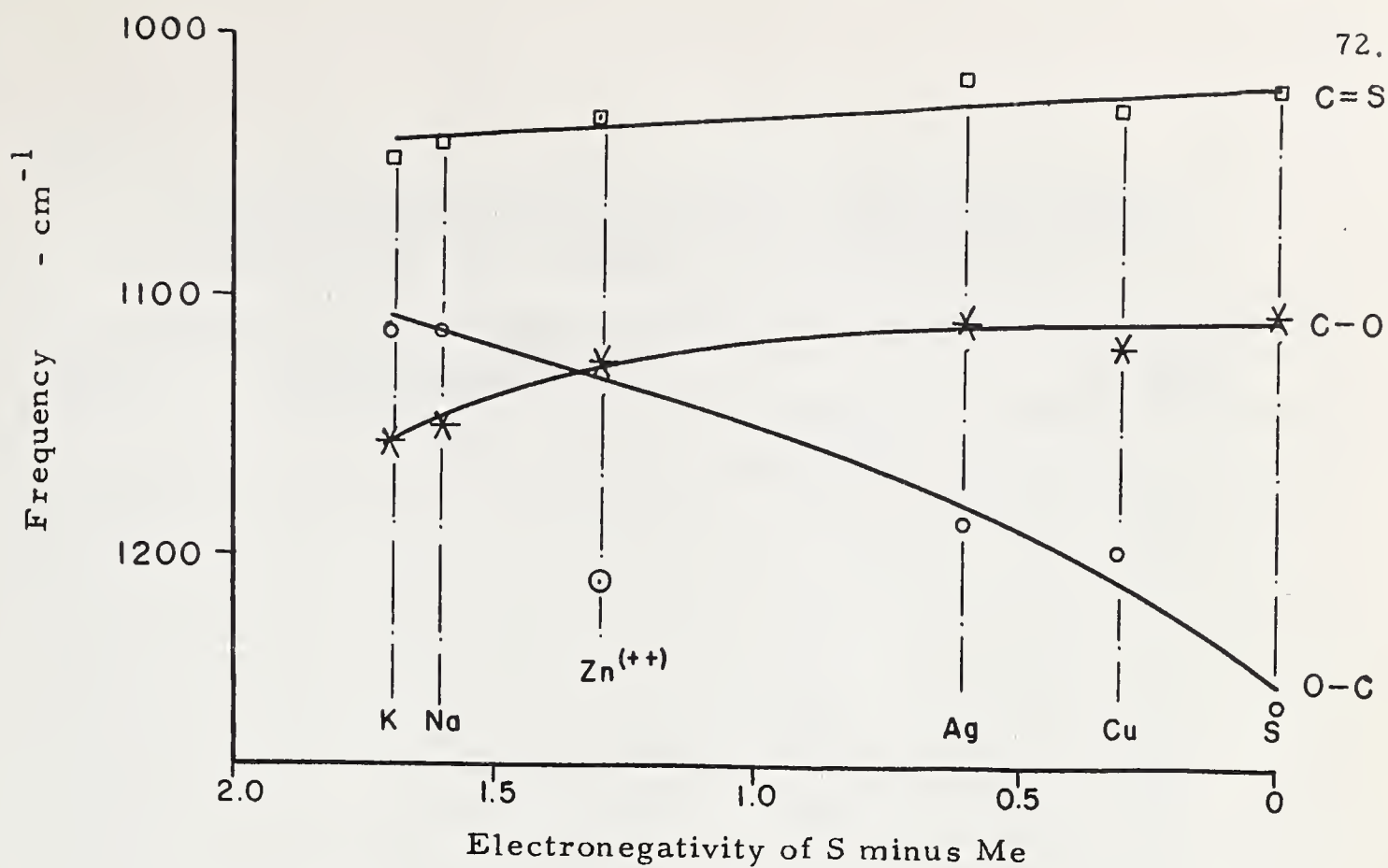


Fig. 22 Metal Ethyl Xanthates  
Group Frequency Shifts (Solid State Spectra)

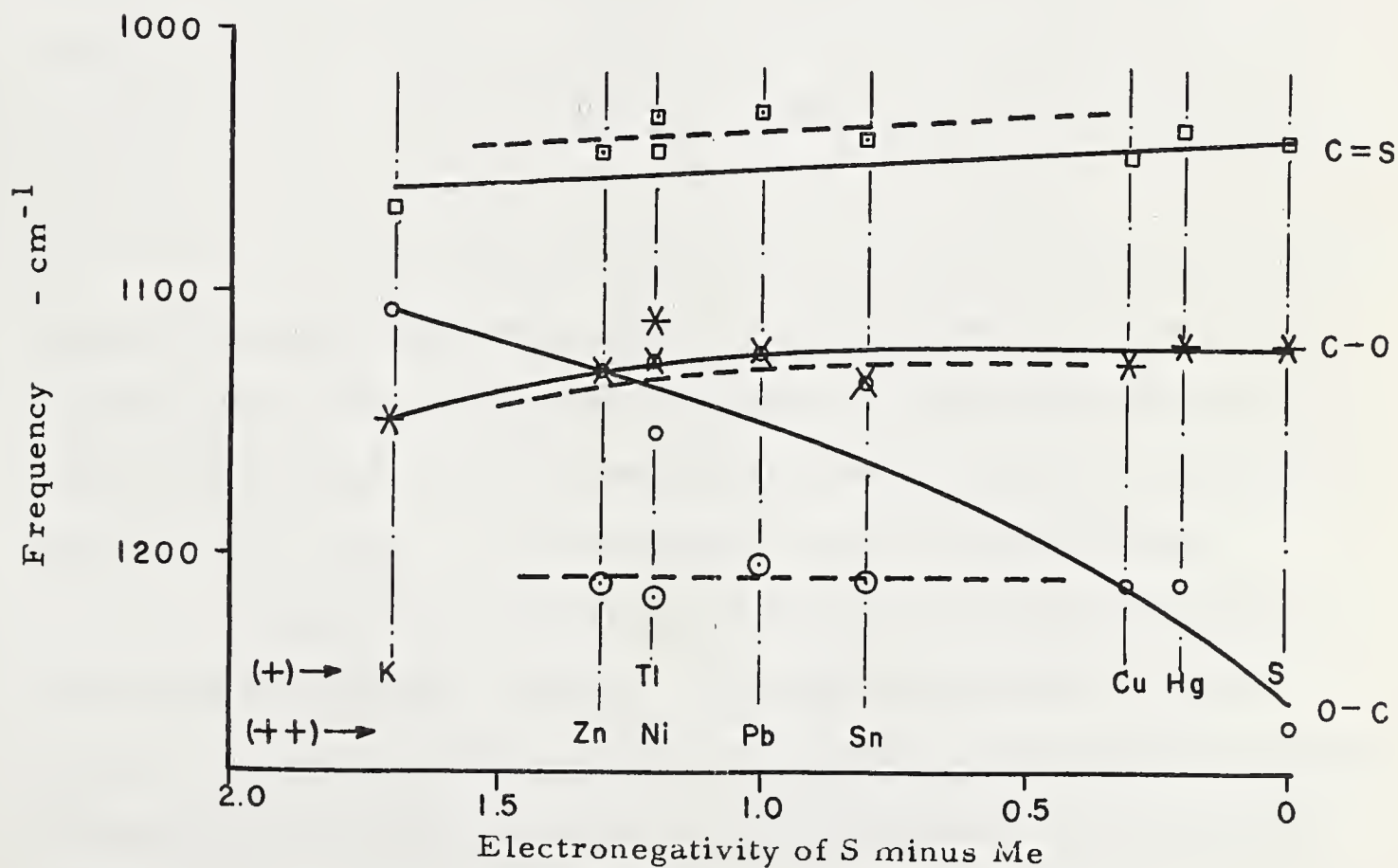


Fig. 23 Metal n-Butyl Xanthates  
Group Frequency Shifts (Solid State Spectra)





TABLE 3

ELECTRONEGATIVITY VALUES AND PARTIAL IONIC  
CHARACTER OF THE METAL-SULPHUR BONDS<sup>40, 41</sup>

Metal	Electronegativity $X_{Me}$	$X_S - X_{Me}$	S-Metal % Ionic Character
K ( <sup>+</sup> )	0.8	1.7	50%
Na ( <sup>+</sup> )	0.9	1.6	47
Hg ( <sup>+</sup> )	1.0	1.5	43
Zn ( <sup>++</sup> )	1.2	1.3	35
Ni ( <sup>++</sup> )	1.3	1.2	30
Tl ( <sup>+</sup> )	1.3	1.2	30
Pb ( <sup>++</sup> )	1.5	1.0	22
Sn ( <sup>++</sup> )	1.7	0.8	15
Ag ( <sup>+</sup> )	1.9	0.6	8
Cu ( <sup>+</sup> )	2.2	0.3	2
S ( <sup>-</sup> )	2.5	0	0

This may mean that the normal mercury electronegativity value is not representative of the "mercurous" linkages. In Figure 23, mercurous xanthate has therefore been located between copper xanthate and dixanthogen (i.e.  $X_S - X_{Hg} = 0.2$ ) to conform to the solubility sequence.

Figure 22 illustrates the proposed group frequency shifts for mono-valent metal ethyl xanthates. The band positions of zinc ethyl xanthate are also included to indicate that the two-chain molecular structure of xanthate has a marked influence on the band position of the one C=O group.



Figure 23 presents group frequency shifts for both mono and divalent metal n-butyl xanthates. (Represented in full and dotted lines respectively). The group frequency shifts for the monovalent metal butyl xanthates are seen to correspond well to those shown in Figure 22 for the similar ethyl xanthates. In addition the divalent metal xanthate "C=S" and "C-O" bands (marked  $\square$  and  $\otimes$  respectively) agree well with those of the monovalent metal xanthates. However, the frequencies of the "O-C" bands (marked  $\odot$ ) in the divalent metal xanthates, are markedly different from those of the monovalent metal xanthates. The divalent metal atoms appear not only to strengthen the "O-C" bonds but also to stabilize them. Further work is required to confirm the tentative assignments and explanations given above. To this end, the substitution of secondary and tertiary hydrocarbon chains should spread the oxygen and metal atoms further apart and thus decrease their interactions if the molecular configuration is that as proposed above. Additional work on the spreading of metal xanthates at the air liquid interface should also aid in the elucidation of their structures.

Organic Solvent Studies: With the recent publication of a paper by Bellamy<sup>34</sup> describing the identification of C=S absorption bands by a study of solvent effects, an attempt was made to apply this method to confirm our previous<sup>6</sup> C=S band assignment for xanthates. Zinc n-butyl xanthate, n-butyl dixanthogen and S-octadecyl O-octadecyl xanthate were studied in the same solvent sequence employed by Bellamy. Most of this work was conducted by Dr. L.H. Little while working with us for two months on this project. It will suffice to state that in general the frequency shifts of the bands attributed to the C=S groups were in accordance with



those found by Bellamy. The shifts were quite small, however, indicating that the polarity of the C=S group in xanthates is low. The (C-O) absorption band at about  $1200\text{ cm}^{-1}$  shifted to higher frequencies in the solvent sequence (from cyclohexane to  $(\text{CHBr}_2)_2$ ) thus eliminating it as a possible C=S band.

Thus, from this study, the C=S band assignment of  $1020\text{-}1070\text{ cm}^{-1}$  is fully confirmed.





## II. NATURE OF THE ADSORBENT

Due to hydration and oxidation, the mineral surface, offered to a xanthate molecule for adsorption, is seldom if ever that of the parent mineral. The adsorbing molecular species must either adsorb onto the oxidation product itself or react chemically with it thereby opening a path for other xanthate molecules to reach the parent mineral.

The following consideration will be limited to the study of a galena surface. A great number of investigations have been conducted on the physical and chemical states of galena surfaces by researchers interested in its flotation, smelting or photoconducting properties. In this regard there appears to have been little liaison between physicists studying the remarkable photoconductive properties of PbS (with its required sensitization by oxygen) and metallurgists interested in its flotation or smelting. Since chemisorption, oxidation and current conduction are all closely linked to electronic transfers and mobilities, these studies should be complementary.

The electron diffraction studies of galena surfaces by H. Hagihara<sup>45</sup>, conducted since 1950, have received widespread attention in the field of flotation. His electron diffraction patterns of galena, oxidized both in air and water, revealed that the lowest oxidation product was  $\text{PbSO}_4$  in all cases. If oxidation was prolonged or if the temperature was raised above  $250^\circ\text{C}$  the compound lanarkite ( $\text{PbO}\cdot\text{PbSO}_4$ ) was also detected. Both types of oxidation products were found to be oriented with respect to the PbS crystal substrate. Earlier electron diffraction work by H. Wilman<sup>22</sup> indicated that when the galena was baked in oxygen, lanarkite was the predominant oxidation product. Hagihara found that during



prolonged soaking of galena in water (i. e. up to 40 days) the  $\text{PbSO}_4$  was dissolved by the water, causing a roughening of the galena surface. The dissolved  $\text{PbSO}_4$  reacted with the carbon dioxide, dissolved in the water, to precipitate basic lead carbonate. According to Hagihara<sup>45</sup> and Taylor and Knoll<sup>46</sup> the rate of oxidation of galena is much faster in water than in air at room temperatures.

Taylor and Knoll<sup>46</sup> presented a hypothesis that compounds formed in the initial oxidation of galena are firmly held by the galena and that they are probably isomorphous with the "cubic" galena (bulk  $\text{PbSO}_4$  is normally orthorhombic). The electron diffraction work of Hagihara, however, did not indicate the presence of a "cubic" lead sulfate but it did show that the normal orthorhombic  $\text{PbSO}_4$  can orient itself in two ways each maintaining a close relationship between the agreement of atoms at the interface:  $\text{PbS/PbSO}_4$ .

The development of lead sulfide detectors with high photoconductive sensitivity and rapid response to radiation, in the wave length region of 1-3 microns, has provoked much interest in the mechanism of oxygen sensitization of this material. These detectors are made of thin films of PbS prepared either by chemical deposition<sup>25</sup> from a colloidal solution or by vacuum evaporation. In either case, the film consists mainly of oriented PbS crystallites of sizes varying from 100-1000 Å. Using electron diffraction, Wilman<sup>22</sup> showed the chemically deposited films to be initially free of oxidation while the evaporated films were always partially oxidized.

The generally accepted theories of photoconductivity involve the transference of an electron into a conduction band by excitation with an



optical quantum together with energy transference from the thermal energy of the lattice<sup>47</sup>. In pure materials the photo effect occurs at preferred lattice points such as vacant anion or cation sites or at interstitial ions. On a statistical thermodynamical basis, Schottky and Wagner<sup>48</sup> have shown that the free energy of a stoichiometric crystal is a minimum when a certain amount of disordering occurs. Stoichiometric lead sulfide has a low conductivity but the excess of either lead or sulfur converts it into a good semi-conductor (electron conduction = sulfur deficiency; positive hole conduction = sulfur excess).

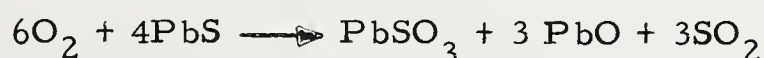
Evaporated PbS films have been found to be "n" type semi-conductors or in other words they are "electron conducting". Various workers<sup>49, 50</sup> have found that PbS films can be reversibly changed from "n" to "p" type (positive hole conducting) upon exposure to oxygen. The first chemisorption of oxygen onto electron conducting PbS causes a marked decrease in the conduction, which, upon increasing the oxygen pressure from  $10^{-5}$  mm Hg decreases steadily to a minimum and then increases again. Measurements<sup>49</sup> have shown that the thermoelectric effect changes in sign upon passing through the minimal value of conductivity. There is fairly conclusive evidence<sup>21, 51</sup> to show that the number of chemisorbed oxygen-electron acceptors adsorbed on evaporated PbS films is more than sufficient to trap out the entire free electron content of the film interior. Further, the ready reversibility of the conductivity on changing the conditions of oxidation, substantiates the photoconductivity theory based on chemisorption of oxygen rather than bulk diffusion of oxygen to lattice vacancies or imperfections. Minden<sup>52</sup> concludes that since evaporated PbS films consist of mirror-like layers of PbS ( $\approx 0.1$  thick) next to the substrate





with non-conducting layers on top of this, two photoconductive effects may be present. The mirror-like conducting layer consists of PbS microcrystals which can reversibly adsorb oxygen and then act as bulk acceptor impurities since the barrier formed is low and the Fermi level is altered throughout the crystal. Since the particle size of the outer PbS layer is relatively much larger, the adsorbed oxygen acts as a higher energy barrier to photoconductivity (i. e. a conducting "n" type interior surrounded by an insulating "p" type film). This theory has recently been upheld by R.H. Jones<sup>53</sup>. Minden<sup>52</sup> has calculated that the adsorption of oxygen as described above is energetically possible from a thermodynamic standpoint with a net free energy change of -0.4 eV (= -9 k cal/mole). At a pressure of  $1\mu$  Hg, oxygen gas is thus predicted to be nearly in equilibrium with oxygen ions adsorbed on the PbS. During the oxygen sorption tests, Minden<sup>21</sup> and Harada<sup>51</sup> found that considerable quantities of SO<sub>2</sub> were evolved and could be condensed out (the condensed gas was identified as SO<sub>2</sub> by vapor pressure measurements). When the SO<sub>2</sub> was frozen out of the system during the test, the mole ratio of O<sub>2</sub> adsorbed to SO<sub>2</sub> evolved was approximately 2:1 over a wide range of conditions: but, if the SO<sub>2</sub> was allowed to remain in contact with the PbS film during the sorption, very little SO<sub>2</sub> was evolved (i. e. ratio O<sub>2</sub>ads./SO<sub>2</sub> evolved  $\approx$  15). The kinetics of the O<sub>2</sub> adsorption, with SO<sub>2</sub> being frozen out, was first order in oxygen pressure. It was also shown that in the absence of oxygen no SO<sub>2</sub> was adsorbed by an evaporated PbS film.

Minden<sup>21</sup> tentatively proposed the following oxidation reaction to account for the observed 2:1 ratio of O<sub>2</sub> adsorbed to SO<sub>2</sub> evolved, viz.,







He was not, however, convinced of the existence of a surface  $\text{PbSO}_3 \cdot 3\text{PbO}$  compound.

Harada<sup>51</sup> considered the principal reactions to be:



He claims that most of the chemical reactions occur at the source during the evaporation and, since  $\text{PbSO}_4$  decomposes before evaporating, only Pb, PbS and PbO are able to evaporate onto the substrate.

Our infrared spectroscopic studies on PbS evaporated films indicate that the initial oxidation product of PbS is lead thiosulfate ( $\text{PbS}_2\text{O}_3$ ). Both films evaporated onto aluminum mirrors (for use in the reflectance technique) and films evaporated onto salt windows (for transmission studies) gave spectra identical to that shown in part (a) of Figure 24. Below spectrum (a) are shown the spectra of (b)  $\text{PbS}_2\text{O}_3$ , (c)  $\text{PbSO}_4$ , (d)  $\text{PbO} \cdot \text{PbSO}_4$  which were all high purity reagent grade materials. The spectrum of pure PbS shows no absorption bands in this region ( $1300\text{--}700 \text{ cm}^{-1}$ ) as determined by A. F. Gibson<sup>54</sup> on single crystals of PbS. Numerous other lead compounds such as PbO,  $\text{Pb}_3\text{O}_4$ ,  $\text{PbCO}_3$ ,  $2\text{PbCO}_3$ ,  $\text{Pb}(\text{OH})_2$ , etc. have been eliminated as the predominant oxidation species largely on the basis of their infrared spectra. The spectral differences shown in Figure 24 between  $\text{PbS}_2\text{O}_3$  and  $\text{PbSO}_4$  are in general agreement with similar spectra presented by Mme. T. Dupuis<sup>55</sup>.



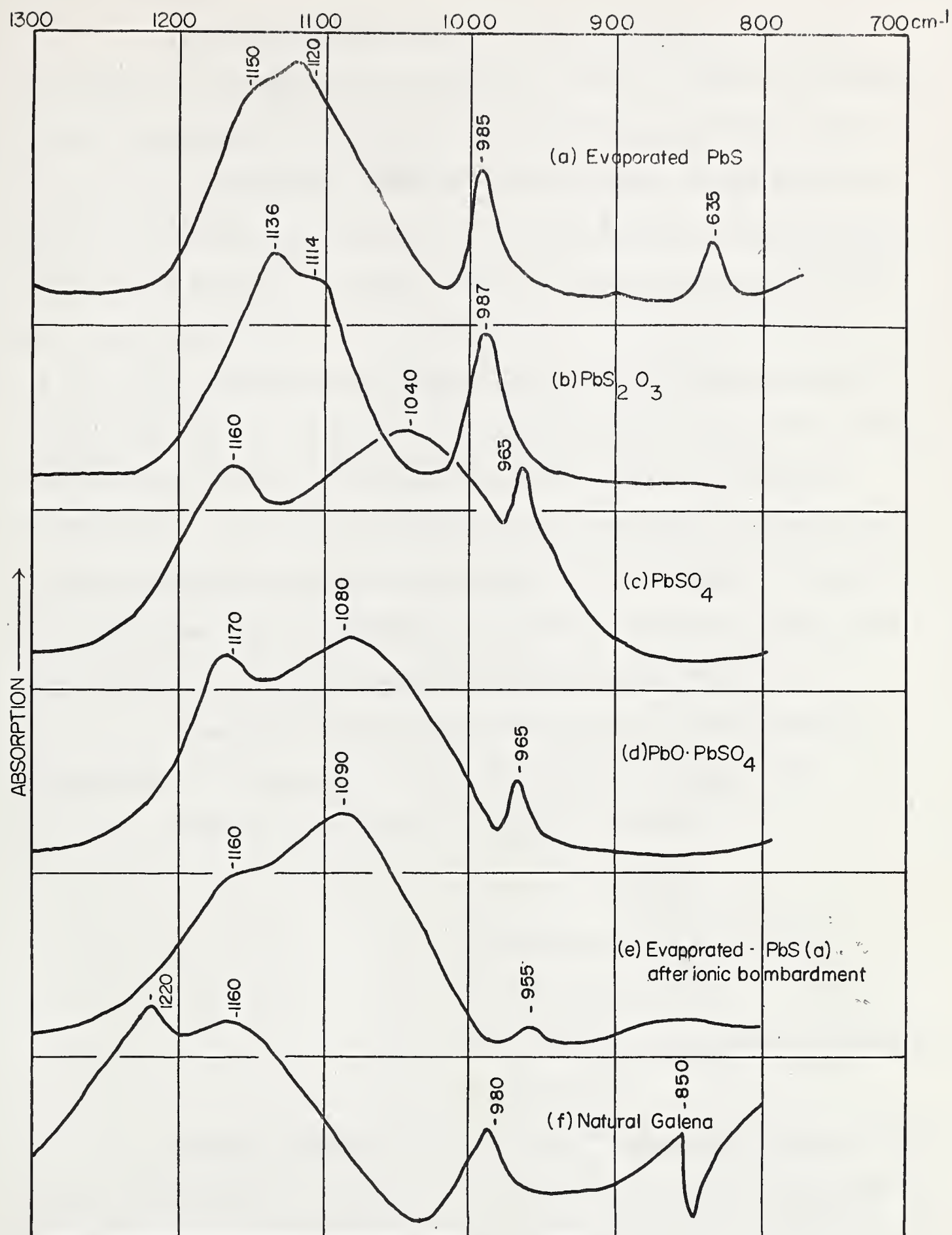


Fig. 24 Lead Sulfide and Oxidation Products



It was found that exposure of the evaporated film to ionic bombardment, in the vacuum evaporation chamber, resulted in a definite shift of the spectrum toward that of lanarkite (Spectrum (d) ) as shown in Spectrum (e) of Figure 24. The ionic bombardment treatment utilized a 1000 v ac potential at a current of 10 ma over an area of approximately  $30 \text{ cm}^2$  for a period of 1/2 hour. Since the accelerating potential was only 1000 volts compared to 35-50 kilo-volts in electron diffraction cameras it is possible that although  $\text{PbS}_2\text{O}_3$  may have been the initial oxidation product in Wilman's and Hagihara's work, the incidence of the electron beam may have resulted in further oxidation to  $\text{PbSO}_4$  or  $\text{PbO} \cdot \text{PbSO}_4$ . Numerous investigators have reported on the caution that must be employed in examining compounds of low stability by electron microscopy and electron diffraction, particularly when the compounds being studied are not bulk phases but rather surface films<sup>23</sup>.

Heavens<sup>23</sup> gives an approximate formula for the rise in temperature of a sample in an electron diffraction camera, viz.,

$$\text{Rise in temperature} = \frac{2 \times 10^3 i V d}{\lambda A} \quad (^\circ\text{C})$$

where  $i$  = beam current in amp.

$V$  = accelerating potential in volts

$d$  = film thickness in cm.

$\lambda$  = mean free path of electrons in the sample

$A$  = irradiated area.

Although Hagihara<sup>45</sup> and Wilman<sup>22</sup> have given only accelerating potentials (35-65 k-volts), a calculation of the order of magnitude of sample temperature rise can be made, viz.,





If:  $V = 50,000$  volts

$i/A = 5 \mu$  Amp./cm. (typical for electron diffraction)

$d = 100 \text{ \AA}$

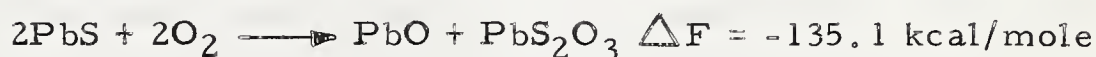
$\lambda = 500 \text{ \AA}$  (estimation for galena - error probably  $\pm 200 \text{ \AA}$ )

$$\begin{aligned} \text{Therefore: Rise in temp.} &= \frac{2 \times 10^3 \times 5 \times 10^{-6} \times 5.0 \times 10^4 \times 100}{500} \\ &= 100^\circ \text{ C.} \end{aligned}$$

According to J. W. Mellor<sup>56</sup>, decomposition of  $\text{PbS}_2\text{O}_3$  begins at about  $100^\circ \text{ C}$  in air. The reaction was represented as

$4\text{PbS}_2\text{O}_3 \longrightarrow \text{PbS} + 4\text{S} + 3\text{PbSO}_4$ . Lead sulphate decomposes at approximately  $1000^\circ \text{ C}$  which explains why this material would persist.

A possible oxidation mechanism, which would produce  $\text{PbS}_2\text{O}_3$ , is as follows:



For the production of  $\text{PbSO}_4$  the following reaction is normally considered typical:



Further oxidation produces  $\text{PbO} \cdot \text{PbSO}_4$  with  $\Delta F^\circ = -260 \text{ kcal/mole}$ .

Many other workers have claimed to have found thiosulfates as oxidation products of metal sulfides<sup>57, 58, 59</sup>.

Taylor and Knoll<sup>46</sup> found that the addition of high concentrations of xanthate liberated (among other ions)  $\text{S}_2\text{O}_3^{2-}$  ions from the surface of galena. Plante and Sutherland<sup>59</sup> found thio-salts present in an alkaline aqueous suspension of galena, but not in a slightly acid suspension.



Spectrum (f) of Figure 24 shows the infrared spectrum of freshly polished natural galena recorded with the use of the reflectance attachment. With the exception of the  $980\text{ cm}^{-1}$  absorption band the bands do not correspond to any of the other spectra (a to c). It does, however, more closely resemble that of the thiosulfate shown in spectrum (b). Since a microscopic examination of the polished galena revealed considerable intergranular quartz which has absorption in this region the predominant band at  $1220\text{ cm}^{-1}$  may be due to the impurity and not the surface oxidation product of the galena.

A curious phenomenon exhibited in spectrum (f) at about  $850\text{ cm}^{-1}$  is that of the "Christiansen Filter Effect"<sup>60</sup>. This phenomenon is related to anomalous dispersion occurring either when the refractive index of the solid becomes equal to that of the surrounding medium or when the refractive index of the material changes rapidly and discontinuously due to the excitation of an electronic transition by the incident light. This phenomenon is generally observed in the vicinity of an absorption band of the material. No attempt has been made to correlate this with the photoconductive properties of galena but presumably this could be done.

In summary, the oxidation of evaporated films of galena is initiated by the adsorption of oxygen atoms (or adsorption of oxygen molecules which subsequently dissociate into atoms) which are then ionized by the trapping of electrons from the interior. The oxygen adsorbs preferentially onto S atom sites forming  $\text{SO}_2$  which can remain in a mobile adsorbed state or be evolved depending on the concentration gradients involved. The  $\text{SO}_2$  interacts with adsorbed Pb-O and S-O groups to form  $\text{PbS}_2\text{O}_3$  which is quite stable in air at ordinary temperatures but which can



be further oxidized to  $\text{PbSO}_4$  and  $\text{PbO} \cdot \text{PbSO}_4$  upon ionic or electronic bombardment in a vacuum or possibly by contact with water having a high dissolved oxygen content.

Specific Density and Area of PbS Evaporated Films: A typical deposit of PbS, evaporated onto an aluminum mirror substrate, was treated as follows to determine the average film density. (As previously described the deposit consisted of a sooty-type layer of PbS on top of a mirror-like layer of PbS.)

Procedure and Data:

1. Geometrical area of mirror covered by  
PbS film . . . . . =  $30.0 \text{ cm}^2$
2. Weight of mirror plus film . . . = 12.0424 gms.
3. Weight of mirror plus shiny PbS film  
remaining after sooty PbS carefully  
wiped off . . . . . = 12.0393 gms.
4. Weight of mirror substrate alone after  
shiny PbS film removed by  $\text{HNO}_3$  = 12.0345 gms.

Therefore: Weight of sooty PbS . . . . . = 3.1 mgms.  
Weight of shiny PbS . . . . . = 4.8 mgms.  
Total weight of PbS film . . . . . = 7.9 mgms.  
Average density of PbS film . . =  $\frac{7.9}{30} = 0.26 \text{ mg/cm}^2$ .

Specific Surface Area Calculation: According to R.H. Harada<sup>51</sup> the average specific surface area of a freshly evaporated PbS film is about  $63 \text{ m}^2/\text{gm}$ . corresponding to a particle size of  $130 \text{ \AA}$ . Wilman<sup>22</sup> has given a mean crystallite size of  $150\text{-}500 \text{ \AA}$  for evaporated PbS films. The agreement is good considering that Harada's value was determined by a





B.E.T.<sup>61</sup> krypton gas adsorption technique while Wilman used an electron microscope.

If, on the basis of the above information, an average particle size of 300 Å<sup>0</sup> is assumed for the sooty type deposit, this corresponds roughly to a specific surface area of  $3 \times 10^5$  cm<sup>2</sup>/gm (30 m<sup>2</sup>/g). Since the density of the sooty PbS deposit was found to be 3.1 mgms. per 30 cm<sup>2</sup> geometrical area, the ratio of the sooty particle surface area to the geometrical area of the mirror substrate becomes:

$$\frac{3.1}{30} \times 3 \times 10^2 = 31 \text{ cm}^2 \text{ per cm}^2.$$

In addition to this, the mirror-like PbS would contribute to the specific surface area of the deposit. However, this contribution is assumed to be small compared to the specific surface area of the sooty deposit and shall thus be neglected.

Therefore a specific surface area of 30 cm<sup>2</sup> per cm<sup>2</sup> geometrical area will be considered as typical for the evaporated PbS films used as adsorbents. Future study of such films using both gas adsorption techniques (B.E.T. method) and electron microscopic techniques are planned to verify the above result.





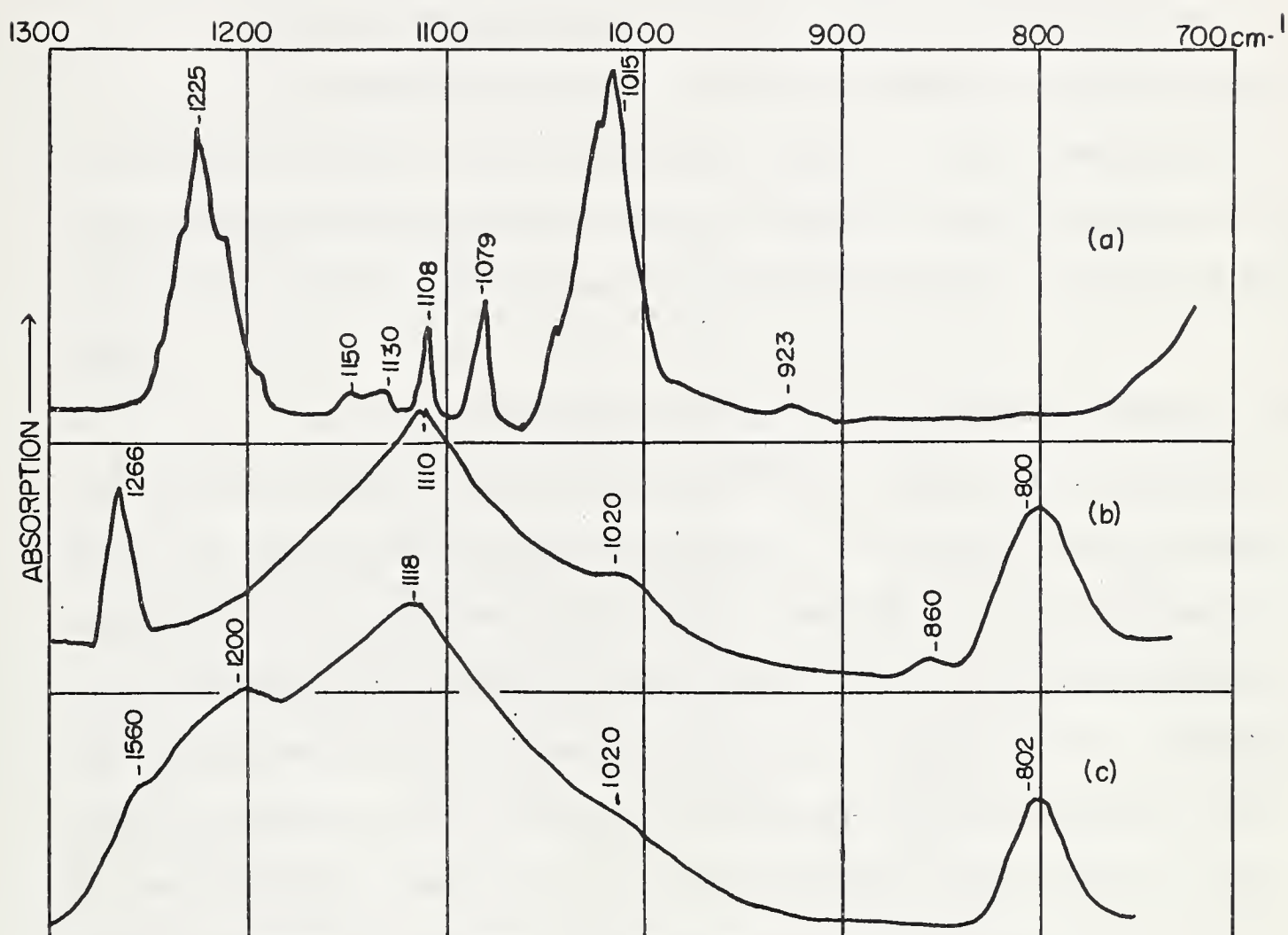
### III SPECTRA OF LANGMUIR BLODGETT MONOLAYER DEPOSITS ON ALUMINUM MIRRORS

To insure that the spectrophotometer equipped with the reflectance attachment was capable of producing reasonable absorption bands from monolayer deposits, such films were deposited onto aluminum mirrors and their spectra recorded. The procedure used in depositing these films has been described in "Experimental Procedures".

Lead n-cetyl xanthate has been spread at the air-water interface, from a benzene solution, and deposited on front surface aluminum mirrors as oriented monomolecular films. Preliminary results indicate that such films are highly compressible, perhaps as a result of the initial random orientation of the hydrocarbon chains. The films were deposited at a film pressure of 12 dynes per cm. and at this pressure the area occupied per molecule was calculated to be about  $30 \text{ \AA}^2$ . The area occupied by the polar group of the zinc n-heptyl xanthate molecular model, having the configuration shown in Figure 19A, was measured to be about  $35 \text{ \AA}^2$ . Further work is required to establish the areas occupied by various metal xanthate molecules in the hope of elucidating their possible molecular configurations.

The spectrum of a monolayer of lead n-cetyl xanthate, deposited on aluminum mirrors under the conditions given above, is shown in Figure 25 (b). This spectrum was recorded versus two clean aluminum mirrors in the reflectance attachment at an ordinate scale expansion factor of 10X. The spectrum of the deposit on the aluminum mirrors was the same as that shown in (b) both immediately after drying and after two weeks exposure to the atmosphere. This indicates that if there were any decomposition or oxidation of the monolayer it must have occurred during the overnight drying of the film in a desiccator.





(a) Bulk Pb n-Cetyl Xanthate at 1X  
 (b) Monolayer Pb n-Cetyl Xanthate at 10X  
 (c) = (b) after 40 mins. Ionic Bombardment

Fig. 25 Infrared Spectra of Lead n-Cetyl Xanthate Monolayers



The spectrum of bulk lead n-cetyl xanthate (randomly oriented in a nujol mill) is shown in spectrum (a) of Figure 25. The band assignments for this spectrum are:

C=S Stretching mode at  $1015\text{ cm}^{-1}$

C-O Stretching modes at  $1225\text{ cm}^{-1}$  and  $(1108-1079)\text{ cm}^{-1}$

The marked dissimilarity of the two spectra (a and b) may be due to decomposition and/or orientation effects. Francis and Ellison<sup>62</sup> have calculated the effect of the angle of incidence of the light beam on the interaction between the radiation and oriented molecules deposited on mirrors.

If the incident beam should strike the surface normal to it, the reflected and incident light would be  $180^\circ$  out of phase and thus produce a "node" or zero electric field at the surface. The dipole moment changes of the molecules adsorbed at the surface would not therefore interact with this radiation and no absorption bands would occur. Francis and Ellison showed that since, with oblique incidence of the beam, the field associated with the radiation would effectively be perpendicular to the surface, only the perpendicular component of the dipole moment of the molecule would effectively absorb radiation. Vibrational modes producing dipole moment changes parallel to the surface would therefore appear very weak in the spectrum. It is to be noted that this condition applies only to oriented molecular films such as Langmuir-Blodgett films deposited on mirrors. It is probable that xanthate molecules adsorbed from solution onto evaporated galena films (crystallites) will show no orientation effects.

If the lead n-cetyl xanthate has a molecular configuration similar to that shown in Figures 19 and 19A, the dipole moment changes associated with stretching of the C=S groups and C-H groups would be





parallel with the surface and thus would be expected to be very weak (assuming that the molecules are oriented perpendicularly to the mirror surface). Spectrum (b) of Figure 25, shows only a weak shoulder at  $1020\text{ cm}^{-1}$  which may therefore be due to the stretching of the C=S group. Strong intermolecular interactions may have caused the O-C band to shift from  $1225\text{ cm}^{-1}$  to  $1266\text{ cm}^{-1}$  (from spectrum a to spectrum b) but the broad strong band at  $1110\text{ cm}^{-1}$  is somewhat puzzling as is the appearance of the strong band at  $800\text{ cm}^{-1}$ . A study of the possible molecular packing using models as shown in Figure 19A indicates that the C-O band adjacent to the hydrocarbon chain is more "open" to interaction with neighboring molecules. This may partially account for the broadening and increased intensity of the  $1110\text{ cm}^{-1}$  band. Further study of these films is required before definite conclusions can be reached.

For interest's sake, the spectrum of the lead cetyl xanthate film after subjection to 40 minutes of ionic bombardment, is shown in (c) of Figure 25. No explanation is tendered for the appearance of the  $1200\text{ cm}^{-1}$  band.



#### IV INFRARED SPECTRA OF XANTHATES ADSORBED ONTO SULFIDE MINERALS FROM THE SOLUTION PHASE

Work on this phase of the project has met with some success only very recently, with the use of the reflection technique and consequently the results reported herein are of a preliminary nature. The spectral studies were confined to the NaCl region of the spectrum ( $4000 - 650 \text{ cm}^{-1}$ ) and therefore only absorption bands associated with bonds within the molecules are considered. Future studies will continue this work and extend the region to lower frequencies where it is hoped the metal-sulfur absorption bands will be found. Recently Miller et al<sup>63</sup> have assigned a band at  $349 \text{ cm}^{-1}$  in the spectrum of cinnabar to the covalent Hg-S bond.

##### A. Preliminary Attempts:

The attempts at infrared spectroscopic adsorption studies using the copper foil cell, sulfide mineral sols, and pressed disks of precipitates, which were unsuccessful, have been sufficiently described in the "Experimental Procedures" section of this thesis.

Adsorption studies using radiation transmitted through evaporated metal sulfide films were abandoned in favor of the reflection technique, largely due to the interfering reactions occurring on the substrate material. This interfering effect (previously mentioned in describing the experimental procedures in recording solution spectra) has been a major impediment in this investigation. Whenever a xanthate organic solvent solution came into contact with an infrared transmitting (halide) window a slow decomposition reaction occurred. Considerable effort was spent in attempting to both identify the reaction product and determine a possible mechanism for the reaction. In all cases when an organic solvent



solution of potassium xanthate was left in contact with  $\text{NaCl}$ ,  $\text{CaF}_2$  or  $\text{BaF}_2$  for a considerable period of time (20 mins. - 2 days) the infrared spectra of the reaction products were the same.

A typical spectrum of the reaction product is shown in Figure 26 (a) and was obtained by soaking a  $\text{NaCl}$  window in a near saturated solution of Kn-butyl xanthate in butyl alcohol for approximately one day after which the  $\text{NaCl}$  window was removed and thoroughly washed in butyl alcohol. This spectrum is typical of the reaction products obtained using either Kn-Butyl Xanthate or Kn-Nonyl Xanthate in acetone, benzene or alcohol solutions. The spectrum of potassium thiosulphate is shown below that of the reaction product, and of numerous compounds studied (by their infrared spectra)  $\text{K}_2\text{S}_2\text{O}_3$  was the only one that proved nearly identical to the reaction product. The appearance of potassium thiosulfate as a decomposition product of potassium xanthates has been mentioned previously<sup>64</sup>. Sulfides, in the presence of alkyl halides, form sulphonium salts and further oxidation can produce sulfoxides or sulphones. The mechanism of the oxidation may be; first, formation of dixanthogen (the oxidation product of xanthate) which is further oxidized on the surface of the halide to form the thiosulfate.





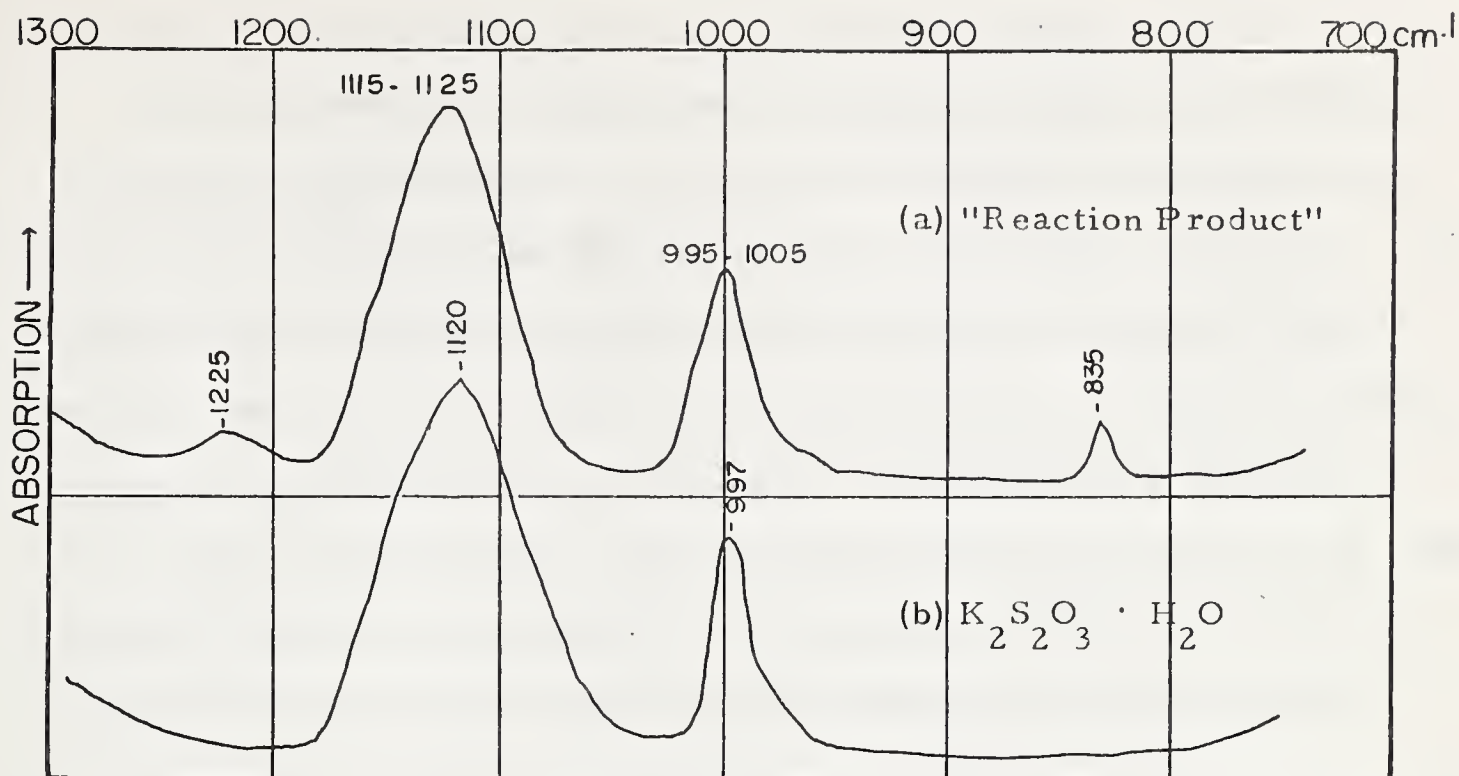


Fig. 26 Spectra of Xanthate "Reaction Product" and  $K_2S_2O_3$

### B. Multiple Reflection Studies

As previously described, galena was evaporated onto aluminum mirrors and attempts were made to record the spectra of monolayer xanthate adsorption on these films by the reflection technique.

The spectra of Langmuir-Blodgett monolayer deposits, using this same technique, have illustrated that the sensitivity of the instrument should be sufficient to detect less than a compact monolayer adsorption coverage. Since the specific surface area of the PbS deposit is about 30 times the geometrical area, adsorbed monolayer patches covering only 1/10 of the surface area available should be detectable.

The following procedure was adopted in studying the adsorption of potassium n-nonyl xanthate on an evaporated PbS film. Figure 27 presents the spectra related to the treatment sequence described below.





- (1) Fresh PbS precipitate was evaporated onto carefully cleaned aluminum mirrors (cleaned by acetone then by prolonged ionic bombardment) at a vacuum of approximately  $5 \times 10^{-6}$  to  $10^{-6}$  mm Hg. The spectrum was recorded immediately upon completion of the evaporation. In one case, the spectrum was recorded immediately after evaporation (approximately 1 minute) and then re-recorded continuously for nearly an hour to study any change in the oxidation state of the film. No changes were detected. A typical spectrum of freshly evaporated PbS is shown in Figure 27 (a). Note that this spectrum corresponds to the spectrum of  $\text{PbS}_2\text{O}_3$  in Figure 24.
- (2) To remove any hydrocarbon surface contamination which may have occurred in the vacuum evaporation, the film was then soaked for 1 hour in warm acetone, dried and its spectrum again recorded. (See spectrum (b) ). Note that the weak bands at  $1260$  and  $900\text{ cm}^{-1}$  have been eliminated.
- (3) The cleaned PbS film was then soaked in a warm, near saturated solution of potassium n-nonyl xanthate in acetone for 1 hour, removed, thoroughly washed in warm acetone, dried and its spectrum immediately recorded. (See spectrum (c) ). Two very weak additional bands appear at  $1248\text{ cm}^{-1}$  and  $1040\text{ cm}^{-1}$  which may be due to adsorbed xanthate C-O and C=S stretching modes respectively. No carbon-hydrogen stretching bands could be detected in spectrum (c). It was expected that the C-H stretching bands would be weak compared to either the C-O or C=S stretching bands and since the  $1248$  and  $1040\text{ cm}^{-1}$  bands are very weak the C-H bands may not have been detectable. Since the film did not exhibit a hydrophobic character after prolonged treatment, if any xanthate did adsorb it must have been a small fraction of a monolayer since 5-10% coverage should have produced a definite bubble contact angle.



(4) The above film was then soaked for 1 hour in an aqueous solution of

K n-nonyl xanthate, removed, thoroughly washed in water and its spectrum recorded (See spectrum (d) ). This spectrum is identical to that of bulk lead nonyl xanthate (see spectrum (b) of Figure 18). Note in particular, that the strong bands due to the oxidation product ( $\text{PbS}_2\text{O}_3$ ) at 1130 and  $\sim 1000 \text{ cm}^{-1}$  have completely disappeared. It would appear that the xanthate anions reacted with the lead sulphide oxidation product to form lead xanthate multilayers. The absorption bands of lead n-nonyl xanthate cannot be ascribed to a monolayer coverage because of their high intensities. (Note spectrum (d) was recorded at 1X ordinate scale expansion while the others shown in Figure 27 were recorded at 5X expansion factors).

(5) In an attempt to wash away the lead xanthate multilayers, the sample

from step (4) was next washed in hot acetone for nearly two hours after which spectrum (e) resulted. This spectrum is no longer exactly that of bulk lead nonyl xanthate for the one C-O stretching band is now at  $1187 \text{ cm}^{-1}$ . The absorption band intensities are approximately 1/3 those of spectrum (d).

(6) The samples were soaked an additional 16 hours in acetone after which

the solid line spectrum of (f) resulted. Again the band intensities were diminished approximately three times (i.e. 1/3 those of spectrum (e) ). The important features of this spectrum are, firstly, the appearance of 1133 and  $983 \text{ cm}^{-1}$  bands, which are presumably due to partial oxidation of the galena surface and secondly, the appearance of weak bands at 1260, 1240 and  $1070 \text{ cm}^{-1}$ . These bands have intensities in the range expected from the first monolayer of adsorbed xanthate but no definite conclusions can as yet be made.





Figure 27 Captions

- (a) Freshly evaporated PbS films.
- (b) PbS films washed in acetone 1 hour (spectrum identical to  $\text{PbS}_2\text{O}_3$ ).
- (c) Treated in K n-nonyl xanthate-acetone solution for 1 hour.
- (d) Treated in aqueous solution K n-nonyl xanthate for 1 hour (Spectrum identical to Pb N-nonyl xanthate).
- (e) Washed in hot acetone for 2 hours.
- (f) Solid Line Spectrum: Samples washed additional 16 hours in acetone.  
  
Dotted Line Spectrum: Exposed to atmosphere for 2 days.
- (g) Sample washed in pyridine 3 hours.



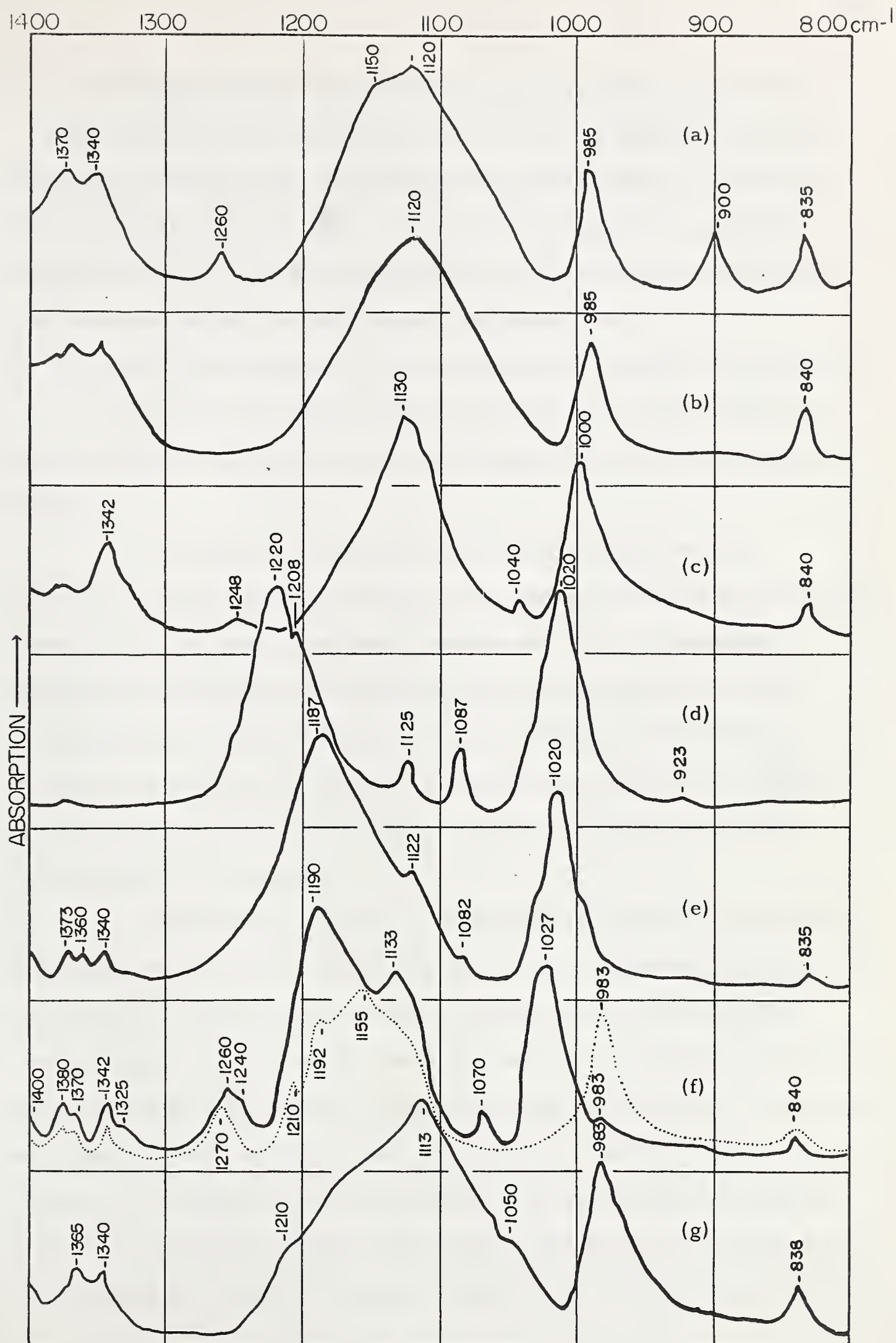


Fig. 27 Adsorption of Kn-Nonyl Xanthate onto Evaporated PbS Film



(7) The dotted line spectrum of (f) is that of the sample from (6) after exposure to the atmosphere for 50 hours. This spectrum is almost identical to that of freshly polished natural galena, given in Figure 24. The disappearance of the  $1027\text{ cm}^{-1}$  band indicates that the xanthate coating has been oxidized forming, possibly, some dixanthogen ( $1270\text{ cm}^{-1}$  band is characteristic of dixanthogen) and thiosulfate.

(8) To complete the sequence, the sample was then soaked in pyridine for about 3 hours after which spectrum (g) resulted. This spectrum is almost identical to spectrum (b); that of the oxidation product of galena,  $\text{PbS}_2\text{O}_3$ .

In summary, xanthate did not adsorb in appreciable quantities onto evaporated PbS films from acetone solutions but did adsorb strongly onto the same films from aqueous solutions. Adsorption of xanthate from aqueous solutions resulted in a replacement of the PbS oxidation product with multilayers of lead xanthate. Hot acetone was not capable of completely solvating the lead xanthate multilayers. Exposure of the adsorbed xanthate to the air for two days resulted in complete decomposition of the xanthate.

Multilayer adsorption of xanthate from aqueous solutions has also been noted by Dr. L. Little and Dr. J. Leja (unpublished work) using infrared spectrophotometry. Their adsorbents were extremely fine ( $\sim 700$  mesh) copper screens, several of which were stacked in the beam path to increase the number of absorbing groups in the beam. The screens were reduced with hydrogen at a temperature of about  $350^\circ\text{C}$  in a sealed capsule. The capsule was then sealed off and broken under an aqueous solution of potassium xanthate thus eliminating exposure of the copper to the atmosphere. (Only the oxygen contained in the water could oxidize the



copper). The infrared spectrum of these screens, recorded after a few minutes of exposure, did not reveal any xanthate absorption bands. Retreatment of the same screens after about 1 hour exposure to the atmosphere, in the same xanthate solution, however, gave a spectrum identical to that of bulk cuprous xanthate. Since the sensitivity was too low to detect a monolayer coverage and the absorption bands obtained were quite intense, the spectrum was concluded to be due to multilayer adsorption. It is not possible to say whether or not oxidation was a prerequisite to xanthate adsorption since a monolayer could have been present without detection. It does, however, appear from this that the extent of multilayer adsorption is directly related to the extent of oxidation.

In order to check the effect of water alone on an evaporated PbS film, two new PbS-Al mirrors were prepared as before. The spectrum of the freshly evaporated films was again that of spectrum (a) in Figure 27. The samples were then soaked in acetone as before and their spectrum was found to be the same as spectrum (b) of Figure 27. Following this the two sample mirrors were soaked in doubly distilled water for 16 hours, removed and quickly dried in a hot air jet and their spectrum immediately recorded. The spectrum was the same as that of a PbS evaporated film after ionic bombardment, Figure 24 (e), except that the weak low frequency band was at  $985\text{ cm}^{-1}$  instead of  $955\text{ cm}^{-1}$ . This would indicate that the film was possibly partially oxidized from  $\text{PbS}_2\text{O}_3$  to  $\text{PbO}\cdot\text{PbSO}_4$ . Very little change in the band intensities was noted.





## V. SUMMARY

The infrared absorption spectra of many xanthate compounds in the solid and solution states have been recorded and absorption band assignments have been presented for the stretching modes of the C-O, C=S, C-S and S-S groups (See Table II).

A possible molecular configuration has been presented for heavy divalent metal xanthates on the basis of their infrared spectra and Langmuir-Blodgett monolayer films (See Figures 19 and 19A).

The infrared spectra of evaporated PbS films showed their oxidation products to be mainly  $\text{PbS}_2\text{O}_3$ . Under either ionic bombardment or prolonged contact with water, the films appeared to be further oxidized to  $\text{PbO} \cdot \text{PbSO}_4$  (See Figure 24).

The design of a reflectance attachment for the spectrophotometer is described which permits the recording of spectra due to monomolecular film coverages. Preliminary results of the adsorption of xanthate onto evaporated PbS films were presented.





## VI. PROPOSALS FOR FURTHER STUDIES

Many aspects of the work described in this thesis are, as yet, incomplete. In particular, a thorough investigation of xanthate adsorption onto sulfide minerals has only been begun; however, before this phase of the project can be extended, two requirements must be met. Absorption band assignment work must be extended into the far infrared spectral region in the hope of locating the absorption bands of the metal sulphur linkages in addition to furthering the study of the C-S linkage. The second requirement is the construction of a vacuum infrared cell for use with the reflectance attachment. This cell should permit the accomplishment of the following:

(1) Evaporation of the minerals onto the mirrors "in situ" under a high vacuum ( $10^{-7}$  mm Hg). Both ionic and electron bombardment facilities should be installed.

(2) The sample mirrors must be positioned, optically adjusted, treated, etc. without ever being exposed to the air or a contaminating medium.

Specific surface area determinations of adsorbents are planned with the use of a recently constructed gas-line and the B.E.T. gas adsorption technique.

An infrared spectroscopic investigation of Langmuir-Blodgett, metal xanthate monolayer films using a polarizer attachment should be valuable in molecular structure determinations. Very little work has been done on the spreading of metal xanthates at the air-water interface and future study of this aspect is planned. Frother-collector interactions may also be studied by combining infrared spectroscopy and monolayer film deposition techniques.



## REFERENCES

1. Cook, M.A., and Nixon, J.C., J. Phys. and Colloid Chem. 54, 445-459 (1950)
2. Last, G.A., and Cook, M.A., J. Phys. Chem. 56, 627 (1952)
3. Wark, I.W., "Principles of Flotation", p. 47, Australasian Institute of Min. and Met., Melbourne (1938)
4. Sutherland, K.L., J. Phys. Chem., 1717, (1959)
5. Eyring, E.M., and Wadsworth, M.E., Mining Eng. 5, 531 (1956)
6. Little, L.H., Poling, G.W., and Leja, J., Can. J. Chem. April (1961)
7. Bak, Borge, "Elementary Introduction to Molecular Spectra", Interscience Pub. Inc., New York, 1954.
8. Colthup, N.B., J. Opt. Soc. Amer., 40, 397-400 (1950)
9. Price, W.C., and Tetlow, K.S., J. Chem. Phys. 16, 1157 (1948)
10. Bellamy, L.J., "The Infrared Spectra of Complex Molecules". II<sup>nd</sup> Edition, p. 405, John Wiley and Sons, Inc., New York, (1958).
11. Hales, J.L., Jones, J.I., and Kynaston, W., J. Chem. Soc., 618 (1957)
12. Strong, F.C., Anal. Chem., 24, 338 (1952)
13. Jones, R.N., and Sandorfy, C., "Technique of Organic Chemistry", Vol. IX, p. 274, (1956), Interscience Pub. Inc., New York.
14. Lorentz, H.A., Proc. Acad. Sci., Amsterdam. 8, 591 (1906)
15. Ramsay, D.A., J. Amer. Chem. Soc., 74, 72 (1952)
16. Eischens, R.P., Z. Elektrochem. (1956) 60, 782.
17. Eischens, R.P., Fifth World Petroleum Congress, Pittsburg, (1959)
18. Little, L.H., and Leja, J., Proc. II<sup>nd</sup> Int. Cong. of Surface Activity, III, p. 261, Butterworth's Sci. Pub., London (1957).
19. Bulmer, G., and Mann, F.G., J. Chem. Soc., 614 (1957)



20. Holland, L., "Vacuum Deposition of Thin Films", p. 330, Chapman and Hall Ltd., London (1958)
21. Minden, H.T., J. Chem. Phys., 23, 1948 (1955)
22. Wilman, H., Proc. Phys. Soc., Lond., V60, 117 (1948)
23. Heavens, O.S., "Optical Properties of Thin Solid Films", p. 8 and 38, Butterworths Scientific Pub., London (1955)
24. Sternglanz, H., App. Spectroscopy, 10, p. 77 (1956)
25. Kicinski, F., Chem. and Industry, p. 54 (1948)
26. Francis, S.A., and Ellison, A.H., J. Opt. Soc. Amer., 49, p. 131 (1959)
27. Blodgett, K.B. and Langmuir, I., Phys. Rev., 51, 964 (1937)
28. Germer, L.H., and Storks, K.H., J. Chem. Phys., 6, 2801 (1938)
29. Blodgett, K.B., J. Amer. Chem. Soc., 57, 1007 (1935)
30. Bowcott, J.E.L., Proc. IIInd Int. Cong. of Surface Activity, III p. 267, Butterworth's Sci. Pub., London, (1957)
31. Pearson, F.G., and Stasiak, R.B., App. Spectroscopy, 12, 116 (1957)
32. Klassen, V.I., and Mokrousov, V.A., "Introduction to the Theory of Flotation", p. 255, Moscow 1959.
33. Kakovsky, I.A., Proceedings of the Mineral Industry, T. 111, Akad. Nauk., SSSR, (1956)
34. Bellamy, L.J., J. Chem. Soc., p. 2218 (1960)
35. Hagihara, H., Uchikoski, H., and Yamashita, S., Proc. IIInd Int. Cong. of Surf. Activity, III, p. 343, Butterworths Sci. Pub., London, (1957).
36. Thompson, H.W., and Torkington, P., J. Chem. Soc. 640 (1945)
37. Trotter, I.F., and Thompson, H.W., J. Chem. Soc., 481 (1946)





38. Wyckoff, R.W.G., "The Structure of Crystals", 1st Ed. Chemical Catalogue, New York, (1931)
39. Hagihara, H., Bulletin of the Kobayasi Inst. of Phys. Research, Vol. 4, p. 30-54 (1954)
40. Gordy, J., Phys. Rev., 69, 604 (1946)
41. Pauling, L., "The Nature of the Chemical Bond", p. 70, Cornell University Press (1948)
42. Kakovsky, I.A., Proc. II<sup>nd</sup> Int. Cong. of Surface Activity, IV, p. 225, Butterworths Scientific Pub., London, (1957)
43. Pilipenko, A.T., et al., Zhur. Anal. Khim., 12, 457-61 (1957)
44. Rietz, C.D., Svensk. Kem. Tidski., 69, 310-27, (1957)
45. Hagihara, H., J. Phys. Chem., 56, 610, (1952)
46. Taylor, T.C., and Knoll, A.F., Trans. Amer. Inst. Min. and Met. Engrs. 169, 259 (1946)
47. Moss, T.S., Proc. Phys. Soc. London, 63B, 167 (1950)
48. Schottky, W., and Wagner, C., Z. Physik. Chem. B11, 163 (1930)
49. Anderson, J.S., Disc. Faraday Soc., No. 4, p. 163 (1948)
50. Sosnowski, L., Starkiewicz, J., and Simpson, O., Nature, 159, 818 (1947)
51. Harada, R.H., J. Chem. Phys., 24, 447 (1956)
52. Minden, H.T., J. Chem. Phys., 25, 241 (1956)
53. Jones, R.H., Proc. Phys. Soc., London,  
a) 70B p. 235 (1957); b) 70B p. 1025 (1957)
54. Gibson, A.F., Proc. Phys. Soc., London, 65B, 378, (1952)
55. Dupuis, Mme. T., Compte Rendus, 242, 2924 (1956)
56. Mellor, J.W., "A Comprehensive Treatise on Inorganic and Theoretical Chemistry, Vol. X, p. 550, (1930)



57. Elisiev, L., and Nagirnyak, F., *Tsvetnye Metall.*, 13, No. 10, 38 (1938)
58. Mitrofanov, S.I., and Benenson, V.D., *Tsvetnye Metall.*, 13, No. 11, 56 (1938)
59. Plante, E.C., and Sutherland, K.L., *Am. Inst. Min. and Met. Engrs.*, Tech. Publ. 2297, *Mining Technology*, Jan. (1948)
60. Price, W.C., and Tetlow, K.S., *J. Chem. Phys.*, 16, 1157 (1948)
61. Brunauer, S., Emmett, P.H., and Teller, W.E., *J. Am. Chem. Soc.*, 60, 309 (1938)
62. Francis, S.A., and Ellison, A.H., *J. Opt. Soc. of Am.*, 49, p. 131-138 (1959)
63. Miller, F.A., Carlson, G.L., Bentley, F.F. and Jones, W.H., *Spectrochimica Acta*, 16, 135-235 (1960)
64. Berl, E., and Schmitt, B., *Kolloid Zeitschrift* 52, 333 (1930)













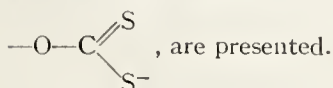
# INFRARED SPECTRA OF XANTHATE COMPOUNDS

## II. ASSIGNMENT OF VIBRATIONAL FREQUENCIES<sup>1</sup>

L. H. LITTLE,<sup>2</sup> G. W. POLING,<sup>3</sup> AND J. LEJA<sup>3</sup>

### ABSTRACT

Discrepant interpretations regarding the frequency of the C=S stretching mode are reviewed and assignments of frequencies for the vibrational modes of the xanthate group,



A band at 1020–1070  $\text{cm}^{-1}$  is assigned to the C=S stretching mode. Bands at 1200  $\text{cm}^{-1}$  and 1110–1140  $\text{cm}^{-1}$  are ascribed to the stretching vibrations of the C—O—C linkage.

The effects of the alkyl hydrocarbon chain length and of metal atoms (alkali metals, copper, and zinc) in displacing some of the frequencies are recorded.

In studying adsorption of xanthates on metals and their sulphide minerals by infrared spectroscopy, it became necessary to assign the spectral frequencies to the vibrational modes of the xanthate group. Previous studies of the spectra of xanthates (1, 2) and similar compounds (3, 4) were mainly exploratory in nature, due largely to the uncertain assignment of the C=S stretching mode for thiocarbonyl compounds (5, p. 293; 6; 7), in general.

Spectra of xanthates and similar compounds have been recorded and compared with recent studies of the thiocarbonyl stretching vibration (8, 9). Assignments of the xanthate vibrational frequencies have been made and conclusions reached with respect to the structures of dioxanthogens, heavy metal xanthates, and alkali metal xanthates.

### PROCEDURE

The spectra were recorded on Perkin–Elmer 21 and 221 double beam infrared spectrophotometers using sodium chloride prisms and on a Beckman IR4 infrared spectrophotometer using a cesium bromide prism. The solid samples were studied as mulls in nujol or in hexachlorobutadiene.

The intensities of the bands given in Table III, measured with the cesium bromide prism, are directly comparable with those of the bands shown in Figs. 1–4 for spectra measured with the sodium chloride prism.

The Raman spectrum of  $(n\text{-C}_4\text{H}_9\text{—S})_2\text{C=O}$  was recorded on a Cary Raman spectrophotometer. The other compounds are colored and, thus, are unsuitable for study by Raman spectroscopy.

#### (1) Xanthates\*

Potassium xanthate homologues,  $\text{C}_n\text{H}_{2n+1}\text{—O—C} \begin{array}{l} \text{=S} \\ \text{—SK} \end{array}$ , listed in Table I, were prepared

<sup>1</sup>Manuscript received November 17, 1960.

Contribution from the Division of Applied Chemistry, National Research Council, Ottawa, Canada, and the Department of Mining and Metallurgy, University of Alberta, Edmonton, Alberta.

Issued as N.R.C. No. 6222.

<sup>2</sup>Postdoctorate Research Fellow, National Research Council, Ottawa.

<sup>3</sup>Department of Mining and Metallurgy, University of Alberta, Edmonton, Alberta.

\*The dotted bands shown in Fig. 1 occur where bands due to the compounds being studied are masked by those of the nujol mulling agent.

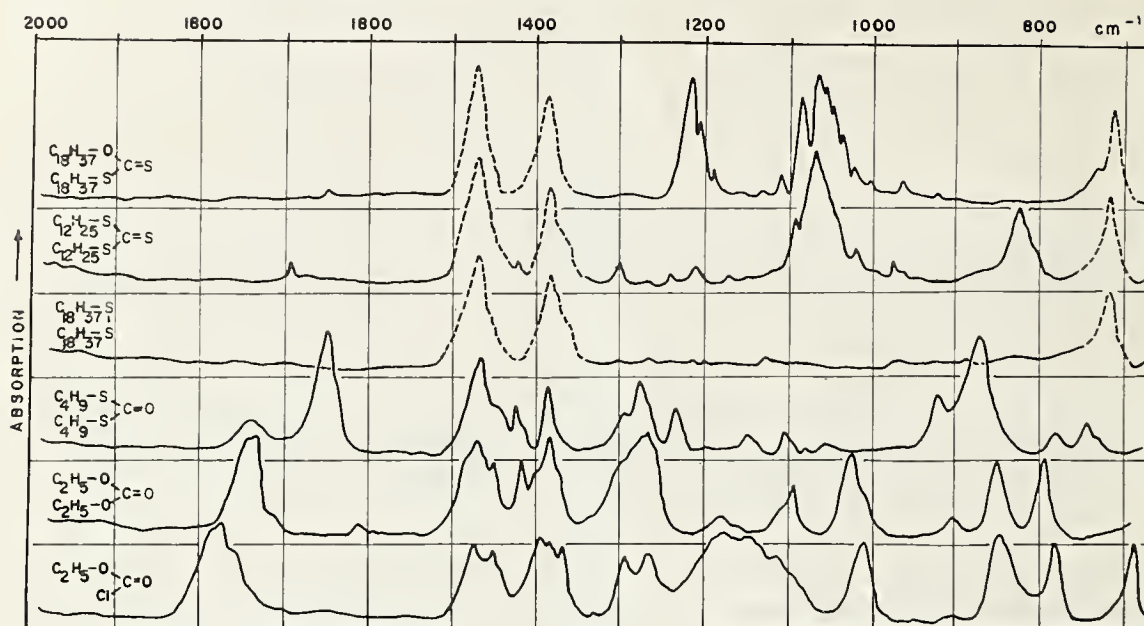


FIG. 1. Selected carbonyl and thiocarbonyl compounds.

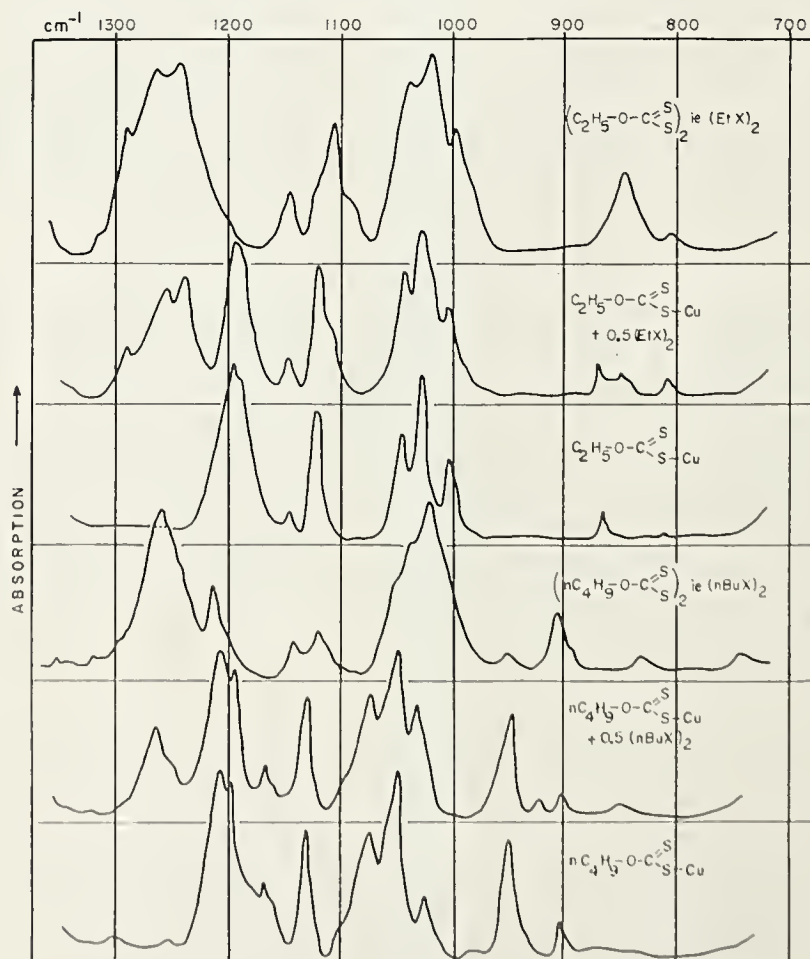


FIG. 2. Ethyl and butyl xanthates of copper and dioxanthogens.

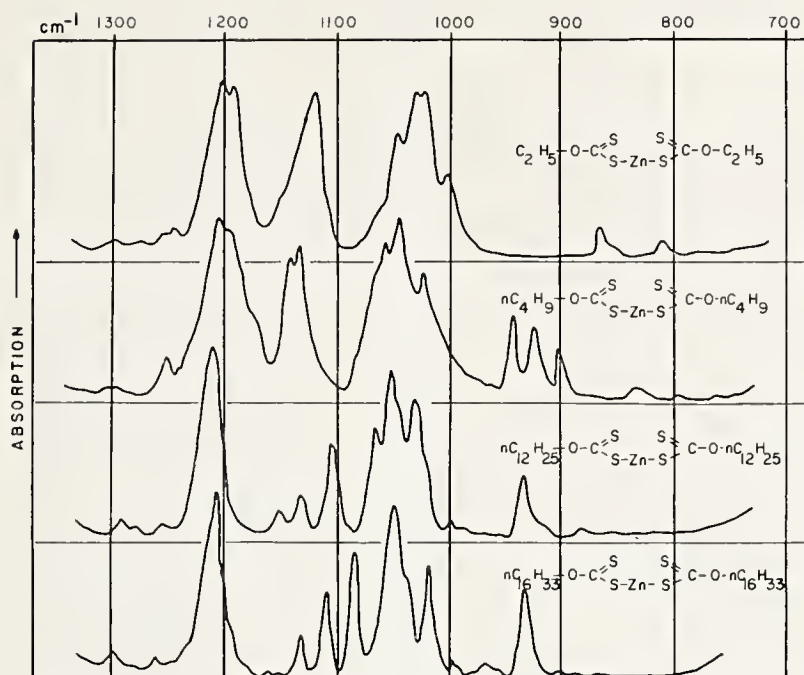


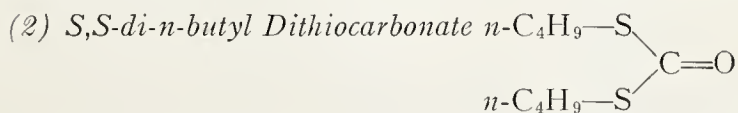
FIG. 3. Zinc alkyl xanthates.

TABLE I  
Analysis of xanthates

Potassium salt of alkyl xanthate	% C		% H		% S	
	Calc.	Chem. anal.	Calc.	Chem. anal.	Calc.	Chem. anal.
K-methyl xanthate	16.45	16.38	2.07	2.10	43.84	43.59
K-ethyl xanthate	22.48	22.62	3.14	3.20	40.01	38.04
K- <i>n</i> -propyl xanthate	27.56	27.14	4.05	4.01	36.79	36.50
K- <i>n</i> -butyl xanthate	31.89	30.97	4.82	4.63	34.05	33.19
K- <i>n</i> -amyl xanthate	35.61	34.79	5.48	4.78	31.69	28.83
K- <i>n</i> -hexyl xanthate	38.85	38.78	6.05	6.04	29.73	29.40
K- <i>n</i> -nonyl xanthate	46.47	46.53	7.41	7.35	24.81	23.77
K- <i>n</i> -cetyl xanthate	57.25	55.63	9.32	9.15	17.98	17.86

as described previously (1).

AnalaR grade cupric sulphate and zinc sulphate were used to prepare heavy metal xanthates from solutions of alkali xanthates. It has been shown previously (1) by spectroscopic methods that dixanthogen is produced during the precipitation of copper xanthate from solutions of cupric salts, while no dixanthogen is produced during the precipitation of zinc xanthate. These findings are now confirmed by analytical results (see Table II).



The dithiocarbonate was prepared by the method described by Bulmer and Mann (10). Phosgene was passed through a solution of sodium *n*-butyl mercaptide in ethanol





TABLE II  
Analysis of Zn and Cu xanthates

Material	Formula for calculations	% C		% H		% S		% metal	
		Calc.	Chem. anal.	Calc.	Chem. anal.	Calc.	Chem. anal.	Calc.	Chem. anal.
Zinc <i>n</i> -butyl xanthate	$(n\text{-C}_4\text{H}_9\text{-O-C}\begin{array}{c} \text{S} \\ // \\ \text{S} \end{array})_2\text{Zn}$	33.00	33.21	4.98	5.19	35.25	34.80	% Zn 17.97	% Zn 18.03
Copper <i>n</i> -butyl xanthate	$(n\text{-C}_4\text{H}_9\text{-O-C}\begin{array}{c} \text{S} \\ // \\ \text{S} \end{array})_2\text{Cu}$ (cupric)	33.17		5.01		35.43		% Cu 17.55	% Cu
Ether-extracted copper xanthate precipitate	$n\text{-C}_4\text{H}_9\text{-O-C}\begin{array}{c} \text{S} \\ // \\ \text{S} \end{array}\text{-Cu}$ (cuprous)	28.22		4.26		30.14		29.86	
Non-extracted fresh precipitate			28.67		4.26		29.79		28.37
Mixture of 2:1 moles cuprous xanthate- dixanthogen (calculated)		33.17	33.07	5.01	5.11	35.43	35.02	17.55	18.44

The original sample has been purified by  $\text{Al}_2\text{O}_3$  column chromatography and gave the following analysis: Calculated: 74.18% C; 12.45% H; 10.70% S. Found: 73.80% C; 12.00% H; 10.97% S.

(5) *Dialkyl Carbonates*

Dialkyl carbonates (ethyl, *n*-butyl, and *n*-amyl) were commercial high-purity reagents.

(6) *Alkyl Chloroformates*

Alkyl chloroformates (ethyl and *n*-butyl) were commercial high-purity reagents.

## INFRARED SPECTRA OF CARBONYL AND THIOCARBONYL COMPOUNDS

### *C=S Stretching Mode*

Figure 1 shows the spectra of thiocarbonate compounds of the types  $\text{R}-\text{O}-\text{C} \begin{smallmatrix} \text{S} \\ \text{S}-\text{R} \end{smallmatrix}$

and  $(\text{RS})_2\text{C}=\text{S}$ . It is seen that spectra of both types of compounds have strong bands at 1060–1070  $\text{cm}^{-1}$ . Intense bands in this region are absent in molecules which do not contain the  $\text{C}=\text{S}$  group, although some weaker bands appear in this region for diethyl carbonate and ethyl chloroformate (Fig. 1).

The shape of the band at 1060  $\text{cm}^{-1}$  is similar throughout the series of spectra of molecules containing the  $\text{C}=\text{S}$  group (Figs. 1, 2, and 3) and is composed of several peaks. This band has been assigned to the  $\text{C}=\text{S}$  stretching mode.

The  $\text{C}=\text{S}$  stretching mode has been assigned over a wide range of frequencies by different workers. Jones *et al.* (11) have discussed the variation of frequencies, depending on the environment of the  $\text{C}=\text{S}$  group, over the range 1000–1400  $\text{cm}^{-1}$ . Hazeldine and Kidd (6) assigned to the  $\text{C}=\text{S}$  stretching vibration a band at 1050–1120  $\text{cm}^{-1}$  in the spectra of the compounds  $(\text{RO})_2\text{C}=\text{S}$  and  $(\text{RS})_2\text{C}=\text{S}$ , while Marvel *et al.* (7) assigned to this vibration a band at 1170–1195  $\text{cm}^{-1}$ . Recently, Mecke *et al.* (8, 9) have investigated the spectra of a considerable number of molecules containing the  $\text{C}=\text{S}$  group and they ascribed its stretching frequency to the range 1053–1234  $\text{cm}^{-1}$ ; in the trithiocarbonate compounds the range was 1050–1060  $\text{cm}^{-1}$ . An extremely intense absorption band between 1110 and 1145  $\text{cm}^{-1}$  in the spectra of two mercaptopyridines has been assigned by Spinner (12) to the stretching vibration of conjugated  $\text{C}=\text{S}$  groups.

Felumb (3, 4) studied the spectra of many thiocarbonate molecules and assigned the  $\text{C}=\text{S}$  stretching mode to a band occurring at 1200–1250  $\text{cm}^{-1}$ . The series of compounds studied by Felumb was, however, incomplete insofar as the compounds  $(\text{RS})_2\text{C}=\text{S}$  and  $(\text{RS})_2\text{C}=\text{O}$  were omitted. The former molecule, which contains the  $\text{C}=\text{S}$  group, has no strong absorption band in the region 1200–1250  $\text{cm}^{-1}$  (Fig. 1). Moreover, all the molecules studied by Felumb contained the  $\text{C}-\text{O}-\text{C}$  linkage, which would be expected to show strong absorption bands at about 1200  $\text{cm}^{-1}$  (5, p. 161). The molecule  $(\text{RS})_2\text{C}=\text{O}$ , which has neither  $\text{C}-\text{O}-\text{C}$  nor  $\text{C}=\text{S}$  groups, has no strong bands between 1000  $\text{cm}^{-1}$  and 1300  $\text{cm}^{-1}$  (Fig. 1).

### *C—O—C Stretching Modes*

Thompson and Torkington (13) have assigned two bands in the region of 1200  $\text{cm}^{-1}$  to the stretching of the  $\text{C}-\text{O}$  bonds in esters. The assignment of absorption bands in the range 1000–1200  $\text{cm}^{-1}$  in molecules containing the  $\text{C}-\text{O}-\text{C}$  group has been discussed



by Hales *et al.* (14). Their conclusion was that the two bands in this region may be associated with the stretching vibrations of the C—O—C group.

The spectra of copper and zinc xanthates, dioxanthogens, and O,S-dioctadecyl xanthate (Figs. 1, 2, and 3) show two bands in the region 1100–1250  $\text{cm}^{-1}$ : an intense band at 1200–1250  $\text{cm}^{-1}$  and a weaker band at 1110–1140  $\text{cm}^{-1}$ . The latter band is of variable intensity, being sensitive to the length of the hydrocarbon chain and the nature of the metal atoms incorporated in the compounds. It can be seen from the spectra of the zinc alkyl xanthates (Fig. 3) that the intensity of this band decreases as the chain length increases.

In the spectra of ethyl and *n*-butyl dioxanthogens (Fig. 2), the frequency of the intense band is shifted to 1250  $\text{cm}^{-1}$  (from 1200  $\text{cm}^{-1}$  for copper and zinc xanthates) and the intensity of the band at lower frequency (1110  $\text{cm}^{-1}$ ) is greatly decreased for the dioxanthogens. These bands appear at 1220  $\text{cm}^{-1}$  and 1110  $\text{cm}^{-1}$  for O,S-dioctadecyl xanthate (Fig. 1).

The spectra of compounds which do not contain the C—O—C linkage, i.e.,  $(\text{RS})_2\text{C}=\text{O}$  and  $(\text{RS})_2\text{C}=\text{S}$  (Fig. 1) do not have strong bands between 1100  $\text{cm}^{-1}$  and 1250  $\text{cm}^{-1}$ .

The spectra of ethyl chloroformate and diethyl carbonate (Fig. 1) show the intense high-frequency bands at 1160  $\text{cm}^{-1}$  and 1260  $\text{cm}^{-1}$ , respectively, for these two compounds, and a considerably weaker band at a lower frequency, 1020  $\text{cm}^{-1}$ . This band is weaker than the intense band ascribed to the C=S stretching mode of xanthates.

The bands at 1120  $\text{cm}^{-1}$  and 1200  $\text{cm}^{-1}$  appearing in the spectra of xanthates are here ascribed to the stretching vibrations of the C—O—C linkage.

#### C=O Stretching Mode

The intense band at 1650–1780  $\text{cm}^{-1}$ , which occurs in the spectra of compounds containing the C=O group, viz. dialkyl carbonates, alkyl chloroformates, and  $(n\text{-C}_4\text{H}_9\text{S})_2\text{C}=\text{O}$ , (Fig. 1), is absent from the spectra of trithiocarbonate and of all the xanthate compounds. This band has been ascribed to the C=O stretching mode of the carbonyl compounds.

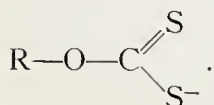
In addition to the carbonyl absorption of  $(n\text{-C}_4\text{H}_9\text{S})_2\text{C}=\text{O}$ , which occurs as a very intense band at 1650  $\text{cm}^{-1}$  (Fig. 1), a weaker band is found at 1750  $\text{cm}^{-1}$ . This is probably an overtone or combination band of the intense bands at 870  $\text{cm}^{-1}$  and 920  $\text{cm}^{-1}$ .

#### Structure of Xanthates

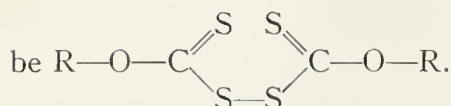
The spectra of copper and zinc xanthates (Figs. 2 and 3) show well-defined bands at 1200  $\text{cm}^{-1}$  and 1120  $\text{cm}^{-1}$ , which have been attributed to vibrations of the C—O—C linkage, while the intense band at 1060  $\text{cm}^{-1}$  has been assigned to the C=S stretching mode.

The resonance hybrid  $\left[ \text{R}-\text{O}-\overset{\text{C}}{\underset{\text{C}}{\text{S}}} \right]^-$  may be considered to represent the structure of

the metal xanthates (2). However, the xanthate esters (Fig. 1), which do not exist as resonance hybrids, have the same C=S band at 1060  $\text{cm}^{-1}$  as all the heavy metal xanthates. Consequently the structure of the heavy metal xanthates must be



For similar reasons the structure of the dixanthogens, retaining the C=S group, must



#### *C—S and S—S Stretching Modes*

Intense absorption bands occur at  $830\text{ cm}^{-1}$  and  $870\text{ cm}^{-1}$  in the spectra of  $(n\text{-C}_{12}\text{H}_{25}\text{S})_2\text{C}=\text{S}$  and  $(n\text{-C}_4\text{H}_9\text{S})_2\text{C}=\text{O}$  respectively (Fig. 1), while a band of medium intensity appears at  $850\text{ cm}^{-1}$  in the spectrum of ethyl dixanthogen (Fig. 2). The intensities of the bands for  $(n\text{-C}_4\text{H}_9\text{S})_2\text{C}=\text{O}$  and ethyl dixanthogen are far greater than those of bands at lower frequencies (Table III). It is probable, therefore, that the bands at lower frequencies are associated with fundamental vibrations and not with overtones or combinations. An intense band also occurs at  $870\text{ cm}^{-1}$  in the Raman spectrum of  $(n\text{-C}_4\text{H}_9\text{S})_2\text{C}=\text{O}$  (Table III).

The frequencies of these bands are considerably higher in value than those usually associated with the stretching of C—S or S—S bonds. Bellamy (5, p. 290) has discussed the assignments of C—S and S—S stretching modes to weak bands in the spectrum, occurring between  $600\text{--}700\text{ cm}^{-1}$  and  $400\text{--}500\text{ cm}^{-1}$ , respectively.

The intense bands ( $830$  to  $870\text{ cm}^{-1}$ ) may be associated with an asymmetric C—S stretching mode of the C—S—C—S—C chain in the molecules  $(n\text{-C}_{12}\text{H}_{25}\text{S})_2\text{C}=\text{S}$  and  $(n\text{-C}_4\text{H}_9\text{S})_2\text{C}=\text{O}$  or the C—S—S—C chain in ethyl dixanthogen. It must be noted, however, that the disulphide  $(n\text{-C}_{18}\text{H}_{37}\text{S})_2$  (Fig. 1) does not have an intense absorption band in this region. Moreover, the metal xanthates, which have only one C—S bond also show bands in the region  $800\text{--}950\text{ cm}^{-1}$  (Figs. 2 and 3), although these bands are generally weaker than those discussed above.

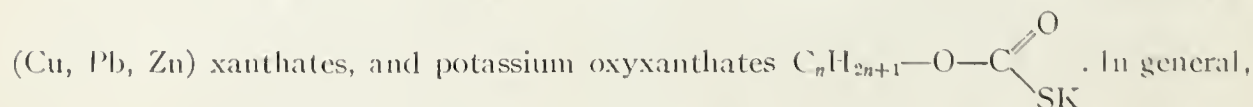
Jones *et al.* (11) have tentatively assigned bands occurring at  $880\text{--}700\text{ cm}^{-1}$  in the spectra of "carbon sulphonyl chloride" and dimeric thiocarbonyl chloride to the stretching of the C—S bond. It is possible that, due to the environment of the C—S bond in the xanthate group, the frequency of the C—S stretching mode may be raised above the normal limits discussed by Bellamy.

An intense band appearing at  $600\text{ cm}^{-1}$  in the Raman spectrum of  $(n\text{-C}_4\text{H}_9\text{S})_2\text{C}=\text{O}$  is probably due to a C—S stretching mode of this compound (5, p. 290).

Several bands appear between  $300$  and  $550\text{ cm}^{-1}$  in the spectra of xanthates (Table III). Although the spectrum of ethyl dixanthogen has more bands in this region than those of the metal xanthates, no definite assignment can be given to the S—S stretching mode of dixanthogens.

#### PRECIPITATION OF COPPER XANTHATE

Pearson and Stasiak (2) have published spectra of potassium xanthates, heavy metal



their spectra of corresponding xanthates are identical with those shown previously (1) and with those reported here. However, their spectrum of cupric xanthate corresponds to our spectrum of cuprous xanthate. The latter material was obtained after washing off the dixanthogen, which was coprecipitated with cuprous xanthate during the addition of cupric salts to solutions of alkali xanthates (1).

TABLE III  
Cesium bromide infrared and Raman spectra of thiocarbonates

$\text{C}_2\text{H}_5\text{-O-C-S-Cu}$		$\left[ \text{C}_2\text{H}_5\text{-O-C} \begin{array}{c} \text{S} \\ \text{S} \end{array} \right]_2 \text{Zn}$		$\text{C}_2\text{H}_5\text{-O-C-SK}$		$\text{C}_2\text{H}_5\text{-O-C-SNa}$		$\left[ \text{n-C}_4\text{H}_9\text{-O-C} \begin{array}{c} \text{S} \\ \text{S} \end{array} \right]_2 \text{Zn}$		$\text{n-C}_4\text{H}_9\text{-O-C-SK}$		$(\text{n-C}_4\text{H}_9\text{S})_2\text{C=O}$	
$\nu^*$	$\Delta\nu_{\frac{1}{2}}^\dagger$	% A $^\ddagger$	$\nu$	$\Delta\nu_{\frac{1}{2}}$	% A	$\nu$	$\Delta\nu_{\frac{1}{2}}$	% A	$\nu$	$\Delta\nu_{\frac{1}{2}}$	% A	Infrared spectrum $\nu$ $\Delta\nu_{\frac{1}{2}}$ % A	Raman spectrum $\nu$ % A
300	9	8	345	~7~20		290	~4	6	308	~10	10	~295	170
350	9	8				308	9	15	327	2	10	~303	220
453	9	10	360	~15~20		350	~5	2				395	440
547	10	8	452	10	18	447	8	29	470	~90	55		
667	~10	6				540	~15	2				~670	600
						565	10	2				750	660
						647	~25	6	620	~60	30		740
						673	~20	6				842	740
815	~10	4	820	~10	7	672	~20	9					800
						820	~10	9	805	~15	6	925	870
873	10	13	875	~15	11	840	~15	2	850	~10	2	962	900
						875	~10	2	865	~10	3	1065	900
									927	7	13		1050
1015	43					1015		43	945	8	37	1107	1060
1040	80		1035		78				1026			1107	1080
1053	37								1040	74	38	1153	1100
											93		1105
1127	66		1130		72	1055		75					1147
						1107		78					1235
1200	82		1213		80	1122		78	1115	74	70	1300	1220
						1145		79	1153	70	90	1345	1280
									1170	69		~20	1310
												~10	1345
												~10	1387
												10	1420
												15	1420
												10	1460
												17	1460
												24	1650
												~25	1650
												17	1750
												~40	1750
												20	
												6	

\* Band frequency ( $\text{cm}^{-1}$ ).† Half-band width ( $\text{cm}^{-1}$ ).

‡ % absorption at band maximum.



Pearson and Stasiak do not state whether their copper xanthate precipitate was washed with solvents, yet in their spectrum no band appears at  $1250\text{ cm}^{-1}$ , characteristic of dioxanthogen in the precipitate. Nor do they state whether their elemental analysis was made before or after washing with solvents. Results of the analysis of the precipitate both before and after ether extraction are shown in Table II. In the absence of knowledge that the precipitate was a mixture of cuprous xanthate and dioxanthogen, the results would indicate that it was cupric xanthate.

Infrared spectra (Fig. 2) and chemical analysis (Table II) suggest that the reaction between cupric ions and xanthate ions results in the coprecipitation of cuprous xanthate and dioxanthogen in the molar ratio 2:1;  $4\text{RX}^- + 2\text{Cu}^{++} \rightarrow 2\text{RXCu} + (\text{RX})_2$  where  $\text{X}^-$

denotes the  $\text{—O—C}\begin{smallmatrix} \text{S} \\ \text{S}^- \end{smallmatrix}$  group. With zinc ions a zinc dioxanthate, but no dioxanthogen, is formed.

#### ALKALI METAL XANTHATES

Spectra of some alkali metal xanthates are shown in Fig. 4. The absorption bands in the region  $1000\text{--}1200\text{ cm}^{-1}$  are not well resolved but it is possible to distinguish three more or less distinct groups of bands, corresponding to the bands at  $1200\text{ cm}^{-1}$ ,  $1130\text{ cm}^{-1}$ , and  $1060\text{ cm}^{-1}$  for the heavy metal xanthates in Figs. 2 and 3.

If such a grouping of bands in the spectra of alkali metal xanthates is accepted, then the frequencies of the C—O—C linkage, discussed earlier, would appear to be displaced to lower values than those given for the C—O—C linkage in the heavy metal xanthates. The frequency of the band assigned to the C=S stretching mode varies from  $1040$  to  $1080\text{ cm}^{-1}$  in the spectra of alkali metal xanthates. The presence of this band suggests that the C=S bond is preserved in the structure of the alkali metal xanthates.

#### ACKNOWLEDGMENTS

The authors gratefully acknowledge the assistance of Dr. K. Noack, Dr. E. C. Horswill, Mr. A. E. Castagne, and Mr. J. A. H. Desaulniers. G. W. Poling and J. Leja express their appreciation for the grants A699 and E140 received from the National Research Council of Canada.

#### REFERENCES

1. L. H. LITTLE and J. LEJA. Proceedings of the Second International Congress of Surface Activity, Vol. III, Butterworth Scientific Publications, London, 1957, p. 261.
2. F. G. PEARSON and R. B. STASIAK. Appl. Spectroscopy, **12**, 116 (1957).
3. R. FELUMB. Compt. rend. **244**, 2038 (1957).
4. R. FELUMB. Bull. soc. chim. France, Ser. 5, **24**, 890 (1957).
5. L. J. BELLAMY. The infrared spectra of complex molecules. 1st ed. Methuen & Co., Ltd., London, 1954.
6. R. N. HAZELDINE and J. M. KIDD. J. Chem. Soc. 3871 (1955).
7. C. S. MARVEL, P. DERADZITZKY, and J. J. BRADER. J. Am. Chem. Soc. **77**, 5997 (1955).
8. R. MECKE, R. MECKE, and A. LÜTTRINGHAUS. Z. Naturforsch. Pt. b, **10b**, 367 (1955).
9. R. MECKE, R. MECKE, and A. LÜTTRINGHAUS. Chem. Ber. **90**, 975 (1957).
10. G. BULMER and F. G. MANN. J. Chem. Soc. 666 (1945).
11. J. I. JONES, W. KYNASTON, and J. L. HALES. J. Chem. Soc. 614 (1957).
12. E. SPINNER. J. Org. Chem. **23**, 2037 (1958).
13. H. W. THOMPSON and J. TORKINGTON. J. Chem. Soc. 640 (1945).
14. J. I. HALES, J. I. JONES, and W. KYNASTON. J. Chem. Soc. 618 (1957).



**B29792**